COMPARATIVE ONTOGENY OF THE HOMINID PELVIS AND IMPLICATIONS FOR THE EVOLUTION OF BIRTH

Dissertation

zur

Erlangung der naturwissenschaftlichen Doktorwürde

(Dr. sc. nat.)

vorgelegt der

Mathematisch-naturwissenschaftlichen Fakultät

der

Universität Zürich

von

Alik Huseynov

von/aus

Deutschland

Promotionskomitee

Prof. Dr. Christoph P. E. Zollikofer (Vorsitz der Dissertation)

Dr. Marcia S. Ponce de León (Leiterin der Dissertation)

Prof. Dr. Marcelo Sánchez-Villagra

Prof. Dr. Carel van Schaik

Zürich, 2016

Contents

Abstract

Sex-specific phenotypic differences – known as somatic sexual dimorphism – are present in the pelvis of various primate species, but particularly conspicuous in humans. It is generally agreed that the human female pelvis is under selection to be adequately capacious for childbirth, but the proximate (developmental) and ultimate (evolutionary) mechanisms that lead distinct adult female and male pelvic morphologies remain largely unknown. This thesis investigates these mechanisms in humans and great apes, using methods of biomedical imaging and geometric morphometrics. The first part focuses on human pelvic development. Results show that male and female pelves follow largely similar development trajectories until puberty. The female trajectory then diverges from the prepubertal course, resulting in rapid expansion of birth canal dimensions up to the age of 25-30 y. In males, however, the postpubertal developmental trajectory remains largely similar to the prepubertal course. In postmenopausal women, the pelvis resumes a male-like trajectory, resulting in the constriction of birth canal dimensions. These developmental changes are likely linked to major changes in sex steroid levels during puberty and menopause, implying a substantial role of developmental plasticity as a response to changing physiological and environmental conditions during an individual's lifetime. The second part of this thesis focuses on changing patterns of modularity/integration in the developing chimpanzee pelvis. Results indicate that, during ontogeny, the developmental units of the pelvis (ilium, ischium and pubis) become more integrated, while the functional units (locomotion versus obstetrics) become more modular. The latter patterns suggests more independence between units, implying high evolvability (potential to evolve and adapt), which likely constitutes the basis for developmental divergence between sex-specific pelvic shapes. The third part of this thesis focuses on the question whether the pattern of adult pelvic sexual dimorphism in humans represents evolutionary-developmental novelty, or whether it builds upon shared ancestral processes of dimorphic development and evolution. The results show that great apes and humans share similar patterns of sex-related differences in pelvic morphology, indicating shared processes of sex-specific development that predate the evolution of obstetric constraints in hominins.

Zusammenfassung

Somatischer Sexualdimorphismus ist bei Primaten relativ weit verbreitet. Beim Menschen ist er vor allem im Becken stark ausgeprägt. Während allgemein angenommen wird, dass beim Menschen das weite weibliche Becken eine Adaptation an den Geburtsprozess darstellt, bleiben die proximaten (entwicklungsmechanischen) und ultimaten (evolutionären) Ursachen für die unterschiedlichen weiblichen und männlichen Beckenmorphologien weitgehend unbekannt. In dieser Arbeit werden Methoden der Medizinischen Bildgebung und der Geometrischen Morphometrie gebraucht, um die Beckenentwicklung beim Menschen und bei Menschenaffen zu untersuchen. Der erste Teil der Arbeit analysiert die Beckenentwicklung beim Menschen. Bis zur Pubertät entwickeln sich männliche und weibliche Becken ähnlich, Dann divergiert das weibliche Becken vom präpubertären Entwicklungsmuster, was zu einer raschen Ausdehnung der Geburtskanaldimensionen bis zum Alter von 25-30 Jahren führt. Bei Männern bleibt das Entwicklungsmuster jedoch weitgehend unverändert. Bei postmenopausalen Frauen folgt das Becken einem „männlichen“ Entwicklungsmuster, was zur Verengung des Geburtskanals führt. Diese Entwicklungsveränderungen sind wahrscheinlich mit Veränderungen des Sexualhormonspiegels während der Pubertät und der Menopause verbunden. Dank diesem Mechanismus kann sich das weibliche Becken „in-vivo“ an veränderte physiologische und Umweltbedingungen anpassen. Der zweite Teil dieser Arbeit konzentriert sich auf die ontogenetische Veränderung der Modularität/Integration im Becken von Schimpansen. Während der Ontogenese nimmt die Integration der Entwicklungseinheiten des Beckens (Ilium, Ischium und Pubis) zu, während die Modularität der funktionalen Einheiten (Fortbewegung versus Gebären) zunimmt. Das letztgenannte Muster deutet auf eine ausgeprägte Evolvabilität (Potenzial zur evolutionären Adaptation) des Beckens hin und bildet wahrscheinlich die evolutionäre und entwicklungsbiologische Grundlage für die Divergenz zwischen weiblichen und männlichen Beckenformen. Der dritte Teil dieser Arbeit konzentriert sich auf die Frage, ob das Muster des erwachsenen Becken-Sexualdimorphismus beim Menschen eine evolutionär-entwicklungsbiologische Neuheit darstellt oder ob es auf evolutionär alten Mustern aufbaut. Die Ergebnisse zeigen, dass Menschenaffen und Menschen ähnliche Muster des Becken-Sexualdimorphismus aufweisen, was auf Prozesse der geschlechtsspezifischen Entwicklung hindeutet, die evolutionär älter sind als der spezifisch menschliche Geburtsprozess.

Abstract for non-academic audience

Various evolutionary and developmental mechanisms produce distinct male and female pelvic morphologies. This thesis demonstrates that the human female pelvis changes substantially during pubertal development to accommodate large neonates. The human pattern of pelvic sexual dimorphism is also found in the great apes, indicating that it has deep evolutionary roots.

Zusammenfassung für nicht-akademisches Publikum

Diese Doktorarbeit zeigt, dass sich beim Menschen das weibliche Becken während der Pubertätsentwicklung stark verändert, um grosse Babys gebären zu können. Die geschlechtsspezifischen Formen des menschlichen Beckens lassen sich auch bei den Menschenaffen nachweisen, was auf gemeinsame evolutionäre und entwicklungsbiologische Wurzeln des Sexualdimorphismus hinweist.

Development of sexual dimorphism in the human pelvis in relation to obstructed labor

One central aspect of phenotypic differences in vertebrates is secondary sexual dimorphism, i.e., differences between males and females of the same species. Such differences are pervasive, and are most obviously expressed in macroscopic features such as body size and shape, and the morphology of soft and hard tissue structures (Badyaev, 2002; McPherson and Chenoweth, 2012). Secondary sexual dimorphism is largely due to sex-biased autosomal gene expression that in turn is regulated by various hormones, such as growth hormone/insulin-like growth factor 1, and androgen/estrogen and associated signaling pathways (Williams and Carroll, 2009; Callewaert et al., 2010; Parsch and Ellegren, 2013). In vertebrates sexual differentiation mostly happens once the development of testes and ovaries is complete (Williams and Carroll, 2009). Somatic sexual dimorphism of the pelvis – which is at the center of this thesis work – has been shown to be largely the outcome of such molecular/ developmental processes. It is not only found in humans and non-human primates (Schultz, 1949; Leutenegger, 1970; Gingerich, 1972; Leutenegger, 1974; Rosenberg, 1992; LaVelle, 1995; Tague, 1995; Lovejoy, 2005; Wittman and Wall, 2007; Weiner et al., 2008; Bilfeld et al., 2011; 2012; 2015; Gruss and Schmitt, 2015; Wells, 2015), but also in rodents (Bernstein and Crelin, 1967; Iguchi et al., 1989; Uesugi et al., 1992; Berdnikovs et al., 2006), and other vertebrates (Chapman et al., 1994; Tague, 2003).

In humans, pelvic sexual dimorphism (PSD) is substantial, and clearly more expressed than in our closest living relatives, the great apes. The evolution of human PSD has traditionally been discussed in the framework of the obstetrical dilemma (OD) hypothesis of Washburn (1960). According to this hypothesis, conflicting or antagonistic selective regimes constitute the "dilemma": selection for biomechanically efficient (narrow) pelves versus selection for large-brained/big-bodied neonates requiring obstetrically efficient (wide) female pelves (Schultz, 1949; Rosenberg, 1992; LaVelle, 1995). In its original form, the OD hypothesis mostly tried to explain the early timing of birth that results in human altriciality (Portmann, 1941): humans are born in a comparatively helpless state, and newborns have been interpreted as extrauterine fetuses (Montagu, 1961). The high maternal-neonatal mortality (Hofmeyr, 2004; McClure et al., 2007; Harrison et al., 2015) in modern human societies has been associated with the high prevalence of cephalopelvic disproportion and

resulting obstructed labor. Accordingly, obstetric constraints, i.e. a tight fit between the female pelvis and neonatal head/body dimensions, have been proposed to play a major role in the evolution of PSD.

Recently, however, the OD hypothesis has been challenged on various grounds: the energetics of gestation and growth (EGG) hypothesis (Ellison, 2008; Dunsworth et al., 2012; Dunsworth and Eccleston, 2015) suggests that the timing of birth is constrained by the limited metabolic output of the mother rather than by spatial limitations of her pelvis. In fact, experimental evidence and biomechanical modeling suggest that a wide pelvis does not reduce bipedal locomotor efficiency (Dunsworth et al., 2012; Warrener et al., 2014). Furthermore, it has been proposed that rapidly changing environmental conditions may result in a generational lag between maternal and neonate developmental plasticities, resulting in fetopelvic mismatch and obstructed labor (Jasienska et al., 2006; Ellison, 2008; Gruss and Schmitt, 2015; Wells, 2015). Also, on biocultural grounds, it has been hypothesized that increased maternal mortality is due to increased pregnancy/obstetrics-related medical interventions without previous risk assessment, which tend to interfere with natural biological processes of childbirth (Stone, 2016). On the other hand, there is new support for a significant role of obstetric constraints during the evolution of modern human PSD: a recent study examined the correlation between pelvic form, head size and stature in humans and showed that females with large heads tend to have obstetrically more favorable pelvic morphologies than females with small heads, thus reflecting correlational selection for those traits (Fischer and Mitteroecker, 2015). More generally, several recent studies reported sexual dimorphism in the human coxal bone, ilium and pubis separately, suggesting that most of the sex-specific differences in these pelvic regions become evident already at 10-13 years of age (Bilfeld et al., 2011; 2012; 2015).

Experimental endocrinological studies in rodents, such as mice, provided evidence for hormonal/molecular mechanisms for sex-biased pelvic development. For instance, gonadectomized and testicular-feminized (i.e. lacking androgen receptors) males develop a female-like pelvis, whereas ovariectomized female mice under administration of androgens develop male-like pelvic morphologies (Bernstein and Crelin, 1967; Iguchi et al., 1989; Uesugi et al., 1992). These studies further suggested that male development deviates from the prepubertal course under testosterone influence, and this hypothesis was also proposed for humans and primates in general (Tague, 1995; 2005). However, others (Gingerich, 1972; Berdnikovs et al., 2006) suggested that estrogens are important for female pelvic

development, and for a female-specific developmental trajectory during puberty (Berdnikovs et al., 2006). Moreover, since such hormonal changes are sensitive to ecological and nutritional factors, it has been suggested that the pelvis exhibits substantial *in-vivo* "modifiability" (Wilson, 1894), i.e., developmental plasticity (Wells et al., 2012; Wells, 2015).

In the first chapter of this thesis, I test the OD hypothesis from a developmental perspective. Specifically, I propose the developmental obstetric dilemma (DOD) hypothesis, which postulates that the female pelvic morphology reflects *in-vivo* changes in obstetric needs (versus other needs such as locomotion) during an individual's lifetime, and thus is subject to developmental plasticity. This hypothesis states that (i) sex-specific differences in human pelvic morphology become pronounced during puberty (Bilfeld et al., 2011; 2012; 2015); (ii) the female pelvis reaches its obstetrically most adequate morphology around the age of highest fertility (Bamberg Migliano et al., 2007; Martin et al., 2015); (iii) during postmenopausal life, the female pelvis reverts to an obstetrically less adequate morphology, which is probably most adequate for locomotion and other functions; (iv) the male pelvis does not show these developmental changes. To test the DOD hypothesis I quantify and analyze pelvic morphology and developmental changes from late fetal stages to late adulthood. Since pelvic elements fuse relatively late during development, and the three-dimensional morphology of the pelvis critically depends on the presence of the surrounding soft tissues, the sample used here consists of Computer Tomography (CT) data of anonymized known-age and known-sex forensic/clinical cases. Based on this sample, I perform a geometric-morphometric analysis of three-dimensional (3D) pelvic shape change; the results of this study provide clear support for the DOD hypothesis.

Modularity and integration of the human and great ape pelvis in an evolutionary-developmental context

In order to understand the evolutionary and developmental mechanisms that lead to the specific pelvic morphologies of humans and our closest living relatives, the great apes, and also lead to PSD, several lines of research need to be followed: (a) comparative studies of taxon-specific patterns of pelvic development; (b) studies of the relative interdependence of different pelvic units (integration and modularity), permitting inferences on the "evolvability" of the pelvis; and (c) comparative analyses of taxon-specific patterns of pelvic sexual

dimorphism. The second and third chapters of this thesis are dedicated to (b) and (c), while (a) will be the focus of a future publication.

Chapter 2 focuses on the ontogenetic patterns of modularity and integration in the chimpanzee pelvis. Modularity is known as a heterogeneous pattern or process in organismal development and/or morphology, where different modules are viewed as internally strongly integrated units having weak connectivity to other such units (Kitano, 2004; Wagner et al., 2007; Klingenberg, 2008; Kuratani, 2009; Klingenberg, 2010; Wagner and Zhang, 2011; Klingenberg, 2014; Esteve-Altava, 2015). The concept of modularity can also be related to network models of biological structures. For example, in neural networks, direct selection to minimize connection costs (such as maintenance, efficient energy transmission, physical limits and signal transmission delays due to high connection numbers) tend to produce modularity as a side effect (Striedter, 2005). Basically, any biological network under external or internal pressure to minimize connection costs between network nodes may evolve modularity and is able to adapt more quickly to changing environmental factors than an integrated system (Clune et al., 2013). Modularity and integration have been studied in various animals and their substructures, for example fruit fly wings (Klingenberg and Zaklan, 2000), bird beaks (Abzhanov et al., 2004; 2006), mammalian skulls (Klingenberg et al., 2003; Klingenberg, 2004; Mitteroecker and Bookstein, 2008; Zelditch et al., 2008; Delezene, 2015), and the primate and human pelvis (Berge, 1998; Williams and Orban, 2007; Grabowski et al., 2011; Grabowski, 2012; Lewton, 2012). It is generally agreed that the modular organization of an organism can facilitate its capacity to evolve and adapt (evolvability), because selection can act independently on each module (Hansen, 2003; Hendrikse et al., 2007; Wagner et al., 2007; Kuratani, 2009; Goswami and Polly, 2010; Goswami et al., 2014; 2015).

While concepts of modularity and integration are well developed, there is currently no agreement on how to quantify them. The basic approach to study morphological modularity and integration is to quantify patterns of intra/interspecific and developmental morphological (co-)variation. In a majority of studies, the covariation within pre-defined morphological units is compared to covariation between these units. These measures of covariation are then used to assess modularity (loose between-unit compared to within-unit covariation) and integration (strong between-unit compared to within-unit covariation). While patterns of covariation are often considered to be static, I focus here on their modification during ontogeny. Analyzing changes in covariation patterns permits inferences on changes in modularity and integration. In technical terms, measuring such changes from one ontogenetic stage to the subsequent one

represents a challenge; “ontogenetic stages” are typically defined by an externally set time frame. They do not represent a point of developmental homology among same-aged individuals, because these individuals will exhibit natural variation in growth and developmental rates.

The bony pelvis of great apes and humans represents an interesting model system for such studies. It is composed of several developmental units (ilium, ischium, pubis) representing independent chondrification/ossification regions (Scheuer et al., 2000). These elements are fusing during skeletal development and likely become more integrated with increasing individual age. At the same time the pelvis serves various functions, such as parturition, locomotion, abdominal stability, and more generally as an attachment site for muscles, tendons and ligaments. Functional demands tend to change during an individual’s lifetime. Consequently, one expects complex interactions between evolutionary, developmental and environmental factors influencing modularity/integration. Earlier studies on modularity/integration of the pelvis demonstrated that, in humans compared to great apes, morphological integration is reduced in obstetric versus to locomotor regions, indicating higher evolvability of birth canal in human than great apes, and low integration and high evolvability of the pelvis in general (Berge, 1998; Williams and Orban, 2007; Grabowski et al., 2011; Grabowski, 2012; Lewton, 2012). However these studies focused on phenotypic variation in adults, such that what happens to modularity/integration of the pelvis during development remains largely unknown. More generally, it has been shown that modularity/integration patterns tend to change during ontogeny of craniofacial elements (Willmore et al., 2006; Zelditch et al., 2006; Hallgrimsson et al., 2009; Gonzalez et al., 2011; González et al., 2011). It has been suggested that modules tend to become integrated, or integrated units become modular (e.g. due to external stimuli), such that the original pattern of modularity/integration is “overwritten” by subsequent ones, resulting in a “palimpsest” of modularity/integration (Hallgrimsson et al., 2009).

Given this theoretical and methodological framework, I investigate here the development of the chimpanzee pelvis, and test the following hypotheses: a) the modularity of developmental units of the pelvis decreases during ontogeny, while their integration increases; b) the modularity of functional pelvic units increases during ontogeny, while their integration decreases. Testing these hypotheses in chimpanzees (rather than in humans, were larger samples are available) has the advantage that effects of obstetric constraints and/or sexual dimorphism can be expected to be minimal (Schultz, 1949; Tague, 2005), such that a smaller

number of factors needs to be considered. As mentioned, there are various ways to quantify patterns of modularity/integration in morphometric data; likewise, there are various ways to assess the potential for evolutionary change ("evolvability") from such patterns (Wagner, 1990; Klingenberg, 2005; McGuigang, 2006; Hansen and Houle, 2008; Hallgrimsson et al., 2009; Klingenberg, 2009; Smilde et al., 2009; Young et al., 2010; Klingenberg et al., 2012; Adams, 2016). One needs to keep in mind that modularity/integration are developmental processes that can only be quantified by direct observation and experimental modification of these processes (Hallgrimsson et al., 2009; Bookstein, 2016). In primates, this is not possible, such that the majority of studies focuses on patterns of covariation, while the underlying processes of integration remain unexplored. The approach followed here is largely similar to that proposed by Klingenberg (2014) and Adams (2016).

The third chapter of this thesis provides a comparative analysis of the patterns of adult PSD in humans and great apes. Previous studies have shown that PSD is present in apes, but that it is minimal compared to humans (Schultz, 1949; Tague, 2005). Intriguingly, PSD is present not only in humans, but also in the obstetrically unconstrained great apes (Schultz, 1949; Tague, 2003). Also, it has been shown that actual morphological patterns of PSD have been shown to be similar in obstetrically constrained and unconstrained species of the lesser apes (hylobatids) (Zollikofer et al.). Here I compare 3D patterns of PSD in adult humans (obstetrically constrained) and great apes (obstetrically unconstrained). Specifically, I address the following questions: does the observed pattern of human PSD reflect (a) true evolutionary novelty or (b) an ancestral pattern shared with great apes that had increased in magnitude in humans because of obstetrics-related selection? The results of this study provide support for hypothesis (b), indicating that the conspicuous PSD of modern humans has deep phylogenetic roots, which predate the evolution of human-specific obstetric constraints.

Each of the chapters characterized here represents a peer-reviewed journal paper, either published (Huseynov et al., 2016) (chapter 1) or accepted (Huseynov et al., accepted) (chapter 2), or ready to submit (chapter 3). The Appendix provides a detailed account of the sample structure, and of the methods of data acquisition and analysis used in all three studies.

Future perspectives

One has to recognize that the: "...development is intimately connected to evolution because it is through changes in embryos that changes in form arise,, (Carroll, 2005, p 13) and "...understanding how alterations in the mechanisms of embryonic development influence or

direct evolutionary changes in any and all stages of the life cycle,, (Hall, 2012, p 184) is a key to understand the phenotypic evolution. I am planning a follow-up paper on the development of the pelvis in great apes as compared to humans from the fetal stage to adulthood. This paper will explore the sex-specific and sex-neutral components of developmental trajectories per taxon in order to infer the ancestral developmental trajectory, and underlying processes that led to the shared pattern of pelvic sexual dimorphism in adult great apes and humans.

References:

Abzhanov A, Kuo WP, Hartmann C, Grant BR, Grant PR, Tabin CJ. 2006. The calmodulin pathway and evolution of elongated beak morphology in Darwin's finches. Nature 442:563–567.

Abzhanov A, Protas M, Grant BR, Grant PR, Tabin CJ. 2004. Bmp4 and morphological variation of beaks in Darwin's finches. Science 305:1462–1465.

Adams DC. 2016. Evaluating modularity in morphometric data: challenges with the RV coefficient and a new test measure. Methods Ecol Evol 7:565–572.

Badyaev AV. 2002. Growing apart: an ontogenetic perspective on the evolution of sexual size dimorphism. Trends Ecol Evol 17:369–378.

Bamberg Migliano A, Vinicius L, Lahr MM. 2007. Life history trade-offs explain the evolution of human pygmies. Proc Natl Acad Sci USA 104:20216–20219.

Berdnikovs S, Bernstein M, Metzler A, German RZ. 2006. Pelvic growth: ontogeny of size and shape sexual dimorphism in rat pelves. J Morphol 268:12–22.

Berge C. 1998. Heterochronic processes in human evolution: An ontogenetic analysis of the hominid pelvis. Am J Phys Anthropol 105:441–459.

Bernstein P, Crelin ES. 1967. Bony pelvic sexual dimorphism in the rat. Anat Rec 157:517–525.

Bilfeld MF, Dedouit F, Rousseau H, Sans N, Braga J, Rougé D, Telmon N. 2011. Human coxal bone sexual dimorphism and multislice Computed Tomography: geometric morphometric analysis of 65 adults. J Forensic Sci 57:578–588.

Bilfeld MF, Dedouit F, Sans N, Rousseau H, Rougé D, Telmon N. 2012. Ontogeny of size and shape sexual dimorphism in the ilium: a multislice computed tomography study by geometric morphometry. J Forensic Sci 58:303–310.

Bilfeld MF, Dedouit F, Sans N, Rousseau H, Rougé D, Telmon N. 2015. Ontogeny of size and shape sexual dimorphism in the pubis: a multislice Computed Tomography study by geometric morphometry. J Forensic Sci.

Bookstein FL. 2016. The inappropriate symmetries of multivariate statistical analysis in geometric morphometrics. Evol Biol 43:277–313.

Callewaert F, Sinnesael M, Gielen E, Boonen S, Vanderschueren D. 2010. Skeletal sexual dimorphism: relative contribution of sex steroids, GH-IGF1, and mechanical loading. J Endocrinol 207:127–134.

Carroll SB. 2005. Endless forms most beautiful: The new science of evo devo and the making of the animal kingdom. New York: Norton.

Chapman A, Hall LS, Bennett MB. 1994. Sexual Dimorphism in the Pelvic Girdle of Australian Flying Foxes. Aust J Zool 42:261–265.

Clune J, Mouret J-B, Lipson H. 2013. The evolutionary origins of modularity. Proc R Soc B 280:20122863–20122863.

Delezene LK. 2015. Modularity of the anthropoid dentition: Implications for the evolution of the hominin canine honing complex. J Hum Evol 86:1–12.

Dunsworth H, Eccleston L. 2015. The evolution of difficult childbirth and helpless hominin infants. Annu Rev Anthropol 44:55–69.

Dunsworth HM, Warrener AG, Deacon T, Ellison PT, Pontzer H. 2012. Metabolic hypothesis for human altriciality. Proc Natl Acad Sci USA 109:15212–15216.

Ellison P. 2008. Energetics, reproductive ecology, and human evolution. PaleoAnthropology: 172–200.

Esteve-Altava B. 2015. Systematic review of the research on morphological modularity. bioRxiv:027144.

Fischer B, Mitteroecker P. 2015. Covariation between human pelvis shape, stature, and head size alleviates the obstetric dilemma. Proc Natl Acad Sci USA 112:5655–5660.

Gingerich PD. 1972. The development of sexual dimorphism in the bony pelvis of the squirrel monkey. Anat Rec 172:589–595.

Gonzalez PN, Oyhenart EE, Hallgrimsson B. 2011. Effects of environmental perturbations during postnatal development on the phenotypic integration of the skull. J Exp Zool B Mol Dev Evol 316B:547–561.

González PN, Hallgrimsson B, Oyhenart EE. 2011. Developmental plasticity in covariance structure of the skull: effects of prenatal stress. J Anat 218:243–257.

Goswami A, Binder WJ, Meachen J, O'Keefe FR. 2015. The fossil record of phenotypic integration and modularity: A deep-time perspective on developmental and evolutionary dynamics. Proc Natl Acad Sci USA 112:4891–4896.

Goswami A, Polly PD. 2010. The influence of modularity on cranial morphological disparity in carnivora and primates (Mammalia). PLoS ONE 5:e9517.

Goswami A, Smaers JB, Soligo C, Polly PD. 2014. The macroevolutionary consequences of phenotypic integration: from development to deep time. Philos Trans R Soc B 369:20130254–20130254.

Grabowski MW, Polk JD, Roseman CC. 2011. Divergent patterns of integration and reduced constraint in the human hip and the origins of bipedalism. Evolution 65:1336–1356.

Grabowski MW. 2012. Hominin obstetrics and the evolution of constraints. Evol Biol 40:57–75.

Gruss LT, Schmitt D. 2015. The evolution of the human pelvis: changing adaptations to bipedalism, obstetrics and thermoregulation. Philos Trans R Soc Lond, B, Biol Sci 370:20140063–20140063.

Hall BK. 2012. Evolutionary Developmental Biology (Evo-Devo): Past, Present, and Future. Evo Edu Outreach 5:184–193.

Hallgrimsson B, Jamniczky H, Young NM, Rolian C, Parsons TE, Boughner JC, Marcucio RS. 2009. Deciphering the palimpsest: studying the relationship between morphological integration and phenotypic covariation. Evol Biol 36:355–376.

Hansen TF, Houle D. 2008. Measuring and comparing evolvability and constraint in multivariate characters. Journal of Evolutionary Biology 21:1201–1219.

Hansen TF. 2003. Is modularity necessary for evolvability? Remarks on the relationship between pleiotropy and evolvability. Biosystems 69:83–94.

Harrison MS, Ali S, Pasha O, Saleem S, Althabe F, Berrueta M, Mazzoni A, Chomba E, Carlo WA, Garces A, Krebs NF, Hambidge K, Goudar SS, Dhaded SM, Kodkany B, Derman RJ, Patel A, Hibberd PL, Esamai F, Liechty EA, Moore JL, Koso-Thomas M, McClure EM, Goldenberg RL. 2015. A prospective population-based study of maternal, fetal, and neonatal outcomes in the setting of prolonged labor, obstructed labor and failure to progress in low- and middle-income countries. Reprod Health 12 Suppl 2:S9.

Hendrikse JL, Parsons TE, Hallgrimsson B. 2007. Evolvability as the proper focus of evolutionary developmental biology. Evol Dev 9:393–401.

Hofmeyr GJ. 2004. Obstructed labor: using better technologies to reduce mortality. Int J Gynaecol Obstet 85 Suppl 1:S62–72.

Huseynov A, Ponce de León MS, Zollikofer CPE. (*accepted*). Development of modular organization in the chimpanzee pelvis. Anat Rec.

Huseynov A, Zollikofer CPE, Coudyzer W, Gascho D, Kellenberger C, Hinzpeter R, Ponce de León MS. 2016. Developmental evidence for obstetric adaptation of the human female pelvis. Proc Natl Acad Sci USA 113:5227–5232.

Iguchi T, Irisawa S, Fukazawa Y, Uesugi Y, Takasugi N. 1989. Morphometric analysis of the development of sexual dimorphism of the mouse pelvis. Anat Rec 224:490–494.

Jasienska G, Thune I, Ellison PT. 2006. Fatness at birth predicts adult susceptibility to ovarian suppression: an empirical test of the Predictive Adaptive Response hypothesis. Proc Natl Acad Sci USA 103:12759–12762.

Kitano H. 2004. Biological robustness. Nat Rev Genet 5:826–837.

Klingenberg CP, Duttke S, Whelan S, KIM M. 2012. Developmental plasticity, morphological variation and evolvability: a multilevel analysis of morphometric integration in the shape of compound leaves. Journal of Evolutionary Biology 25:115–129.

Klingenberg CP, Mebus K, Auffray JC. 2003. Developmental integration in a complex morphological structure: how distinct are the modules in the mouse mandible? Evol Dev 5:522–531.

Klingenberg CP, Zaklan SD. 2000. Morphological integration between development compartments in the Drosophila wing. Evolution 54:1273.

Klingenberg CP. 2004. Integration and modularity of quantitative trait locus effects on geometric shape in the mouse mandible. Genetics 166:1909–1921.

Klingenberg CP. 2005. Developmental constraints, modules, and evolvability. In: Hallgrimsson B, Hall BK, editors. Themes on Variation. San Diego: Academic Press. p 219–247.

Klingenberg CP. 2008. Morphological integration and developmental modularity. Annu Rev Ecol Evol Syst 39:115–132.

Klingenberg CP. 2009. Morphometric integration and modularity in configurations of landmarks: tools for evaluating a priori hypotheses. Evol Dev 11:405–421.

Klingenberg CP. 2010. Evolution and development of shape: integrating quantitative approaches. Nat Rev Genet 11:623–635.

Klingenberg CP. 2014. Studying morphological integration and modularity at multiple levels: concepts and analysis. Philos Trans R Soc Lond, B, Biol Sci 369:20130249.

Kuratani S. 2009. Modularity, comparative embryology and evo-devo: Developmental dissection of evolving body plans. Developmental Biology 332:61–69.

LaVelle M. 1995. Natural selection and developmental sexual variation in the human pelvis. Am J Phys Anthropol 98:59–72.

Leutenegger W. 1970. Relation between newborn size and sex dimorphism of pelvis in simian primates. Folia Primatol 12:224–235.

Leutenegger W. 1974. Functional aspects of pelvic morphology in simian primates. J Hum Evol 3:207–222.

Lewton KL. 2012. Evolvability of the primate pelvic girdle. Evol Biol 39:126–139.

Lovejoy CO. 2005. The natural history of human gait and posture. Gait & Posture 21:95–112.

Martin JA, Hamilton BE, Osterman MJ, Curtin SC, Matthews TJ. 2015. Births: final data for 2013. Natl Vital Stat Rep 64:1–65.

McClure EM, Goldenberg RL, Bann CM. 2007. Maternal mortality, stillbirth and measures of obstetric care in developing and developed countries. Int J Gynaecol Obstet 96:139–146.

McGuigang K. 2006. Studying phenotypic evolution using multivariate quantitative genetics. Mol Ecol 15:883–896.

McPherson FJ, Chenoweth PJ. 2012. Mammalian sexual dimorphism. Animal Repr Sci 131:109–122.

Mitteroecker P, Bookstein F. 2008. The evolutionary role of modularity and integration in the hominoid cranium. Evolution 62:943–958.

Montagu A. 1961. Neonatal and infant immaturity in man. JAMA 178:56–57.

Parsch J, Ellegren H. 2013. The evolutionary causes and consequences of sex-biased gene expression. Nat Rev Genet 14:83–87.

Portmann A. 1941. Die Tragzeiten der Primaten und die Dauer der Schwangerschaft beim Menschen: ein Problem der vergleichenden Biologie. [Gestation length in primates and humans: a topic of comparative biology.]. Rev Suisse Zool 48:511–518.

Rosenberg KR. 1992. The evolution of modern human childbirth. Am J Phys Anthropol 35:89–124.

Scheuer L, Black S, Cunningham C. 2000. Developmental juvenile osteology. London: Academic Press.

Schultz AH. 1949. Sex differences in the pelves of primates. Am J Phys Anthropol 7:401–423.

Smilde AK, Kiers HAL, Bijlsma S, Rubingh CM, van Erk MJ. 2009. Matrix correlations for high-dimensional data: the modified RV-coefficient. Bioinformatics 25:401–405.

Stone PK. 2016. Biocultural perspectives on maternal mortality and obstetrical death from the past to the present. Am J Phys Anthropol 159:S150–S171.

Striedter GF. 2005. Principles of brain evolution (Sinauer, Sunderland, MA).

Tague RG. 1995. Variation in pelvic size between males and females in nonhuman anthropoids. Am J Phys Anthropol 97:213–233.

Tague RG. 2003. Pelvic sexual dimorphism in a metatherian, Didelphis Virginiana: implications for eutherians. Journal of Mammalogy 84:1464–1473.

Tague RG. 2005. Big-bodied males help us recognize that females have big pelves. Am J Phys Anthropol 127:392–405.

Uesugi Y, Taguchi O, Noumura T, Iguchi T. 1992. Effects of sex steroids on the development of sexual dimorphism in mouse innominate bone. Anat Rec 234:541–548.

Wagner GP, Pavlicev M, Cheverud JM. 2007. The road to modularity. Nat Rev Genet 8:921–931.

Wagner GP, Zhang J. 2011. The pleiotropic structure of the genotype–phenotype map: the evolvability of complex organisms. Nat Rev Genet 12:204–213.

Wagner GP. 1990. A comparative study of morphological integration in Apis mellifera (Insecta, Hymenoptera). Journal of Zoological Systematics and Evolutionary Research 28:48–61.

Warrener AG, Lewton KL, Pontzer H, Lieberman DE. 2014. A wider pelvis does not increase locomotor cost in humans, with implications for the evolution of childbirth. PLoS ONE 10:e0118903–e0118903.

Washburn SL. 1960. Tools and Human Evolution. Sci Am 203:62–75.

Weiner S, Monge J, Mann A. 2008. Bipedalism and parturition: an evolutionary imperative for Cesarean delivery? Clinics Perinatol 35:469–478.

Wells JCK, DeSilva JM, Stock JT. 2012. The obstetric dilemma: an ancient game of Russian roulette, or a variable dilemma sensitive to ecology? Am J Phys Anthropol 149:40–71.

Wells JCK. 2015. Between Scylla and Charybdis: renegotiating resolution of the “obstetric dilemma” in response to ecological change. Philos Trans R Soc Lond, B, Biol Sci 370:20140067–20140067.

Williams FL, Orban R. 2007. Ontogeny and phylogeny of the pelvis in Gorilla, Pongo, Pan, Australopithecus and Homo. Folia Primatol 78:99–117.

Williams TM, Carroll SB. 2009. Genetic and molecular insights into the development and evolution of sexual dimorphism. Nat Rev Genet 10:797–804.

Willmore KE, Leamy L, Hallgrimsson B. 2006. Effects of developmental and functional interactions on mouse cranial variability through late ontogeny. Evol Dev 8:550–567.

Wilson EB. 1894. The embryological criterion of homology. Biol Lect MBL, Woods Hole: 101–124.

Wittman AB, Wall LL. 2007. The evolutionary origins of obstructed labor: bipedalism, encephalization, and the human obstetric dilemma. Obstetr Gynecol Survey 62:739–748.

Young NM, Wagner GP, Hallgrimsson B. 2010. Development and the evolvability of human limbs. Proc Natl Acad Sci USA 107:3400–3405.

Zelditch ML, Mezey J, Sheets HD, Lundrigan BL, Garland T. 2006. Developmental regulation of skull morphology II: ontogenetic dynamics of covariance. Evol Dev 8:46–60.

Zelditch ML, Wood AR, Bonett RM, Swiderski DL. 2008. Modularity of the rodent mandible: Integrating bones, muscles, and teeth. Evol Dev 10:756–768.

Zollikofer CPE, Scherrer M, Ponce de León MS. (*accepted*). Development of pelvic sexual dimorphism in hylobatids: testing the obstetric constraints hypothesis. Anat Rec.

Chapter 1

Developmental evidence for obstetric adaptation of the human female pelvis

Reference: *Proceedings of the National Academy of Sciences USA* 113.19 (2016): 5227-5232

Abstract

The bony pelvis of adult humans exhibits marked sexual dimorphism, which is traditionally interpreted in the framework of the "obstetrical dilemma" hypothesis: Giving birth to large-brained/ large-bodied babies requires a wide pelvis, whereas efficient bipedal locomotion requires a narrow pelvis. This hypothesis has been challenged recently on biomechanical, metabolic, and biocultural grounds, so that it remains unclear which factors are responsible for sex-specific differences in adult pelvic morphology. Here we address this issue from a developmental perspective. We use methods of biomedical imaging and geometric morphometrics to analyze changes in pelvic morphology from late fetal stages to adulthood in a known-age/known-sex forensic/clinical sample. Results show that, until puberty, female and male pelves exhibit only moderate sexual dimorphism and follow largely similar developmental trajectories. With the onset of puberty, however, the female trajectory diverges substantially from the common course, resulting in rapid expansion of obstetrically relevant pelvic dimensions up to the age of 25-30 y. From 40 y onward females resume a mode of pelvic development similar to males, resulting in significant reduction of obstetric dimensions. This complex developmental trajectory is likely linked to the pubertal rise and premenopausal fall of estradiol levels and results in the obstetrically most adequate pelvic morphology during the time of maximum female fertility. The evidence that hormones mediate female pelvic development and morphology supports the view that solutions of the obstetrical dilemma depend not only on selection and adaptation but also on developmental plasticity as a response to ecological/nutritional factors during a female's lifetime.

Key words: pelvis, development, evolution, obstetric dilemma, sex steroids

INTRODUCTION

Females and males of most mammalian species differ in various morphological characteristics, such as the size and shape of the body as a whole and of soft and hard tissue structures (McPherson and Chenoweth, 2012). Sex-specific differences are also well documented in humans and nonhuman primates, particularly in the pelvis, and various hypotheses have been proposed to explain how pelvic sexual dimorphism evolves and develops (Schultz, 1949; Leutenegger, 1970; Gingerich, 1972; Rosenberg, 1992; LaVelle, 1995; Tague, 1995; Lovejoy, 2005; Wittman and Wall, 2007; Gruss and Schmitt, 2015; Wells, 2015). There is general agreement that the female pelvis is under obstetric selection to be adequately capacious for childbirth. However, the exact nature of selective pressures and developmental mechanisms yielding female and male pelvic phenotypes is still largely unknown, and whether obstetric adaptations involve trade-offs with other aspects of pelvic function, such as locomotor efficiency and abdominal stabilization, continues to be debated (Dunsworth et al., 2012; Warrener et al., 2014).

One key hypothesis discussed in this context is Washburn's obstetrical dilemma (OD) (Washburn, 1960). In its original form (Washburn, 1960), the OD hypothesis posits a conflict between the evolution of bipedal locomotion (selection for biomechanically efficient, narrow pelves) and of large brains (selection for large-brained neonates, and obstetrically efficient, wide pelves). According to Washburn, the dilemma is "solved by delivery of the fetus at a much earlier stage of development" (ref. (Washburn, 1960), p. 74) than in our closest living relatives the great apes. Although the OD hypothesis thus primarily seeks to explain the early timing of birth and human altriciality (Portmann, 1941), it also provides an explanation for pelvic sexual dimorphism: Selection favored wider female pelves to reduce the risks involved in birthing large-brained/large-bodied babies, but did so at the expense of locomotor efficiency (Schultz, 1949; Rosenberg, 1992; LaVelle, 1995). According to this hypothesis, the tight fit between the neonate head and maternal pelvis (obstetric constraints) and the high prevalence of obstructed labor in humans (Hofmeyr, 2004; McClure et al., 2007; Harrison et al., 2015) reflect a trade-off between obstetric and locomotor selection pressures on the female pelvis.

Over the past years, the OD hypothesis has been reexamined extensively and has been challenged on various grounds (Kurki, 2011; Dunsworth et al., 2012; Warrener et al., 2014; Brown, 2015; Dunsworth and Eccleston, 2015; Gruss and Schmitt, 2015; Wells, 2015; Stone, 2016). The energetics of gestation and growth (EGG) hypothesis (Ellison, 2008; Dunsworth et

al., 2012; Dunsworth and Eccleston, 2015) provides a new perspective, proposing that the timing of birth is constrained by the limited metabolic output of the mother rather than by spatial limitations of her pelvis. Furthermore, inverse-dynamics models and experimental data indicate that a wide pelvis does not reduce bipedal locomotor efficiency (Dunsworth et al., 2012; Warrener et al., 2014). Because these studies effectively falsify a major tenet of the OD, the tight fit between neonate head and maternal pelvis and the high prevalence of obstructed labor require alternative explanations. It has been proposed that solutions to the OD can be renegotiated (Wells, 2015) through ecologically mediated phenotypic plasticity of pelvic and fetal dimensions but that rapid changes in environmental conditions may result in fetopelvic mismatch (Ellison, 2008; Gruss and Schmitt, 2015; Wells, 2015). Obstructed labor thus would be a consequence of a mismatch between maternal and neonate developmental plasticity (Jasienska et al., 2006a; Ellison, 2008) or of biocultural factors (Stone, 2016) rather than an evolutionary trade-off between obstetrics and locomotion.

On the other hand, indirect evidence for gene-mediated constraints on fetopelvic proportions comes from a recent study demonstrating that mothers with large heads (who, because of the high heritability of cranial dimensions, are likely to have large-headed babies) tend to have obstetrically more favorable pelvic dimensions than mothers with small heads (Fischer and Mitteroecker, 2015). However, correlation between head size and these pelvic dimensions is also present in males (Fischer and Mitteroecker, 2015), although the correlation is less pronounced than in females. Thus the extent to which the observed patterns represent female-specific obstetric selection, sex-neutral genetic-developmental integration, and/or developmental plasticity remains to be clarified.

Somatic sexual dimorphism such as that of the pelvis is largely the result of hormonally regulated sex-biased gene expression (Williams and Carroll, 2009; Parsch and Ellegren, 2013). Previous research on the development of pelvic sexual dimorphism in mammals reveals a wide variety of modes of divergence. Several studies in rodents (Bernstein and Crelin, 1967; Iguchi et al., 1989; Uesugi et al., 1992) suggest that the pubertal developmental trajectory of the male pelvis deviates from the prepubertal mode shared by both sexes, presumably under testosterone influence. This hypothesis also was proposed for humans and for other primates (Tague, 1995; 2005). Other studies suggest that estrogen effects are crucial for female pelvic development during puberty (Gingerich, 1972; Berdnikovs et al., 2006).

Here we reevaluate the evidence for the OD and alternative hypotheses from a developmental perspective. We propose the developmental obstetric dilemma (DOD)

hypothesis, which posits that pelvic morphology reflects changing obstetric needs (versus other, possibly locomotor, needs) during a female's life time. Given that female fertility (measured as birth rate per year) reaches its peak around the age of 25-30 y (Bamberg Migliano et al., 2007; Martin et al., 2015) and declines toward 40-45 y, the DOD hypothesis predicts that (i) sex-specific differences in human pelvic morphology become pronounced after puberty; (ii) the female pelvis reaches its obstetrically most adequate morphology around the age of highest fertility; (iii) during postmenopausal life, the female pelvis reverts to an obstetrically less adequate morphology, which is probably most adequate for locomotion and other functions; (iv) the male pelvis does not show these developmental changes.

To test the DOD hypothesis, we track pelvic development from late fetal stages to late adulthood in an anonymized known-age and known-sex forensic/clinical sample (n = 275) (Materials and Methods). The bony elements constituting the pelvis fuse relatively late during development, so that the 3D morphology of the pelvis critically depends on the presence of ligaments and other soft tissue structures. Thus computed tomography (CT) was used to analyze pelvic morphology in the context of surrounding tissues. Pelvic size and shape were quantified with a total number of k = 377 3D anatomical landmarks. Sex-specific patterns of shape variation during development were analyzed and visualized with methods of geometric morphometrics (GM) (Materials and Methods).

RESULTS

Fig. 1 graphs sex-specific trajectories of pelvic shape change along the first three principal components (PCs) of shape space and visualizes actual pelvic morphologies at six developmental stages from birth to late adulthood. Fig. 2 graphs the temporal course of pelvic size and shape change. Pelvic growth trajectories (i.e., age-related increase in size) of females and males are largely similar (Fig. 2A). PC1, which accounts for 45% of the total shape variation in the sample, captures a shared male/female mode of shape change (Fig. 2B). It is closely correlated with increase in size (females: r^2 = 0.91; males: r^2 = 0.92) and thus represents ontogenetic allometry (i.e., growth-related change in shape). PC2 (accounting for 11% of the total shape variation) and PC3 (accounting for 10%) track the development of sex-specific differences in pelvic shape. Female and male trajectories diverge early during infancy (see PC3 in Figs. 1B and 2D) and exhibit further separation during late childhood (see PC2 in Figs. 1A and 2C), resulting in moderate but significant sexual dimorphism at the onset of puberty (age 10-12 y) (Fig. 2E and Table S1). These findings confirm previous studies on the

early development of sexual dimorphism in pelvic substructures (Boucher, 1957; LaVelle, 1995; Wilson et al., 2014; Bilfeld et al., 2015).

From the age of ~10 y onward the female trajectory changes its direction substantially, whereas the male trajectory continues its earlier course (Figs. 1B and 2D and Table S2). Around the age of 40-45 y, the female trajectory changes again, assuming a direction that is largely parallel to that of the male trajectory (Figs. 1B and 2D and Table S2). Overall, the mean difference between male and female pelvic shapes (i.e., pelvic sexual dimorphism) reaches a peak during early adulthood and is reduced during later adult life (Fig. 2E), as has been observed earlier (Walker, 2005).

Fig. 3 visualizes the corresponding modes of sex-specific change in pelvic shape (for additional visualizations and animations, see Fig. S1 and Movies S1-S6). In males, pelvic development from ~15 y to young adulthood (~25 y) is characterized by a relative reduction of anteroposterior and superoinferior dimensions (Fig. 3A and Movies S1-S3). During this process the superior portion of the sacrum is tilted ventrally, and the greater sciatic notch becomes narrower. Development of the female pelvis during the same period (~15 to ~25 y) (Fig. 3A and Movies S1-S3) differs substantially from the male mode (Table S2). The sacrum and the ischiopubic region undergo substantial eversion, and the iliac blades undergo inversion. As a result, the anteroposterior dimensions of the pelvic midplane and outlet and the transverse dimensions of the pelvic inlet and outlet become larger (Figs. 3A and 4). Also, the subpubic angle (Fig. 4A) and the angle formed by the greater sciatic notch become wider. As an additional effect, the biacetabular distance becomes relatively wider, and bi-iliac width is relatively reduced (Fig. 4D). Overall, these developmental changes result in a wide, obstetrically favorable birth canal.

It should be noted that the contrasting patterns of male and female pelvic development from puberty to young adulthood visualized here (Fig. 3) were described in part by Coleman (Coleman, 1969), who used anteroposterior radiographs and a precursor of GM methods to track pelvic development in a longitudinal sample of the Fels Longitudinal Study begun in 1929. Using the same sample, a multivariate analysis of linear pelvic dimensions yielded similar results (LaVelle, 1995).

Around the age of 40-45 y, the female pelvis resumes a mode of shape change which is similar to that of males (Figs. 2 and 3B, Table S2, and Movies S4-S6). This pattern largely corresponds to that present in ~15- to 25-y-old males (Table S2). Anteroposterior and superoinferior pelvic dimensions become relatively shorter. Interspinous distance is reduced,

and the iliac blades become more everted. At the same time, the subpubic angle and the greater sciatic notch become narrower, as observed earlier (Tague, 1994; Walker, 2005). In females, this mode of shape change results in a significant reduction of obstetrically relevant birth canal dimensions (Fig. 4). Although our data show that female and male trajectories diverge substantially before the attainment of sexual maturity, we further assessed whether maternity (pregnancy and lactation) has an influence on the development of pelvic shape, as reported, for example, in mice (Schutz et al., 2009). To this end, we analyzed pelvic shape variation in a subsample of females with known maternity status. Results show that pelvic morphologies of parous and nonparous females (both groups with an average age of 34 y) are statistically indistinguishable (Figs. 1, 2, and 4 and Table S3).

DISCUSSION

The findings presented here provide support for the DOD hypothesis along several lines of evidence: With the onset of puberty, the female developmental trajectory diverges substantially from the childhood trajectory, whereas the male trajectory essentially continues its earlier course (Table S2). As a result, the female pelvis attains its obstetrically most favorable morphology around the age of 25-30 y, i.e., at the age of highest fertility (Bamberg Migliano et al., 2007; Martin et al., 2015). Furthermore, pelves in postmenopausal women assume a developmental mode that is largely similar to that of males (Table S2), with the effect that the birth canal becomes constricted.

Sexual dimorphism is largely the outcome of the sex-biased expression of autosomal genes, which in turn are regulated by sex-specific hormone levels and/or differential hormone receptor sensitivity (Williams and Carroll, 2009; Callewaert et al., 2010; Parsch and Ellegren, 2013). In mice, for example, testicular-feminized males (i.e., males lacking androgen receptors) and gonadectomized males develop female-like pelvic morphologies, whereas experimental administration of androgens to females induces male-like morphologies (Bernstein and Crelin, 1967; Iguchi et al., 1989; Uesugi et al., 1992). In humans, direct evidence for hormone-mediated sex-specific bone remodeling patterns of the pelvis is not yet available. Nevertheless, studies on long bone morphology indicate that sexual skeletal dimorphism develops via complex interactions between sex-specific steroid hormone levels, sex-biased gene expression, and gender differences in sensitivity to bone-loading conditions and to hormones such as the growth hormone/insulin-like growth factor 1 (IGF1) axis (Callewaert et al., 2010; Devlin, 2011; Khosla et al., 2012; Oury, 2012).

Our data on pelvic development thus may be tentatively linked to hormonal change in the following way: The early differentiation of sex-specific pelvic shape might be related to the transient hormonal "minipuberty" during the first year of life (Ober et al., 2008). Directional changes in developmental trajectories during the prepubertal stage (see PC2 in Figs. 1 and 2) may be linked to the increase in IGF1 (Cole et al., 2015). The substantial divergence of the female developmental trajectory during puberty (see PC3 in Figs. 1 and 2) is most likely caused by the sex-specific rise in estradiol levels, triggering a change in pelvic bone-remodeling patterns (Ober et al., 2008; Cole et al., 2015). We further hypothesize that the obstetrically favorable shape of the female pelvis is maintained by the high estradiol levels during the time of maximum fertility and that the significant reduction of obstetric dimensions from age 40 y onwards is related to the premenopausal decline in estradiol levels (Ober et al., 2008). Further testing of these hypotheses will require combined hormonal, morphometric, and life-history data.

Short-term hormonal effects of pregnancy and birthing on sacroiliac and pubic joint motility, as well as the effects of body position on pelvic obstetric dimensions, are well documented (Elden et al., 2009; Dehghan et al., 2014; Reitter et al., 2014). However, the age-matched sample of parous and nonparous individuals studied here does not provide evidence for major effects of pregnancy and lactation on the development of female-specific pelvic morphology. The weak or absent influence of the growing fetus on its mother's pelvic development thus might be one of the reasons for fetopelvic disproportion and obstructed labor.

What are the possible evolutionary implications of hormone-mediated development of pelvic obstetric dimensions? Our data suggest that estrogens have a strong influence on the development of the female pelvic morphology during puberty. At the same time, they imply a weak-to-absent influence of androgens on human male-specific pelvic development during puberty, although such influences are well documented in other developmental modules such as the face (Verdonck et al., 1999; Emery Thompson et al., 2012; Lefevre et al., 2013). As proposed earlier (Gingerich, 1972), testosterone may be involved in the maintenance of the human male pelvic morphology throughout development but does not lead to developmental divergence during puberty.

Referring to recent hypotheses on ecological and nutritional factors influencing the OD (Ellison, 2008), we postulate that the female pelvis is highly sensitive to *in-vivo* modification via environmental modulation of hormone levels. As proposed in the framework of human

reproductive ecology (Ellison, 2008), and specifically by the predictive adaptive response hypothesis (Gluckman et al., 2005), an individual's developmental trajectory may be modified according to the environmental conditions "expected" (i.e., likely) during its reproductive phase. The relationship between the term fetus and its mother's pelvic morphology thus might be mediated via estrogen levels, which in turn are sensitive to the current state of ecological parameters relevant for prenatal and postnatal development.

Based on the evidence presented here, the DOD hypothesis predicts that higher levels of estrogen in females during puberty/ young adulthood result in development/maintenance of an obstetrically more favorable pelvic morphology, which facilitates the delivery of larger babies. The relationships between sex hormone levels, maternal pelvic morphology, fetal size, and pre/postnatal development are complex and are topics of intense research (Ellison, 2008; Gruss and Schmitt, 2015; Moffett et al., 2015; Trevathan, 2015; Wells, 2015). For example, it has been shown that females who are large at birth have comparatively high estradiol levels during adulthood (Jasienska et al., 2006b). Estradiol levels also are influenced by diet and nutritional status (Woods et al., 1996; Bentley et al., 1998; Aubertin-Leheudre et al., 2008) and are good predictors of fertility (Lipson and Ellison, 1996), and, likely, of adult pelvic shape (this study). Given this network of cause and effect, there is ample opportunity for *in-vivo* feedback between ecological/nutritional conditions, sex hormone levels, neonate size, and maternal body and pelvic dimensions. For instance, the observed within-subject correlation of pelvic obstetric dimensions with body size and head size (Fischer and Mitteroecker, 2015) could partly be an effect of higher estradiol levels in larger females (Jasienska et al., 2006b), resulting in obstetrically more favorable morphologies of their pelves.

Evidence for estradiol-mediated female-specific patterns of pelvic development in humans (this study), nonhuman primates (Gingerich, 1972), and rodents (Berdnikovs et al., 2006) may indicate either evolutionarily conserved or convergent developmental mechanisms of sexual dimorphism in mammalian species exhibiting obstetric constraints. Because pelvic width does not correlate with locomotor efficiency (Warrener et al., 2014), the question remains why the female pelvis did not evolve and/or does not develop wider obstetric dimensions, which would significantly reduce the existing perinatal risks for the mother and the infant. Pelvic size might be limited by nutritional conditions, which impose global constraints on body growth (Wells, 2015). The high prevalence of obstructed labor thus might largely represent a modern phenomenon resulting from a mismatch between secular increases

in neonate size and maternal size. However, additional factors must be advanced to explain both the limited expansion of female pelvic dimensions during pubertal development and the reversal to more constricted dimensions during postmenopausal development. One conspicuous feature of the female expansion/reversal pattern is the widening/shortening of the distance between the ischial spines (Figs. 3 and 4C). The ischial spines are larger in humans than in nonhuman primates, because they constitute important attachment sites for the ligaments and fasciae forming the pelvic floor (Abitbol, 1988). The spines and associated ligamentous structures substantially constrain the birth canal dimensions, but they provide support for the abdominal and pelvic organs and contribute to sagittal stabilization of the sacrum (Abitbol, 1988; Ashton-Miller and DeLancey, 2007; Tardieu et al., 2013). Intraabdominal hydrostatic pressure reaches high peak values during walking and running (Grillner et al., 1978), and although that pressure positively influences the stability of the lumbar spine, it results in high strains in the pelvic floor (Hodges et al., 2005). Pelvic floor strains thus might represent a limiting factor of birth canal dimensions, and this hypothesis receives support from the observation that wider dimensions correlate with a higher prevalence of pelvic floor disorders (Handa et al., 2003).

Based on these considerations, we hypothesize that the evolutionary and developmental dilemma of the female pelvis reflects a trade-off between obstetrics and abdominopelvic stability. During a female's lifetime, the dilemma is alleviated first in one direction, by widening the birth canal during the time of highest fertility, and then in the other, by restricting its dimensions during postmenopausal life. Although our data provide support for the obstetric side of the dilemma, testing its locomotor side will require a shift of focus from bipedal locomotor economy toward locomotion-related abdominopelvic stability. It remains to be clarified whether the female postmenopausal reversal to more constricted birth canal dimensions evolved under selective pressures acting on postreproductive life (Hawkes et al., 1998) or whether it represents a proximate effect of reduced estrogen levels and developmental plasticity. Also, when during human evolution the developmental mode of the female pelvis started to diverge from the male mode remains to be investigated.

MATERIALS AND METHODS

The study is based on an anonymized known-age and known-sex forensic/clinical sample of nonsymptomatic humans (n = 275) ranging from late fetal stages to late adulthood (Table S4).

Data sources are the Collections of the Anthropological Institute, the Virtopsy® database of the Institute of Forensic Medicine of the University of Zurich, Children's Hospital of Zurich, the Institute of Diagnostic and Interventional Radiology of the University of Zurich, the digital autopsy database of the Catholic University of Leuven, Belgium (KU Leuven), and clinical datasets freely available from the OsiriX web-page (www.osirix-viewer.com).
Volumetric data were acquired with medical CT (beam collimation 128 × 0.6 mm; in-plane pixel size 0.2 × 0.2-0.7 × 0.7 mm2, slice increment 0.2-1.0 mm). 3D surface models of the bony pelvis were generated with Avizo 6.3.1 (FEI Visualization Sciences Group), and subsequent mesh cleaning was performed with Geomagic XOS (3D Systems). Only well-preserved pelves were used. Several specimens (n = 9 with ages <8 y, n = 5 with ages 12-15 y, and n = 14 with ages 50-80 y) required minor virtual reconstruction (Zollikofer and Ponce de León, 2005; Ponce de León et al., 2008).

The shape of the pelvis was quantified with a total number of k = 377 3D anatomical landmarks, which denote locations of biological and/or geometric homology among specimens of the sample. These comprise fixed landmarks (LMs) (k_f = 63), curve semi-landmarks (SLMs) (k_c = 90), and surface SLMs (k_s = 224) (Fig. S2 and Tables S5 and S6). The fixed-LM set comprises 14 LM pairs, which eventually fuse during pelvic development. For geometric morphometric analyses, the mean position was calculated for each pair, resulting in k_f = 49 fixed LMs and a total of k = 363 LMs. Surface SLMs were generated from an arbitrary specimen's point cloud, and iterative SLM sliding procedures were applied as described in ref. (Gunz et al., 2005). SLM sliding was performed relative to the symmetrized mean configuration, using the minimum bending energy criterion. These data were submitted to generalized Procrustes analysis. All procedures were performed with the R package Morpho, version 2.3.1.1 (Schlager, 2016).

Principal component analysis was used to reduce the dimensionality of shape space and visualize major patterns of shape variation in the sample. Sex-specific moving averages of PC scores, centroid size, and angular and linear pelvic dimensions were calculated to explore patterns of morphological change along developmental trajectories. To test for differences between group-specific pelvic shapes (Tables S1 and S3), Procrustes ANOVA was performed using the R package geomorph, version 3.0.0-1 (Adams et al., 2015). Directions of developmental trajectories through shape space were compared using the methods proposed in ref. (Collyer et al., 2015) (Table S2).

ACKNOWLEDGEMENTS

We thank Michael Thali, Lars Ebert, Steffen Ross, and Wim Develter for preparing the anonymized forensic data and Stefan Schlager and Emma Sherratt for their suggestions regarding R packages Morpho and geomorph, respectively. We also thank the three anonymous reviewers for their constructive comments and suggestions. This study was supported by Swiss National Science Foundation Grant 31003A_135470/1 (to C.P.E.Z.), and the A. H. Schultz Foundation.

Figures and Tables

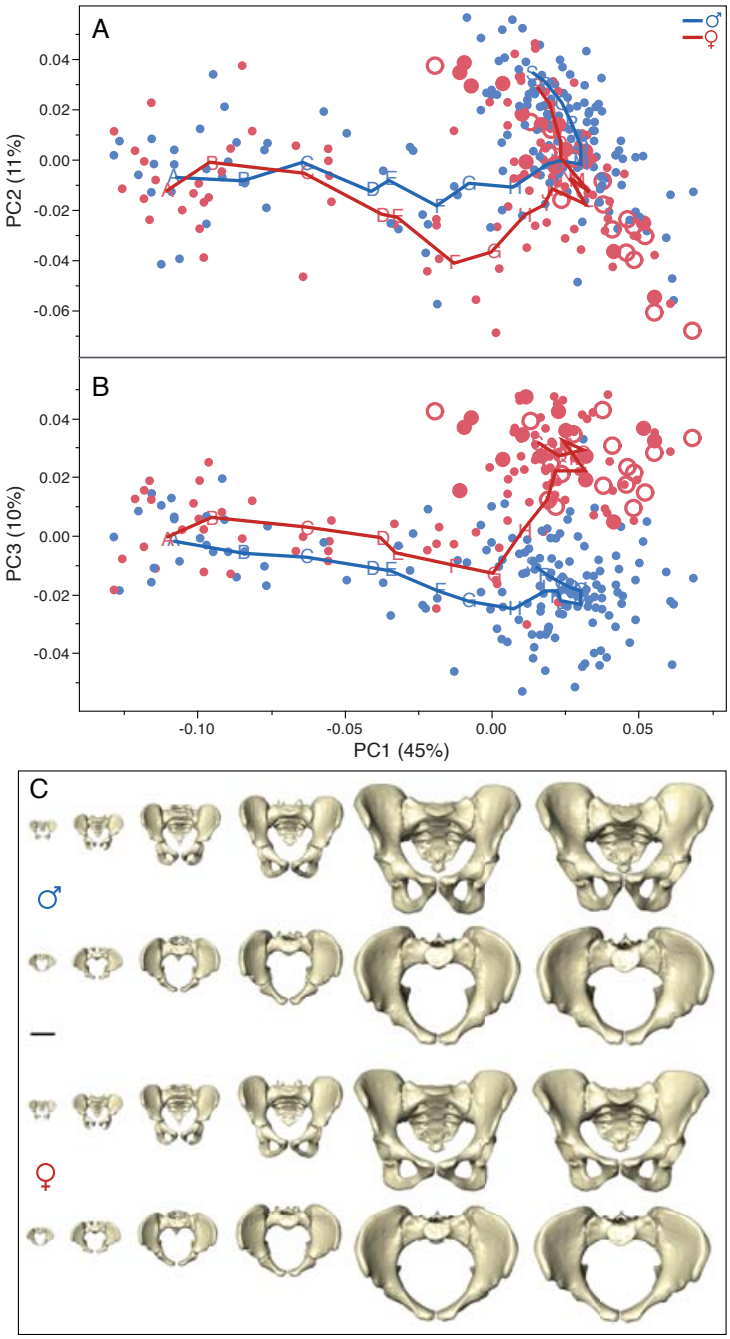

Fig. 1. Developmental changes in human pelvic morphology from late fetal stages to late adulthood. (A and B) Bivariate plots of shape variation along PC1 (45% of total sample variation) and PC2 (11%) (A), and along PC1 and PC3 (10%) (B). Red symbols represent females; dots indicate immature or unknown parity status; filled and open circles indicate parous and non-parous status, respectively. Blue symbols represent males. Points A-S denote moving-average positions calculated at the ages indicated in Fig. 2. (C) Anterior and superior views of sex-specific pelvic mean shapes at birth and around 2, 6, 13, 25, and 80 y. (Scale bar, 5 cm.)

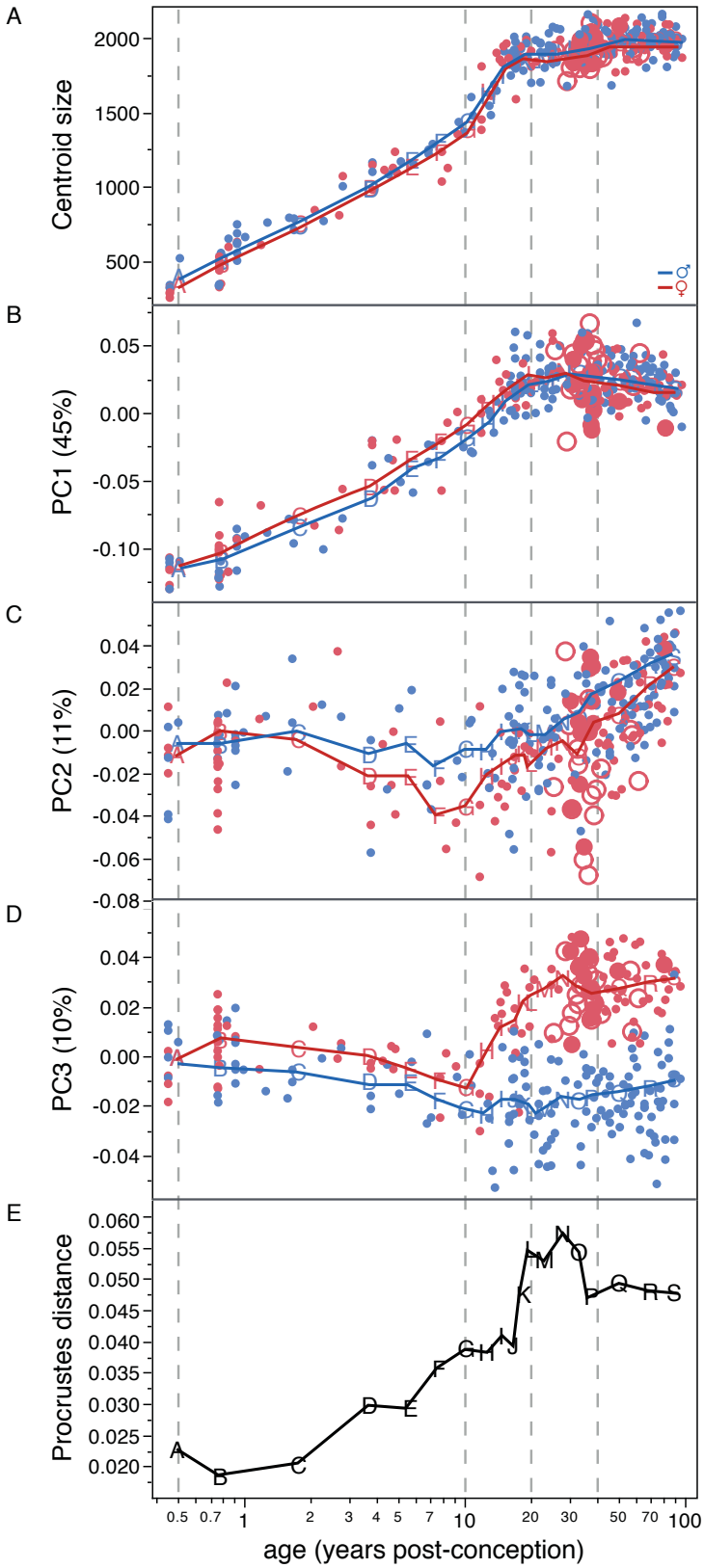

Fig. 2. Age-related change in human pelvic size (A), shape (B-D), and shape dimorphism (E). Colors and symbols are as in Fig. 1; note that the age axis is scaled logarithmically in postconception years.

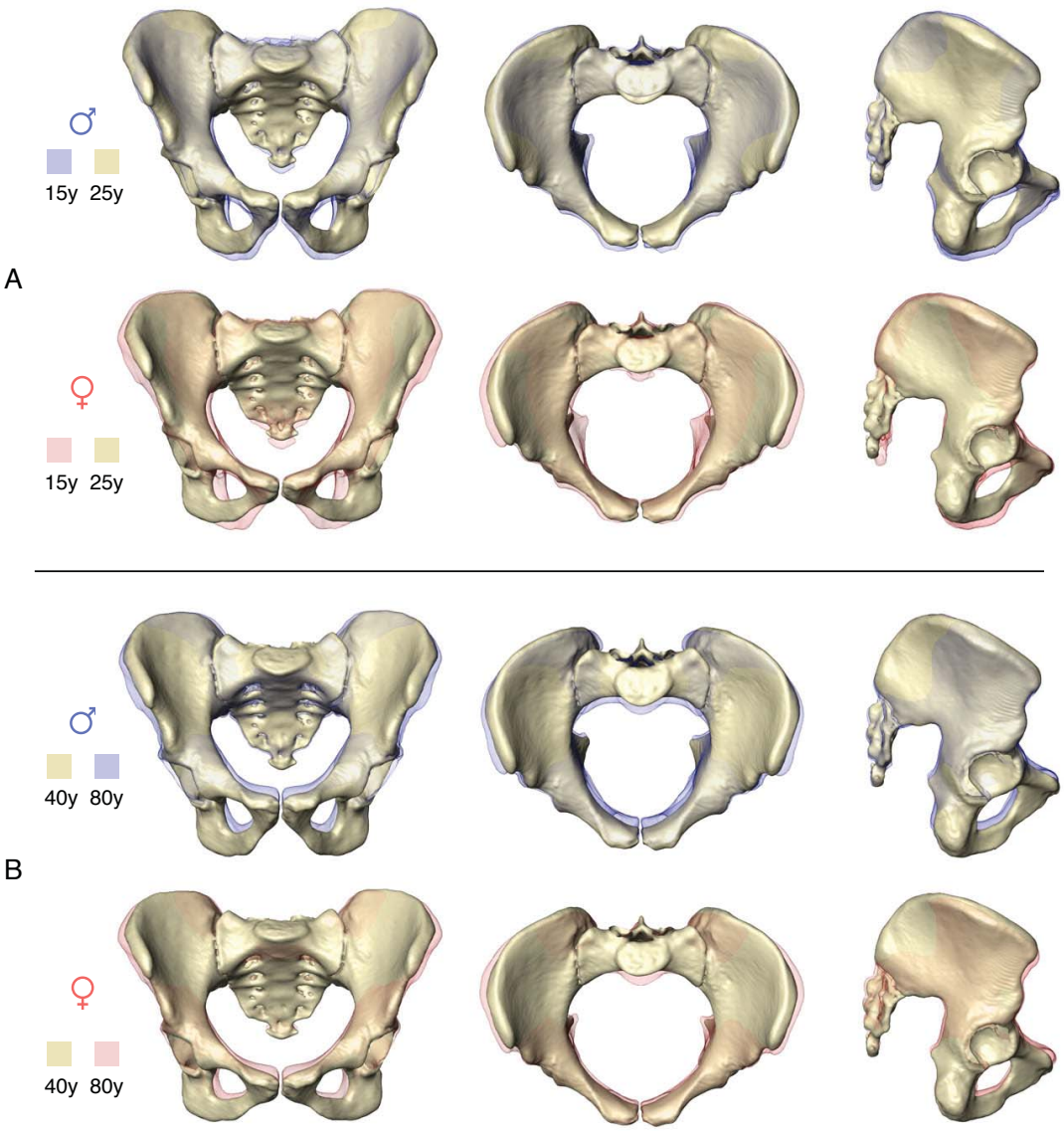

Fig. 3. Anterior, superior, and lateral views showing male and female patterns of pelvic shape change from ~15 y (transparent) to ~25 y (solid) (A), and from ~40 y (solid) to ~80 y (transparent) (B). For additional visualizations of the same patterns of shape change, see Movies S1-S6.

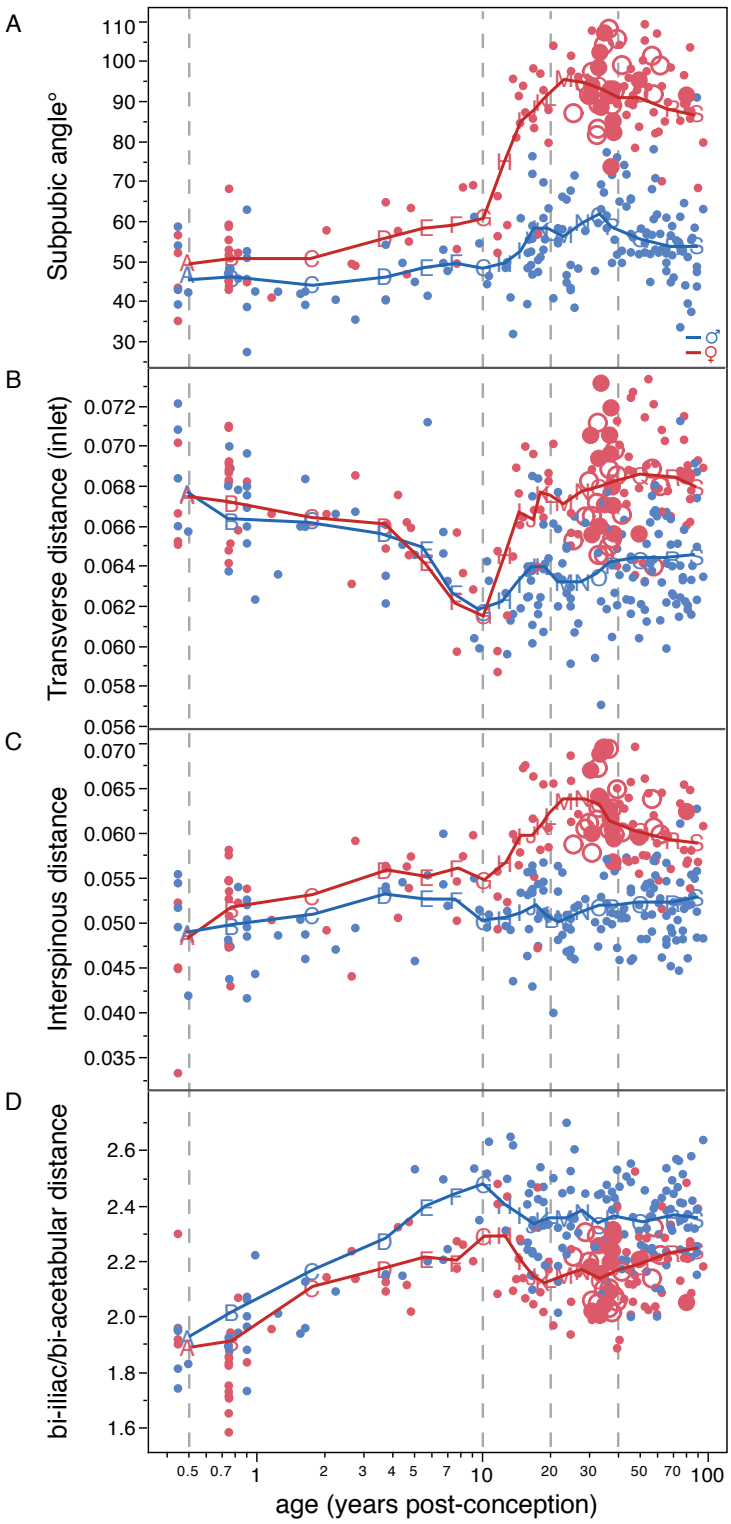

Fig. 4. Sex-specific changes in angular (A) and size-normalized linear (B and C) pelvic dimensions and in pelvic proportions (D). Colors and symbols are as in Figs. 1 and 2.

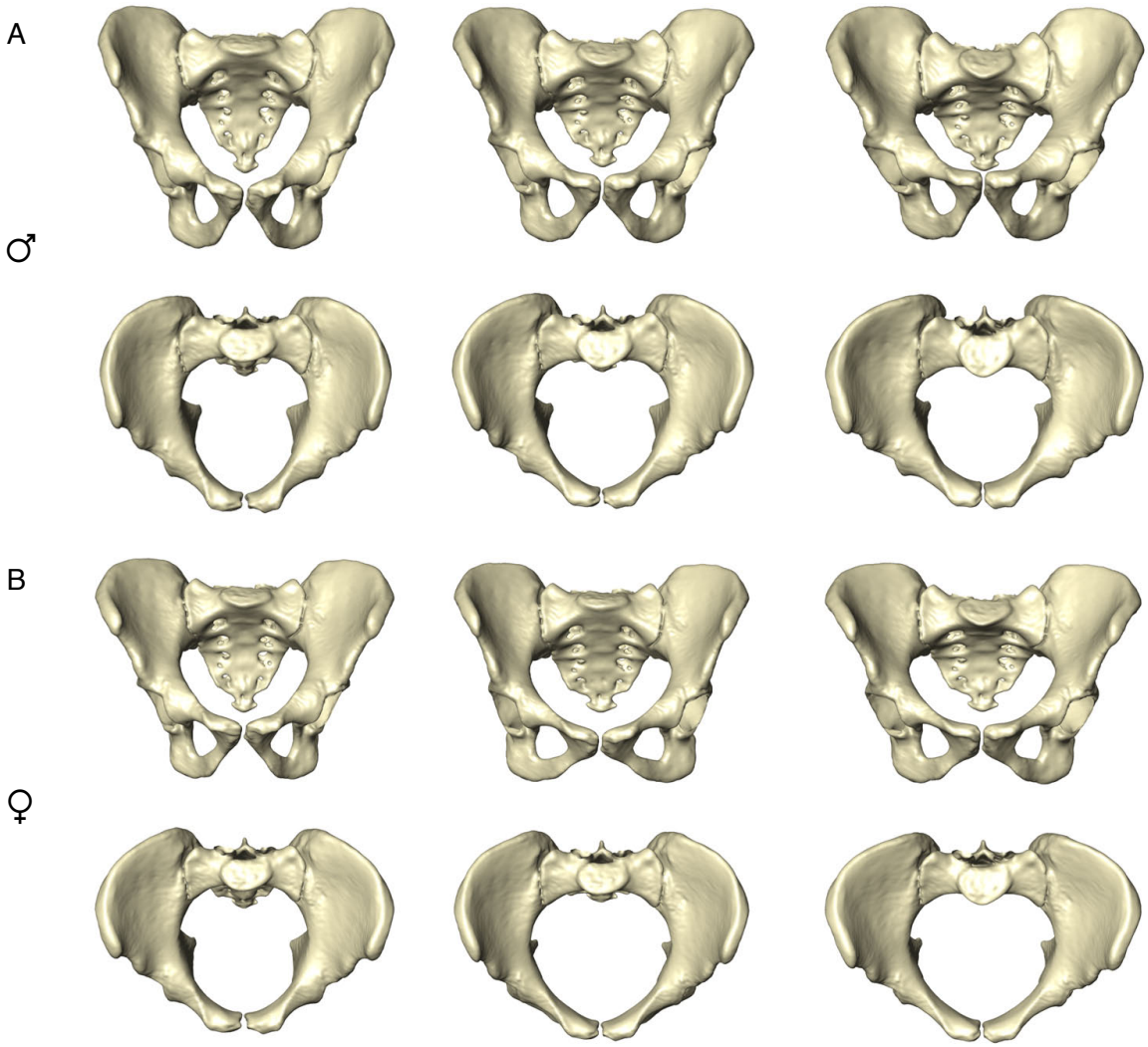

Fig. S1. Anterior and superior views showing male (A) and female (B) pelvic mean shapes at age ~15 y (Left), ~25 y (Center), and ~80 y (Right). For additional visualizations of the same patterns of shape change, see Fig. 3 and Movies S1–S6.

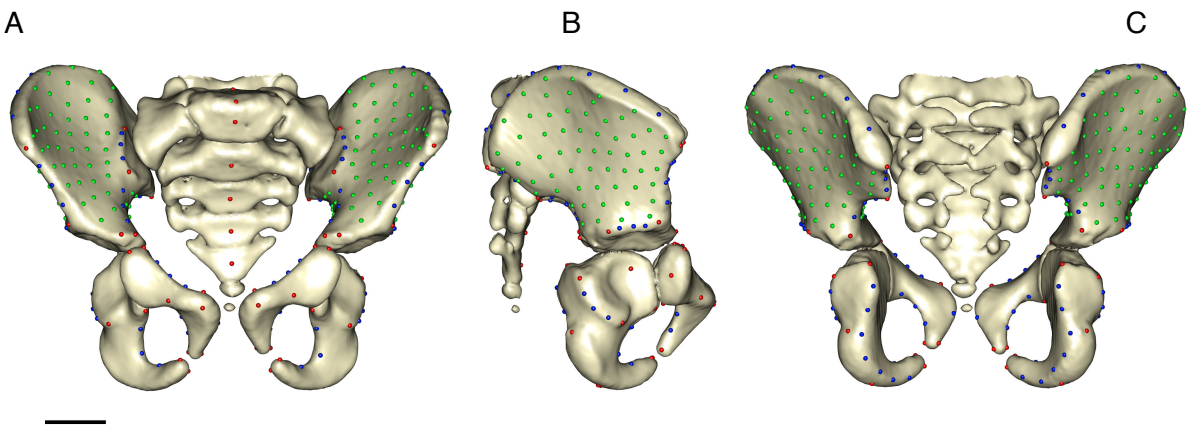

Fig. S2. Anterior (A), lateral (B), and posterior (C) views of an immature pelvis showing pelvic LMs and SLMs. Fixed LMs are shown in red, curve SLMs in blue, and surface SLMs in green. (Scale bar, 2 cm).

Table S1. Differences between male and female pelvic shapes in immature, prime reproductive age, and old adult samples (Procrustes ANOVA).

Age ranges, y	df	SS	MS	Rsq	F	*P*
>0 to <13	1	0.00705	0.00705	0.05781	3.98873	0.00276
Residuals	65	0.11491	0.00176			
Total	66	0.12196				
≥19 to <40	1	0.04584	0.04584	0.19299	15.78333	0.00033
Residuals	66	0.19168	0.00290			
Total	67	0.23752				
≥40 to ≤95	1	0.05741	0.05741	0.19990	24.48527	0.00033
Residuals	98	0.22979	0.00234			
Total	99	0.28720				

df, degrees of freedom; F, F-value; MS, mean square; *P* = P value; Rsq, R^2; SS, sum of squares.

Table S2. Comparison of trajectory directions among sexes and age groups.

Comparison	Angle, degrees	*P*
f1-f2	59.6	0.003*
f2-f3	76.5	0.020*
m1-m2	17.2	0.496
m2-m3	83.5	0.074
f1-m1	6.7	0.280
f2-m2	57.5	0.002*
f3-m3	9.2	0.719

Trajectory directions were evaluated by multivariate regression of PC1-3 on log age (years postconception) for six groups (f1: females, age ≤8 y, *n* = 31; f2: females, age >8 y ≤35 y, *n* = 39; f3: females, age >35 y, *n* = 55; m1: males, age ≤8y, *n* = 31; m2: males, age >8 y ≤ 35 y, *n* = 52; m3: males, age >35 y, *n* = 68).

**P* values ≤0.02 indicate significant divergence between trajectory segments. Note divergence between males and females from puberty to prime reproductive age (f2–m2), but no divergence between sexes during childhood (f1– m1) and late adulthood (f3–m3).

Table S3. Comparison of pelvic shape of parous and nonparous women.

Age range, y	df	SS	MS	Rsq	F	*P*
28-41	1	0.00578	0.00578	0.07291	1.88757	0.10330
Residuals	24	0.07344	0.00306			
Total	25	0.07922				

Sample structure: nonparous: n = 13, mean age = 34.1 y; parous: n = 12 (9 multiparae), mean age = 34.4 y. df, degrees of freedom; F, F-value; MS, mean square; P = P value; Rsq, R^2; SS, sum of squares.

Table S4. Sample structure.

Developmental stage	age range (y)	males	females	total
Perinatal	-0.3 to 0.08	10	16	26
Infancy	0.16 to 2	13	5	18
Early childhood	3 to 8	9	10	19
Middle childhood to adolescence	9 to 18	27	16	43
Prime reproductive age	19 to 40	33	36	69
Old adults	>40 to 95	59	41	100

Table S5. Definition of fixed landmarks.

LM number	Description
1-2	Pubic symphysis: superiormost anterior point
3-4	Pubic symphysis: superiormost posterior point
5-6	Ischiopubic juncture: pubis - posterior fusion point
7-8	Ischiopubic juncture: ischium - posterior fusion point
9-10	Ischiopubic juncture: pubis - obturator foramen inferior fusion point
11-12	Ischiopubic juncture: ischium - obturator foramen inferior fusion point
13-14	Ischiopubic juncture: pubis - obturator foramen superior fusion point
15-16	Ischiopubic juncture: ischium - obturator foramen superior fusion point
17-18	Ischium: posteriormost point (superior from ischial tuberosity)
19-20	Ischium: inferiormost midpoint
21-22	Ilioischial juncture: ischium - fusion point
23-24	Ilioischial juncture: ilium - fusion point
25-26	Ilioischial juncture: ischium - acetabulum lateral fusion point
27-28	Ilioischial juncture: ilium - acetabulum lateral fusion point
29-30	Acetabulum: superiormost lateral point
31-32	Acetabulum: point on pubic part of lunate surface
33-34	Iliopubic juncture: pubis - superior fusion point
35-36	Iliopubic juncture: ilium - superior fusion point
37-38	Iliopubic juncture: pubis - fusion point on pelvic brim
39-40	Iliopubic juncture: ilium - fusion point on pelvic brim
41-42	Pubis: anterior midpoint
43-44	Acetabulum: inferiormost lateral point on lunate surface
45-46	Acetabulum: deepest point on acetabular center (acetabular fossa)
47-48	Pelvic brim and sacroiliac joint: intersection point
49-50	Sacroiliac joint: superiormost point
51	S1: superiormost anterior point
52	S1: superiormost posterior point
53	S1: anterior midpoint
54	S2: anterior midpoint
55	S3: anterior midpoint
56	S4: anterior midpoint
57-58	Anterior supuperior iliac spine
59-60	Iliac crest: posteriormost point (end point)
61-62	Posterior inferior iliac spine
63	S5: anterior midpoint

Table S6. Definition of semilandmarks.

LM number	Description
Iliac crest	Right: start LM 57, end LM 59; Left: start LM 58, end LM 60 with eight subdivisions
Posterior iliac spines	Right: start LM 59, end LM 61; Left: start LM 60, end LM 62 with four subdivisions
Greater sciatic notch	Right: start LM 61, end LM 23; Left: start LM 62, end LM 24 with four subdivisions
Acetabulum: on ilium	Right: start LM 27, end LM 29; Left: start LM 28, end LM 30 with four subdivisions
Anterior iliac spines	Right: start LM 57, end LM 29; Left: start LM 58, end LM 30 with four subdivisions
Acetabulum: on ischium	Right: start LM 25, end LM 43; Left: start LM 26, end LM 44 with four subdivisions
Obturator foramen posterior	Right: start LM 15, end LM 11; Left: start LM 16, end LM 12 with four subdivisions
Obturator foramen anterior	Right: start LM 13, end LM 9; Left: start LM 14, end LM 10 with four subdivisions
Sacroiliac joint	Right: start LM 49, end LM 47; Left: start LM 50, end LM 48 with four subdivisions
Pelvic brim1	Right: start LM 47, end LM 39; Left: start LM 48, end LM 40 with four subdivisions
Pelvic brim2	Right: start LM 37, end LM 3; Left: start LM 38, end LM 4 with four subdivisions
Pubis posterior	Right: start LM 3, end LM 5; Left: startLeft: start LM 4, end LM 6 with two subdivisions
Ischium posterior	Right: start LM 7, end LM 21; Left: start LM 8, end LM 22 with eight subdivisions

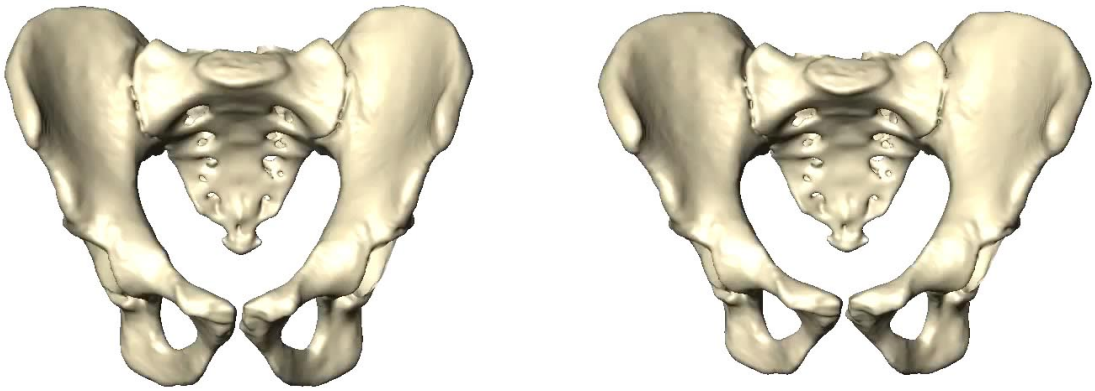

Male and Female ~15 years to ~25 years

Movie S1. Changes in male and female pelvic shape from ~15 y to ~25 y to ~15 y: anterior views.

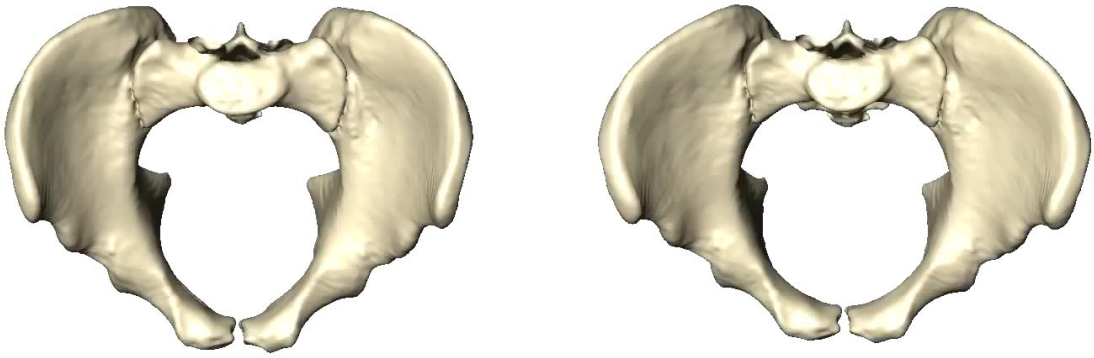

Male and Female ~15 years to ~25 years

Movie S2. Changes in male and female pelvic shape from ~15 y to ~25 y to ~15 y: superior views.

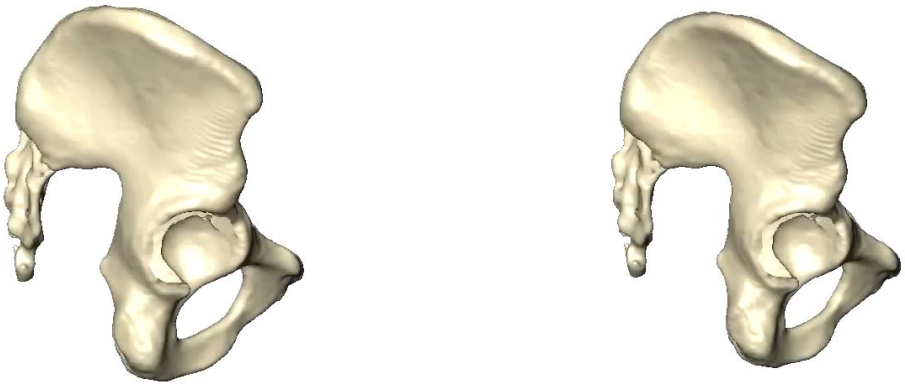

Male and Female ~15 years to ~25 years

Movie S3. Changes in male and female pelvic shape from ~15 y to ~25 y to ~15 y: lateral views.

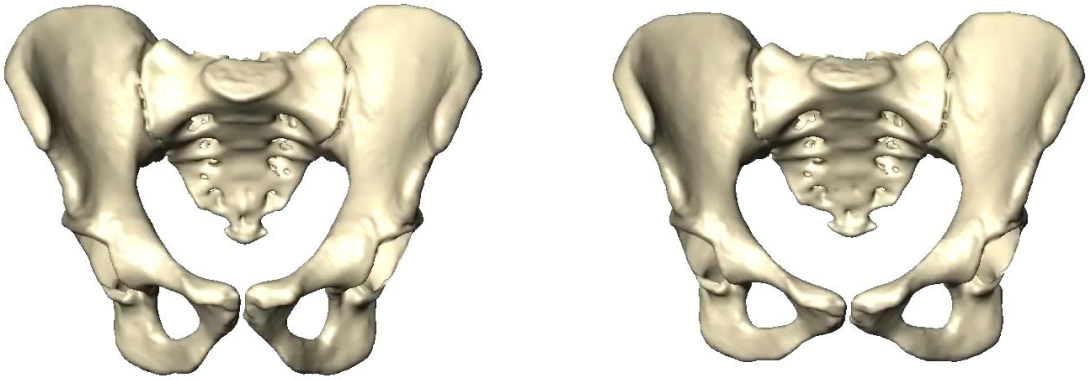

Male and Female ~40 years to ~80 years

Movie S4. Changes in male and female pelvic shape from ~40 y to ~80 y to ~40 y: anterior views.

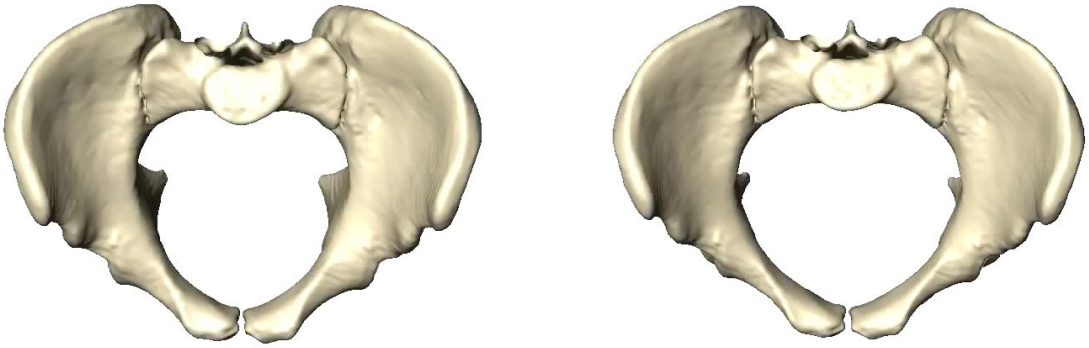

Male and Female ~40 years to ~80 years

Movie S5. Changes in male and female pelvic shape from ~40 y to ~80 y to ~40 y: superior views.

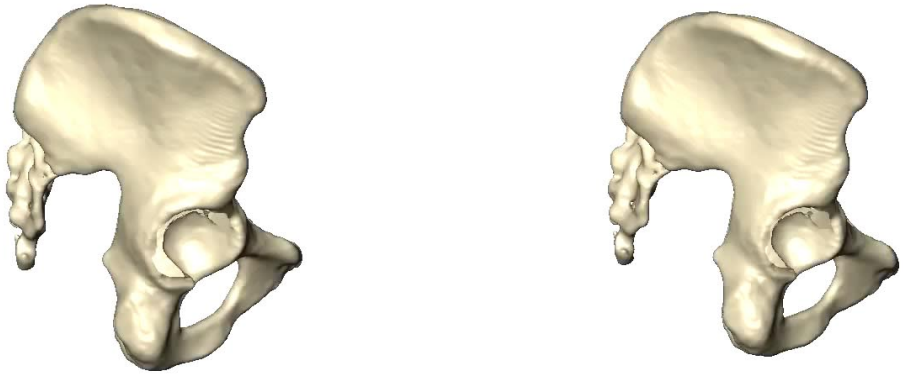

Male and Female ~40 years to ~80 years

Movie S6. Changes in male and female pelvic shape from ~40 y to ~80 y to ~40 y: lateral views.

References:

Abitbol MM. 1988. Evolution of the ischial spine and of the pelvic floor in the hominoidea. Am J Phys Anthropol 75:53–67.

Adams DC, Collyer ML, Sherratt E. 2015. *geomorph*: Software for geometric morphometric analyses. R package version 2.1.7. http://cran.r-project.org/web/ packages/geomorph/ index.html. Available from: http://cran.r-project.org/web/ packages/geomorph/index.html

Ashton-Miller JA, DeLancey JOL. 2007. Functional anatomy of the female pelvic floor. Ann NY Acad Sci 1101:266–296.

Aubertin-Leheudre M, Gorbach S, Woods M, Dwyer JT, Goldin B, Adlercreutz H. 2008. Fat/ fiber intakes and sex hormones in healthy premenopausal women in USA. J Steroid Biochem Mol Biol 112:32–39.

Bamberg Migliano A, Vinicius L, Lahr MM. 2007. Life history trade-offs explain the evolution of human pygmies. Proc Natl Acad Sci USA 104:20216–20219.

Bentley GR, Harrigan AM, Ellison PT. 1998. Dietary composition and ovarian function among Lese horticulturalist women of the Ituri Forest, Democratic Republic of Congo. Eur J Clin Nutr 52:261–270.

Berdnikovs S, Bernstein M, Metzler A, German RZ. 2006. Pelvic growth: ontogeny of size and shape sexual dimorphism in rat pelves. J Morphol 268:12–22.

Bernstein P, Crelin ES. 1967. Bony pelvic sexual dimorphism in the rat. Anat Rec 157:517–525.

Bilfeld MF, Dedouit F, Sans N, Rousseau H, Rougé D, Telmon N. 2015. Ontogeny of size and shape sexual dimorphism in the pubis: a multislice Computed Tomography study by geometric morphometry. J Forensic Sci.

Boucher BJ. 1957. Sex differences in the foetal pelvis. Am J Phys Anthropol 15:581–600.

Brown KM. 2015. Selective pressures in the human bony pelvis: Decoupling sexual dimorphism in the anterior and posterior spaces. Am J Phys Anthropol 157:428–440.

Callewaert F, Sinnesael M, Gielen E, Boonen S, Vanderschueren D. 2010. Skeletal sexual dimorphism: relative contribution of sex steroids, GH-IGF1, and mechanical loading. J Endocrinol 207:127–134.

Cole TJ, Ahmed ML, Preece MA, Hindmarsh P, Dunger DB. 2015. The relationship between Insulin-like Growth Factor 1, sex steroids and timing of the pubertal growth spurt. Clin Endocrinol (Oxf) 82:862–869.

Coleman WH. 1969. Sex differences in the growth of the human bony pelvis. Am J Phys Anthropol 31:125–151.

Collyer ML, Sekora DJ, Adams DC. 2015. A method for analysis of phenotypic change for phenotypes described by high-dimensional data. Heredity 115:357–365.

Dehghan F, Haerian BS, Muniandy S, Yusof A, Dragoo JL, Salleh N. 2014. The effect of relaxin on the musculoskeletal system. Scandinavian J Med Sci Sports 24:e220–e229.

Devlin MJ. 2011. Estrogen, exercise, and the skeleton. Evol Anthropol 20:54–61.

Dunsworth H, Eccleston L. 2015. The evolution of difficult childbirth and helpless hominin infants. Annu Rev Anthropol 44:55–69.

Dunsworth HM, Warrener AG, Deacon T, Ellison PT, Pontzer H. 2012. Metabolic hypothesis for human altriciality. Proc Natl Acad Sci USA 109:15212–15216.

Elden H, Hagberg H, Olsén MF, Ladfors L, Ostgaard HC. 2009. Regression of pelvic girdle pain after delivery: follow-up of a randomised single blind controlled trial with different treatment modalities. Acta Obstetr Gynecol Scand 87:201–208.

Ellison P. 2008. Energetics, reproductive ecology, and human evolution. PaleoAnthropology: 172–200.

Emery Thompson M, Zhou A, Knott CD. 2012. Low testosterone correlates with delayed development in male orangutans. PLoS ONE 7:e47282.

Fischer B, Mitteroecker P. 2015. Covariation between human pelvis shape, stature, and head size alleviates the obstetric dilemma. Proc Natl Acad Sci USA 112:5655–5660.

Gingerich PD. 1972. The development of sexual dimorphism in the bony pelvis of the squirrel monkey. Anat Rec 172:589–595.

Gluckman PD, Hanson MA, Spencer HG. 2005. Predictive adaptive responses and human evolution. Trends Ecol Evol 20:527–533.

Grillner S, Nilsson J, Thorstensson A. 1978. Intra-abdominal pressure changes during natural movements in man. Acta Physiol Scand 103:275–283.

Gruss LT, Schmitt D. 2015. The evolution of the human pelvis: changing adaptations to bipedalism, obstetrics and thermoregulation. Philos Trans R Soc Lond, B, Biol Sci 370:20140063–20140063.

Gunz P, Mitteroecker P, Bookstein FL. 2005. Semilandmarks in three dimensions. In: Slice DE, editor. Modern morphometrics in physical anthropology. Developments in Primatology: Progress and Prospects. New York: Kluwer Academic Publishers-Plenum Publishers. p 73–98.

Handa VL, Pannu HK, Siddique S, Gutman R, VanRooyen J, Cundiff G. 2003. Architectural differences in the bony pelvis of women with and without pelvic floor disorders. Obstet Gynecol 102:1283–1290.

Harrison MS, Ali S, Pasha O, Saleem S, Althabe F, Berrueta M, Mazzoni A, Chomba E, Carlo WA, Garces A, Krebs NF, Hambidge K, Goudar SS, Dhaded SM, Kodkany B, Derman RJ, Patel A, Hibberd PL, Esamai F, Liechty EA, Moore JL, Koso-Thomas M, McClure EM, Goldenberg RL. 2015. A prospective population-based study of maternal, fetal, and neonatal outcomes in the setting of prolonged labor, obstructed labor and failure to progress in low- and middle-income countries. Reprod Health 12 Suppl 2:S9.

Hawkes K, O'Connell JF, Jones NG, Alvarez H, Charnov EL. 1998. Grandmothering, menopause, and the evolution of human life histories. Proc Natl Acad Sci USA 95:1336–1339.

Hodges PW, Eriksson AEM, Shirley D, Gandevia SC. 2005. Intra-abdominal pressure increases stiffness of the lumbar spine. J Biomech 38:1873–1880.

Hofmeyr GJ. 2004. Obstructed labor: using better technologies to reduce mortality. Int J Gynaecol Obstet 85 Suppl 1:S62–72.

Iguchi T, Irisawa S, Fukazawa Y, Uesugi Y, Takasugi N. 1989. Morphometric analysis of the development of sexual dimorphism of the mouse pelvis. Anat Rec 224:490–494.

Jasienska G, Thune I, Ellison PT. 2006a. Fatness at birth predicts adult susceptibility to ovarian suppression: an empirical test of the Predictive Adaptive Response hypothesis. Proc Natl Acad Sci USA 103:12759–12762.

Jasienska G, Ziomkiewicz A, Lipson SF, Thune I, Ellison PT. 2006b. High ponderal index at birth predicts high estradiol levels in adult women. Am J Hum Biol 18:133–140.

Khosla S, Oursler MJ, Monroe DG. 2012. Estrogen and the skeleton. Trends in Endocrinology & Metabolism 23:576–581.

Kurki HK. 2011. Pelvic dimorphism in relation to body size and body size dimorphism in humans. J Hum Evol 61:631–643.

LaVelle M. 1995. Natural selection and developmental sexual variation in the human pelvis. Am J Phys Anthropol 98:59–72.

Lefevre CE, Lewis GJ, Perrett DI, Penke L. 2013. Telling facial metrics: facial width is associated with testosterone levels in men. Evol Hum Behav 34:273–279.

Leutenegger W. 1970. Relation between newborn size and sex dimorphism of pelvis in simian primates. Folia Primatol 12:224–235.

Lipson SF, Ellison PT. 1996. Comparison of salivary steroid profiles in naturally occurring conception and non-conception cycles. Hum Reprod 11:2090–2096.

Lovejoy CO. 2005. The natural history of human gait and posture. Gait & Posture 21:95–112.

Martin JA, Hamilton BE, Osterman MJ, Curtin SC, Matthews TJ. 2015. Births: final data for 2013. Natl Vital Stat Rep 64:1–65.

McClure EM, Goldenberg RL, Bann CM. 2007. Maternal mortality, stillbirth and measures of obstetric care in developing and developed countries. Int J Gynaecol Obstet 96:139–146.

McPherson FJ, Chenoweth PJ. 2012. Mammalian sexual dimorphism. Animal Repr Sci 131:109–122.

Moffett A, Hiby SE, Sharkey AM. 2015. The role of the maternal immune system in the regulation of human birthweight. Philos Trans R Soc Lond, B, Biol Sci 370:20140071–20140071.

Ober C, Loisel DA, Gilad Y. 2008. Sex-specific genetic architecture of human disease. Nat Rev Genet 9:911–922.

Oury F. 2012. A crosstalk between bone and gonads. Annals NY Acad Scis 1260:1–7.

Parsch J, Ellegren H. 2013. The evolutionary causes and consequences of sex-biased gene expression. Nat Rev Genet 14:83–87.

Ponce de León MS, Golovanova L, Doronichev V, Romanova G, Akazawa T, Kondo O, Ishida H, Zollikofer CPE. 2008. Neanderthal brain size at birth provides insights into the evolution of human life history. Proc Natl Acad Sci USA 105:13764–13768.

Portmann A. 1941. Die Tragzeiten der Primaten und die Dauer der Schwangerschaft beim Menschen: ein Problem der vergleichenden Biologie. [Gestation length in primates and humans: a topic of comparative biology.]. Rev Suisse Zool 48:511–518.

Reitter A, Daviss B-A, Bisits A, Schollenberger A, Vogl T, Herrmann E, Louwen F, Zangos S. 2014. Does pregnancy and/or shifting positions create more room in a woman's pelvis? Am J Obstet Gynecol 211:662.e1–662.e9.

Rosenberg KR. 1992. The evolution of modern human childbirth. Am J Phys Anthropol 35:89–124.

Schlager S. 2016. Morpho: Calculations and visualisations related to geometric morphometrics. R package version 2.3.1.1. Available from: http://sourceforge.net/projects/morpho-rpackage/ https://github.com/zarquon42b/Morpho

Schultz AH. 1949. Sex differences in the pelves of primates. Am J Phys Anthropol 7:401–423.

Schutz H, Donovan ER, Hayes JP. 2009. Effects of parity on pelvic size and shape dimorphism in *Mus*. J Morphol 270:834–842.

Stone PK. 2016. Biocultural perspectives on maternal mortality and obstetrical death from the past to the present. Am J Phys Anthropol 159:S150–S171.

Tague RG. 1994. Maternal mortality or prolonged growth: age at death and pelvic size in three prehistoric Amerindian populations. Am J Phys Anthropol 95:27–40.

Tague RG. 1995. Variation in pelvic size between males and females in nonhuman anthropoids. Am J Phys Anthropol 97:213–233.

Tague RG. 2005. Big-bodied males help us recognize that females have big pelves. Am J Phys Anthropol 127:392–405.

Tardieu C, Bonneau N, Hecquet J, Boulay C, Marty C, Legaye J, Duval-Beaupère G. 2013. How is sagittal balance acquired during bipedal gait acquisition? Comparison of neonatal and adult pelves in three dimensions. Evolutionary implications. J Hum Evol 65:209–222.

Trevathan W. 2015. Primate pelvic anatomy and implications for birth. Philos Trans R Soc Lond, B, Biol Sci 370:20140065–20140065.

Uesugi Y, Taguchi O, Noumura T, Iguchi T. 1992. Effects of sex steroids on the development of sexual dimorphism in mouse innominate bone. Anat Rec 234:541–548.

Verdonck A, Gaethofs M, Carels C, de Zegher F. 1999. Effect of low-dose testosterone treatment on craniofacial growth in boys with delayed puberty. Eur J Orthod 21:137–143.

Walker PL. 2005. Greater sciatic notch morphology: Sex, age, and population differences. Am J Phys Anthropol 127:385–391.

Warrener AG, Lewton KL, Pontzer H, Lieberman DE. 2014. A wider pelvis does not increase locomotor cost in humans, with implications for the evolution of childbirth. PLoS ONE 10:e0118903–e0118903.

Washburn SL. 1960. Tools and Human Evolution. Sci Am 203:62–75.

Wells JCK. 2015. Between Scylla and Charybdis: renegotiating resolution of the “obstetric dilemma” in response to ecological change. Philos Trans R Soc Lond, B, Biol Sci 370:20140067–20140067.

Williams TM, Carroll SB. 2009. Genetic and molecular insights into the development and evolution of sexual dimorphism. Nat Rev Genet 10:797–804.

Wilson LAB, Ives R, Cardoso HFV, Humphrey LT. 2014. Shape, size, and maturity trajectories of the human ilium. Am J Phys Anthropol 156:19–34.

Wittman AB, Wall LL. 2007. The evolutionary origins of obstructed labor: bipedalism, encephalization, and the human obstetric dilemma. Obstetr Gynecol Survey 62:739–748.

Woods MN, Barnett JB, Spiegelman D, Trail N, Hertzmark E, Longcope C, Gorbach SL. 1996. Hormone levels during dietary changes in premenopausal African-American women. J Natl Cancer Inst 88:1369–1374.

Zollikofer CPE, Ponce de León MS. 2005. Virtual reconstruction: a primer in computer-assisted paleontology and biomedicine. Hoboken, N. J.: Wiley-Liss.

Chapter 2

Development of modular organization in the chimpanzee pelvis

Reference: AR-SI-HIP-16-0124, *accepted in Anatomical Record*

Abstract

The bony pelvis of primates is a composite structure serving a variety of functions, and exhibiting a complex pattern of modularity and integration. Still little is known, however, about how patterns of modularity and integration arise, and how they change throughout ontogeny. Here we study the ontogeny of modularity and integration in developmental and functional units of the pelvis of our closest living relatives, the chimpanzees. We use methods of biomedical imaging and geometric morphometrics to quantify pelvic shape change from late fetal stages to adulthood, and to track changes in patterns of covariation within and among pelvic regions. Our results show that both developmental and functional units of the pelvis exhibit significant levels of modularity throughout ontogeny. Modularity of developmental units (ilium, ischium, pubis) decreases with increasing age, whereas modularity of functional units tends to increase. We suggest that the decreasing modularity and increasing integration of developmental units reflects their gradual fusion. In contrast, increasing modularity of functional pelvic units likely reflects changing functional demands during an individual's lifetime. Overall, ontogenetic changes in patterns of modularity and integration imply that natural selection could act differently on each module, either developmental or functional, at different stages of ontogeny. This further implies that adult patterns of covariation in the pelvis provide only limited information about its evolvability.

Key words: chimpanzee, development, modularity and integration, pelvis, sexual dimorphism

INTRODUCTION

A heterogeneous pattern in organismal development, function or morphology is known as "modularity", where different modules are viewed as internally strongly integrated units having weak connectivity to other such modules (Kitano, 2004; Wagner et al., 2007; Klingenberg, 2008; Kuratani, 2009; Klingenberg, 2010; Wagner and Zhang, 2011; Klingenberg, 2014; Esteve-Altava, 2015). Modularity has been studied in various structures, such as fruit fly wings (Klingenberg and Zaklan, 2000), bird beaks (Abzhanov et al., 2004; 2006), mammalian skulls (Klingenberg et al., 2003; Klingenberg, 2004; Mitteroecker and Bookstein, 2008; Zelditch et al., 2008; Delezene, 2015), and the primate and human pelvis (Berge, 1998; Williams and Orban, 2007; Grabowski et al., 2011; Grabowski, 2012; Lewton, 2012). It is generally held that the modular organization of an organism tends to facilitate its adaptive evolution (evolvability) as selection can act independently on each module (Hansen, 2003; Hendrikse et al., 2007; Wagner et al., 2007; Kuratani, 2009; Goswami and Polly, 2010; Goswami et al., 2014; 2015). The concept of modularity is also used in network models of biological structures. In neural networks, for example, direct selection to minimize connection cost (maintenance costs, efficient energy transmission, physical limits and signal transmission delays due to high connection number) tend to produce modularity as a side effect (Striedter, 2005). More generally, any biological network under pressure to minimize connection costs between network nodes evolves modularity and is able to adapt more quickly to changing environments than an integrated system (Clune et al., 2013). On the other hand, directional selection was suggested to create modular networks whereas stabilizing selection would actually maintain a modular pattern (Melo and Marroig, 2015).

The pelvis of humans, and of our closest relatives, the great apes, represents an interesting model system for the study of modularity and integration. It is composed of several developmental units (ilium, ischium, pubis) representing separate chondrification/ossification regions (Scheuer et al., 2000). These elements fuse during ontogeny, and can thus be expected to become more integrated with increasing individual age. On the other hand, pelvic morphology serves a diversity of functions, such as locomotion, birthing, and support of abdominal organs during orthograde body position, and there are substantial differences between humans and great apes in pelvic functional constraints. Furthermore, functional demands tend to change during an individual's lifetime, and differ between sexes, resulting in a complex interplay between evolutionary, developmental and environmental factors influencing modularity and integration.

Several studies have analyzed patterns of evolutionary and developmental modularity and integration in the primate and human pelvis (Berge, 1998; Williams and Orban, 2007; Grabowski et al., 2011; Grabowski, 2012; Lewton, 2012). In humans, morphological integration is reduced in obstetric compared to locomotor regions of the pelvis, indicating that the human birth canal region has higher evolvability than that of great apes (Grabowski et al., 2011). Another study (Lewton, 2012) on primates including humans suggested low integration and high evolvability of the pelvis in general, and identified only two pelvic modules, the ilium and the ischiopubic complex, while modularity of the ischium and the pubis was not significant.

These studies focused on patterns of morphological variation in adults, such that it remains to be investigated how modularity changes during pelvic growth and development. Such information is not yet available for the pelvis, but various studies on craniofacial development have shown that modularity/integration patterns tend to change during ontogeny (Willmore et al., 2006; Zelditch et al., 2006; Hallgrimsson et al., 2009; Gonzalez et al., 2011; González et al., 2011). Modular units become integrated, or integrated units become modular (e.g. due to external stimuli), such that the initial pattern of modularity/integration is "overwritten" by subsequent ones, resulting in a "palimpsest" of modularity and integration (Hallgrimsson et al., 2009).

The genetic networks governing pelvic development are best documented in rodents. In mice the three pelvic elements (ilium, ischium, pubis) originate from a single mesenchymal condensation, which later undergoes chondrification and ossification at different centers (Pomikal and Streicher, 2010). Each pelvic element is differentially controlled by *Pixt1* and *Emx2* (ilium), *Alx1*, *Prrx1* and *Twist1* (pubis), and *Pax1* (ischium) (Capellini et al., 2011, p 1185). Experimental studies in mice provided evidence for hormonally induced sex-biased pelvic development. For example, gonadectomized males and those lacking androgen receptors (Tfm mutation) develop a female-like pelvis, whereas under administration of androgens female mice develop male-like pelvic morphologies (Bernstein and Crelin, 1967; Iguchi et al., 1989; Uesugi et al., 1992). A recent study on human pelvic development suggests that changes in female pelvic morphology are correlated with changing estradiol levels throughout an individual's lifetime (Huseynov et al., 2016). Also, there is evidence that pelvic morphology is influenced by developmental plasticity in response to changing ecological/nutritional factors (Wells et al., 2012; Wells, 2015).

Based on the current evidence for proximate to ultimate causes of pelvic morphological variation, two hypotheses can be proposed: a) the modularity of developmental units of the pelvis decreases during ontogeny, while their integration increases; b) the modularity of functional pelvic units increases during ontogeny, while their integration decreases. Here we test these hypotheses for the pelvis of our closest living relatives, the species of the genus *Pan*. There are several reasons why we focus in this study on *Pan* rather than our own species, *Homo sapiens*. In chimpanzees the birth canal is substantially more capacious than fetal head and body dimensions (Schultz, 1949). Obstetric constraints are thus absent, and locomotor functional factors influencing pelvic morphology can be assumed to be largely similar in females and males. Also, pelvic sexual dimorphism is minimal compared to that found in humans (Schultz, 1949; Tague, 2005), and the postreproductive life span is short. Overall, thus, in chimpanzees compared to humans, patterns of variation of the pelvis depend on a smaller number of factors. Earlier studies of pelvic morphology as a whole (Berge, 1998), and of the innominate bone in isolation (Williams and Orban, 2007) revealed fundamental differences between great ape and human developmental trajectories, and also showed that species-specific pelvic morphologies are already present at birth. These studies further indicated that evolutionary changes in rate and duration of growth of pelvic elements played a central role in the evolution of the characteristic pelvic morphology of hominoid species.

Today, volumetric data acquisition by means of computed tomography (CT), and analysis of three-dimensional pelvic shape change by means of geometric morphometrics (Bookstein, 1997) permit a more detailed look at how the chimpanzee pelvis develops, and how patterns of modularity and integration change during ontogeny. Compared with classical multivariate morphometric analysis of linear and/or angular measurements, geometric morphometrics (GM) provides several advantages. First, GM quantifies morphology by the 3D-coordinates of a set of anatomical landmarks that are assumed to represent points of biological and/or geometric homology between the specimens of the sample. Second, GM permits statistical separation of the two main components of morphology, size (extent) and shape (geometry), that are contained in each specimen's landmark configuration. Third, GM permits simultaneous representation of patterns of shape variation in high-dimensional multivariate spaces (amenable to classical multivariate analysis), and in 3-dimensional physical space, thus maintaining the links between statistical and real-space representation of the results.

The analysis of patterns of modularity and integration in morphometric data sets is a topic of growing interest (Klingenberg, 2008; 2009; Klingenberg and Marugán Lobón, 2013; Klingenberg, 2014). Various multivariate and GM-based methods have been proposed to detect and quantify patterns of modularity and integration, and to assess the potential for evolutionary change ("evolvability") that can be inferred from such patterns (Klingenberg, 2005; McGuigang, 2006; Hansen and Houle, 2008; Hallgrimsson et al., 2009; Young et al., 2010; Klingenberg et al., 2012; Adams, 2016). The relationship between patterns of covariation and processes of integration/modularity is complex (Hallgrimsson et al., 2009; Klingenberg, 2014), such that there is currently no consensus as to which approach is best suited to disentangle the developmental and evolutionary factors linking integration/ modularity to covariation (Hallgrimsson et al., 2009; Armbruster et al., 2014; Klingenberg, 2014; Adams, 2016; Bookstein, 2016). The approach used here is detailed in the methods section, and largely follows Klingenberg (2014) and Adams (2016).

RESULTS

Figures 2 and 3 show sex-specific patterns of pelvic shape variation and shape change in the subspace spanned by the first three principal components of shape space. Developmental trajectories are curved, and exhibit marked differences between early (stages A to C) and late (stages C to D) phases of ontogeny. The early phase is characterized by gradual fusion of the pelvic elements, starting with the fusion of the ischium and pubis, and ending with the fusion of the ischiopubic unit with the ilium (Fig. 2C). The onset of the late phase largely coincides with the complete fusion of all elements, and the onset of puberty. During this phase, the pelvis shows a distinct pattern of shape change, with more transverse than superoinferior and anteroposterior expansion, resulting in a wider pelvic inlet, more flaring iliac blades, and a relatively larger ischiopubic region compared to the iliac region (Fig. 2C).

PC1 accounts for 39.7% of total shape variation in the sample and is closely correlated with pelvic size (males: r^2=0.92; females: r^2=0.87), thus largely reflecting ontogenetic allometry, which is most evident during the early phase of ontogeny. PC2 (26.6%) largely captures shape change during the late phase of ontogeny. PC3 (6.6%) reveals small but consistent differences between sex-specific pelvic shapes at all ontogenetic stages (Figs. 2, 3). However, there is no sexual dimorphism in pelvic size along the entire ontogenetic trajectory (Fig. 3A). Sexual dimorphism in pelvic shape at adulthood is visualized in Fig. 4. Compared to the male pelvis, a similarly-sized female pelvis exhibits relatively larger transverse and

anteroposterior inlet dimensions, and more everted ischial regions. However, pelvic sexual dimorphism, as assessed with Procrustes ANOVA on pooled age-group data, is statistically not significant at any ontogenetic stage (Table 2).

Figure 5B graphs covariance ratios CR of the developmental and functional units of the pelvis versus ontogenetic stage. All CR values are significantly different from 1.00 ($p<0.001$, as evaluated by random resampling; see Methods). CR of the developmental units (ilium, ischium, and pubis) increases during mid-to-late ontogeny (stages B-D; Table 3), indicating that integration of these units increases, while modularity decreases. Contrastingly, CR of the functional pelvic units (obstetric/abdominal and locomotor regions) decreases during mid-to-late ontogeny, indicating that integration decreases while modularity increases (Table 3). For left/right modules, CR is consistently larger than 1.0 ($p<0.01$), indicating that covariation between left and right sides of the pelvis is larger than covariation within each side. For user-designed "random" modules, CR is indistinguishable from 1.0. Overall, developmental and functional modules show changes in levels of modularity/integration with increasing age, while no such change is observed in left/right modules and random modules.

DISCUSSION

To the best of our knowledge, this study is the first attempt to quantify ontogenetic changes in developmental and functional modularity of the chimpanzee pelvis. As mentioned in the introduction, a diversity of methods is currently available to quantify modularity/integration of a biological structure, and to draw inferences on the structure's evolvability given the constraints imposed by modularity/integration. No consensus has been reached yet on the choice of methods. We thus first discuss the potential and limitations of the approach followed here in comparison to other approaches. Then we interpret the results presented in this study in terms of modularity/integration and evolvability.

As can be seen in Table 2, the four age bins used in our analyses are relatively wide, such that the morphological variation in the subsamples represented by each bin comprises variation both along and across the ontogenetic trajectory. Bin width in the immature subsample of our study is a function of available specimens; immature full-body specimens that preserve the 3-dimensional morphology of the yet unfused pelvis without "preservation bias" are rare. We thus need to assess how ontogenetic binning might have influenced our results. Generally, one assumes that a fine resolution of ontogenetic stages yields a clear separation of stage-specific variation from between-stage variation. Judging from Figure 2,

however, pelvic shape variation within the adult stage D (which is traditionally used to study "static" patterns of shape variation) is similarly large as in the subsamples representing earlier stages. Moreover, variation among adults has a strong component along the ontogenetic trajectory from stage C to D, thus indicating that variation within a given stage cannot be neatly separated from variation between consecutive stages. This pattern is not a sampling artifact, but reflects a property of the developmental system; due to inter-individual differences in developmental rates, a given chronological age does not represent a point of developmental homology, but a time mark set externally. There are thus principal biological limitations to the separation of "static" (within-stage) from "dynamic" (between-stage) patterns of variation. Based on these considerations, it appears that the specific choice of ontogenetic stages in our study does not principally bias our results.

The degree of modularity and integration of a biological structure has been assessed with quantities such as the scaled variance of eigenvalues (Wagner, 1990; Hallgrimsson et al., 2009), and the RV coefficient (Klingenberg, 2009) or its modified version, the covariance ratio CR (Smilde et al., 2009; Adams, 2016), which is used in this study. Bookstein (2016) has shown in detail that these coefficients have to be interpreted with care, especially because they only represent generalized, global statistical properties of covariance matrices. Whatever measure is chosen, one also needs to be aware that modularity and integration are developmental processes that, ultimately, can only be quantified by direct observation and experimental modification of these processes (Hallgrimsson et al., 2009). Most studies, however, including the present one, observe the outcomes of the processes in terms of patterns of covariation, while the processes themselves remain unexplored. Keeping these caveats in mind, our CR-based study thus represents an initial exploratory approach to track ontogenetic changes in the covariation structure of the pelvis and infer changes in modularity and integration.

An important concept used for the evolutionary interpretation of patterns of modularity and integration is "evolvability". Evolvability, as defined by Hansen and Houle (2008), denotes the potential to evolve into a specific direction imposed by selection, given the constraints imposed on morphological variation by integration. The latter constraints are estimated from the phenotypic variance-covariance matrix, **P**, which serves as a proxy for the additive genetic variance-covariance matrix, **G**. This multivariate "geometric" definition of evolvability has great rigor, but its application to real-life biological problems such as the one studied here is limited. This is because **G** is considered to be a static property of the

population (typically of adults). However, **G** changes during ontogeny, and selection acts throughout ontogeny. The assessment of evolvability in the system studied here thus requires a wider definition of this term.

Given these conceptual and methodological limitations, our data provide support for the two hypotheses stated at the beginning: a) with increasing age (stages B to D) modularity of developmental units decreases, while integration increases (Table 3); b) with increasing age (stages B to D) modularity of functional units increases, while integration decreases (Table 3). CR values further indicate that modularity of developmental and functional units is present already at birth. These findings are consistent with previous studies showing similar effects during the development of the cranium (Willmore et al., 2006; Zelditch et al., 2006; Hallgrimsson et al., 2009; Gonzalez et al., 2011; González et al., 2011). The age-related decrease in developmental modularity likely reflects the gradual fusion of ilium, ischium and pubis. Fusion tends to impose spatial constraints, resulting in coordinated development of previously isolated bony units. Currently, comparative evidence showing similar effects in the developing pelvis of other primates is not available. However, the observed ontogenetic changes in modularity of developmental units have interesting implications for both the evolvability and the *in-vivo* developmental plasticity of the pelvis. High modularity at early ontogenetic stages implies that developmental units are relatively independent, and have high evolvability (Lewton, 2012; Rolian, 2014). Evolutionary changes in the early developmental program are thus most effective in generating phyletic diversity. At the same time, the relative independence of these units facilitates developmental plasticity early during ontogeny (LaVelle, 1995, p 60).

The increase in functional modularity toward adulthood is likely related to two factors: ultimate causes, such as natural selection shaping the genetic underpinnings of the developmental program, and proximate causes, such as developmental plasticity (e.g. bone remodeling) as a response to environmental factors and the individual's behavior. Increasing functional modularity may thus reflect divergent developmental programs of functional regions. At the same time, it may reflect changes in behavior, resulting in "bone functional adaptation" (Ruff et al., 2006) during an individual's lifetime.

CR values quantifying developmental and functional modularity can be directly compared with each other, because CR as a measure of modularity does not depend on the number of variables used to quantify each module (Adams, 2016) (in our case: the number of 3D landmark coordinates), nor does it depend on sample size (in our case: the number of

specimens per age class). Figure 5B shows that the integration of developmental units is generally lower (i.e., covariance ratio CR is lower) than that of functional units. In neonates, low levels of integration among developmental units contrast with high levels of integration among functional units. Toward adulthood, developmental and functional units reach similar levels of integration. One possible interpretation of these findings is that global structural constraints result in tradeoffs between developmental and functional modularity/integration. Higher levels of integration among one set of pelvic subunits imply less integration (thus more modularity) among the other set.

Earlier studies (Grabowski et al., 2011; Grabowski, 2012) suggested that, in the human compared to the great ape pelvis, differential selection pressures resulted in less integration – thus higher evolvability – of the birth canal region versus other pelvic regions. Our results provide evidence for a similar pattern in chimpanzees: the modular organization of obstetric versus locomotor pelvic regions implies that natural selection could act relatively independently on these regions, thus facilitating the evolvability of the pelvis as a whole, as well as the evolution of pelvic sexual dimorphism. Further research is necessary to evaluate whether this modular pattern is a shared feature of all great apes. A shared pattern would imply that the developmental and structural basis for the divergent evolution of hominin versus extant great ape pelves was already present in their last common ancestor, well before the evolution of taxon-specific terrestrial and arboreal locomotor adaptations in these groups.
The consistent (but statistically non-significant) pattern of sexual dimorphism (Fig. 4; Table 2) in the pelvic shape of adult chimpanzees also requires further investigation. While larger sample sizes are needed for a thorough statistical assessment of dimorphism, it is worth noting that the actual pattern of dimorphism (Fig. 4) reflects, to some extent, the proposed subdivision of the pelvis into functional units (Fig. 5A). Male-female shape differences are most conspicuous in the pelvic inlet region. It is thus likely that the evolution and development of pelvic sexual dimorphism is directly related to the modular evolution and development of functional pelvic units.

Furthermore, it is interesting to note that the pattern of pelvic sexual dimorphism in *Pan* revealed here (Fig. 4) is largely similar to the pattern of dimorphism described by Schultz (1949) for *Gorilla*, *Pongo*, *Hylobates*. Schultz (1949, p 412) notes that “Among all the adult primates the ischium length is, on an average, larger in males than in females of the same species, but the pubis length and the pelvic inlet breadth is larger in females than in males in at least those species in which total body size is not extremely different in the two sexes”.

Considering that pelvic sexual dimorphism in hominids is not due to obstetric constraints, Schultz (1949, p 419) further postulates that is most likely related to a "...very marked trend for divergent development of the two sexes". The currently available data indicate that pelvic sexual dimorphism in obstetrically unconstrained hominids (this study, Schultz, 1949; Tague, 2003) exhibits similar patterns as in obstetrically constrained hominid taxa such as hylobatids and humans (Huseynov et al., 2016; Zollikofer et al., accepted). We hypothesize that this represents a shared ancestral pattern of pelvic sexual dimorphism, which is unrelated to obstetric constraints but reflects a shared pattern of modular organization of the pelvis.

Two concepts that are often discussed in the context of modularity/integration and development are "network models" (Esteve-Altava et al., 2013), and the notion of "biological robustness" (Kitano, 2004). Within a biological network, regions with strong local interactions between nodes indicate modules, while global interactions reflect integration among modules. Robustness, on the other hand, "allows changes in the structure and components of the system owing to perturbations, but specific functions are maintained" (Kitano, 2004, p 827). Modularity is considered as one of the main mechanisms providing and maintaining robustness in a biological system (Kitano, 2004), because modular organization keeps perturbations of the system at the level of local networks (Callebaut and Rasskin-Gutman, 2005). At the same time, modularity is the basis for evolvability as well as for developmental plasticity, because different modules (i.e., local networks) can evolve relatively independently under different selective regimes, and develop independently in response to different functional and environmental constraints.

Using these concepts, it is possible to describe the pelvis as a biological network structure, where local interactions within developmental units are partially replaced during ontogeny by functional interactions among units, resulting in similar levels of developmental and functional modularity at adulthood. During early postnatal ontogeny, the localized developmental networks not only provide robusticity against external perturbations, but also permit developmental plasticity for *in-vivo* functional adaptation of the bony elements of the pelvis. Ontogenetic changes in the network structure further indicate that the evolvability and developmental plasticity of the pelvis cannot be fully assessed by focusing on adult patterns of covariation alone. Understanding how the network structure of the pelvis develops while maintaining both robusticity and sensitivity toward external factors is a prerequisite to understand how it evolves in response to different adaptive scenarios.

MATERIALS AND METHODS

The sample consists of n = 86 *Pan* specimens representing development from fetal stages to adulthood (details see Table 1). Since the three-dimensional morphology of the unfused pelvis critically depends on the presence of surrounding soft tissues, the sample comprises a large proportion of "wet" specimens (frozen or formalin/alcohol-preserved). The sample mostly comprises *P. troglodytes spp.* individuals (n = 83); due to the scarcity of suitable immature specimens, we included n = 3 *P. paniscus* individuals, and we combined the evidence available from wild and captive animals. Preliminary analyses showed that the immature pelvic morphology in our sample does not differ significantly between these two species. Data sources are the Collections of the Anthropological Institute (University of Zurich), and the Digital Morphology Museum of the Primate Research Institute (Kyoto University). During data preselection, cases showing congenital or acquired pathologies of the pelvic girdle were excluded from the sample. Actual individual ages at death were available for several immature zoo animals (n = 13). Ages at death of all other immature specimens were estimated from dental eruption patterns (Matsuzawa, 2006, p 11).

Volumetric data of all specimens were acquired with medical computed tomography (CT), using the following acquisition and image reconstruction parameters: beam collimation 1mm; in-plane pixel size between 0.2x0.2 and 0.7x0.7 mm^2, slice increment between 0.2 and 1.0 mm. 3D surface models of the bony pelvis were generated with Avizo 6.3.1 (FEI Visualization Sciences Group), and subsequent mesh cleaning was performed with Geomagic XOS (3D Systems). Only well-preserved pelves were utilized. Several specimens (chimpanzees: n = 8 with ages <2 years, and n = 16 with ages >8 years) required virtual reconstruction (completion of missing parts on one side with mirror-imaged counterparts) following previously published protocols (Zollikofer and Ponce de León, 2005; Ponce de León et al., 2008; Milella et al., 2015).

Pelvic shape was quantified with K = 377 3-dimensional anatomical landmarks, which denote locations of biological and/or geometric homology among specimens of the sample. These comprise fixed landmarks (K_f = 63), curve semilandmarks (K_c = 90), and surface semilandmarks (K_s = 224) (see supplementary Tables S1, S2, and Fig. 1). The fixed-landmark set comprises 14 landmark pairs, which eventually fuse during pelvic development. Surface semilandmarks were generated from an arbitrary specimen‘s point cloud, following the procedures described in (Gunz et al., 2005). In order to minimize among-specimen differences in user-defined semilandmark positions, iterative semilandmark sliding procedures were

applied (Gunz et al., 2005; Schlager, 2013). Semilandmark sliding was performed relative to the symmetrized mean configuration, using the minimum bending energy criterion. All procedures were performed with the R package Morpho, version 2.3.1.1. (Schlager, 2016). After convergence of the iterative sliding procedure, generalized procrustes analysis (GPA) was performed to represent the data in linearized procrustes shape space. Principal components analysis (PCA) was applied to reduce the dimensionality of the procrustes data, and to explore major patterns of shape variation in the sample. Graphs of the data scatter in the low-dimensional shape space represented by the first few principal components (PCs) were produced with software JMP, version 12.1 (Figs. 2A,B, 3). It should be noted that PCs represent statistical rather than biological entities, which facilitate the visualization of patterns of variation in multivariate data sets. In this study, the actual morphological patterns of pelvic shape change were visualized with stage-specific mean shapes (Fig. 2C). Similarly, patterns of pelvic sexual dimorphism were visualized by comparing mean adult female and male pelvic shapes (Fig. 4).

To test for sex-specific differences in pelvic shape, Procrustes ANOVA was performed with the R package geomorph, version 3.0.2 (Adams and Otárola Castillo, 2013; Adams et al., 2015). Since sample sizes per sex and age class are small, tests were performed on pooled age groups (see Table 2). To this end, data of each age group were centered to the age-group-specific mean prior to Procrustes ANOVA.

Analyses of modularity and integration were performed according to the methods proposed by Adams (2016). The proportion of covariance between versus within modules is typically measured by the RV coefficient (Klingenberg, 2009); however, RV has been shown to depend on the dimensionality of the multivariate data, and on sample size (Smilde et al., 2009; Adams, 2016). We thus use the covariance ratio (CR), which is insensitive to dimensionality and sample size (Adams, 2016).

Modularity was tested at four different developmental stages: perinatal, infant, juvenile, and adult (labeled A-D; see Table 1). To test for developmental modularity, landmarks were attributed to three subsets, corresponding to ilium, ischium and pubis. To test for functional modularity, landmarks were attributed to two subsets, representing structures hypothesized to be mainly involved in “obstetric” or “abdominal” functions (the pelvic inlet region), and structures hypothesized to be mainly involved in “non-obstetric” functions (mostly locomotor: muscle attachment regions). These subdivisions are illustrated in Figure 5A. While the developmental subdivision of the pelvis is straightforward, the functional subdivision

proposed here is based on previous observations and hypotheses (Lovejoy, 2005; Hirata et al., 2011; Grabowski, 2012; Gruss and Schmitt, 2015). Modularity/integration was also analyzed in left versus right coxal bones, as well as in "random modules" consisting of user-defined bilaterally symmetrical landmark patches. According to the hypotheses stated above, we expect that developmental modules become more integrated during ontogeny (CR increases), while functional modules become more independent of each other (CR decreases). We further expect in these analyses that CR < 1.0 (more within-module than between-module covariation). For left/right comparisons, we expect that CR > 1.0 (more between-module than within-module covariation). For "random modules", we expect CR ~ 1.0 (Adams, 2016).

ACKNOWLEDGEMENTS

We thank Naoki Morimoto (Kyoto University), Patrick Kircher (VetSuisse Faculty, University of Zurich), and Michael Thali (Institute of Forensic Medicine, University of Zurich) for acquiring/providing chimpanzee CT data. We also thank Ann Margvelashvili for help in assessing dental wear patterns in adult specimens. This study was supported by Swiss NSF grant #31003A_135470/1 to C. P. E. Z., and the A. H. Schultz Foundation.

Figures and Tables

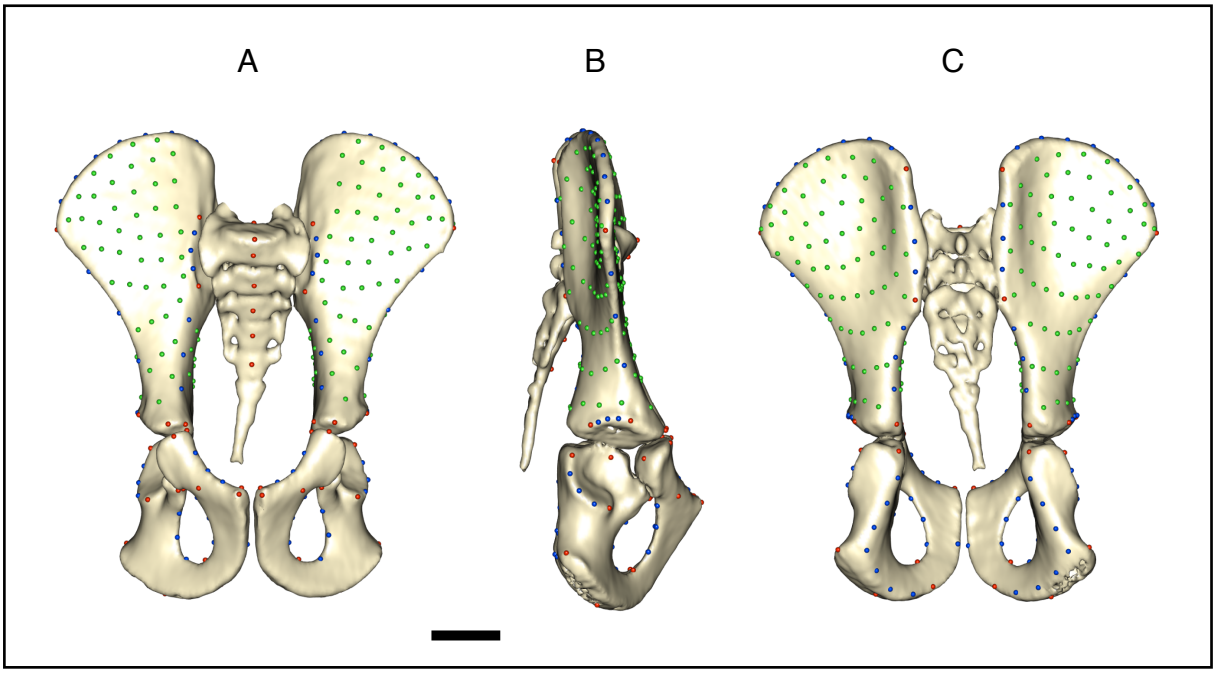

Fig. 1. Pelvic landmarks and semilandmarks. Red: fixed landmarks; blue: curve semilandmarks; green: surface semilandmarks. Anterior, lateral, and posterior views of an immature pelvis (scale bar is 2 cm).

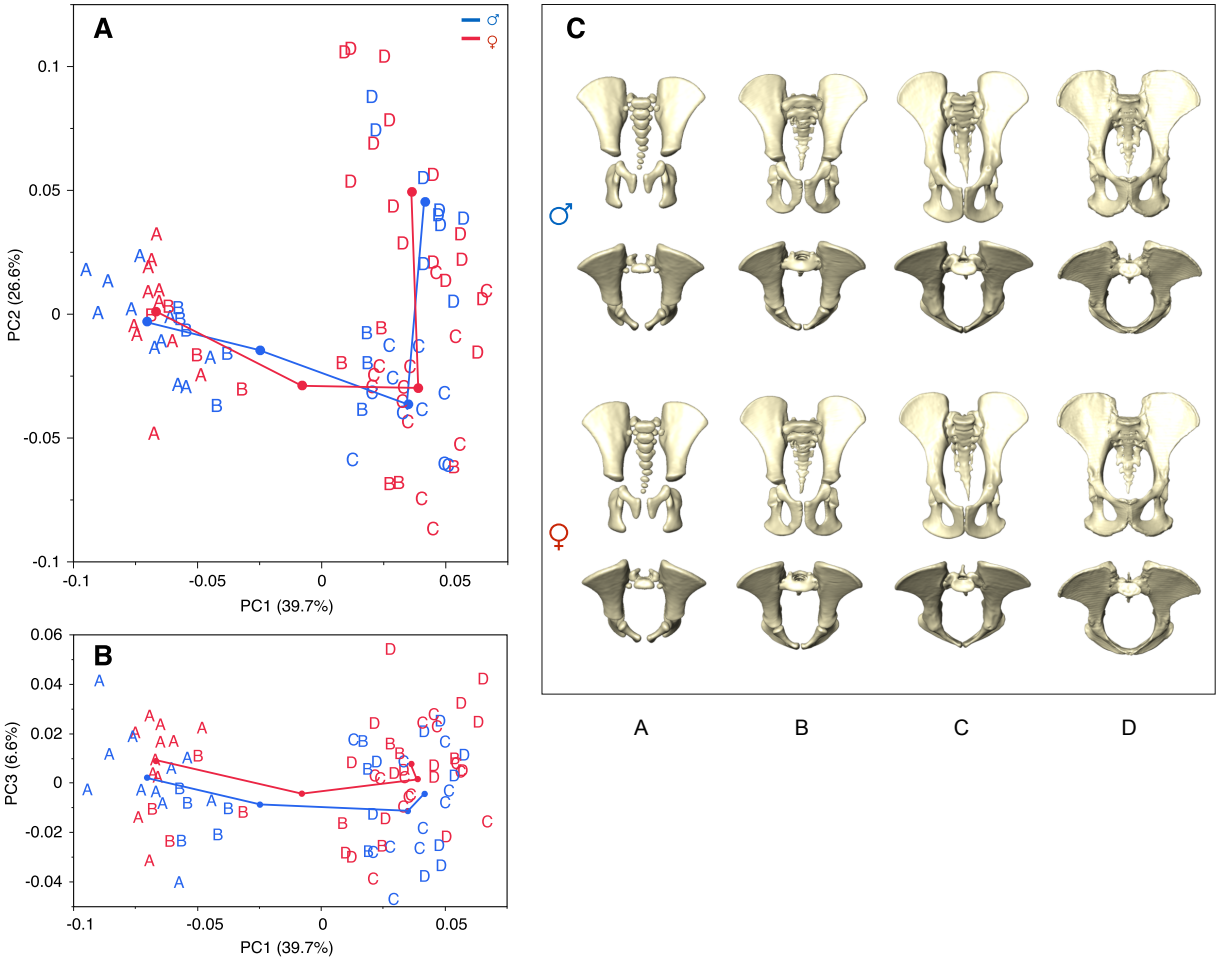

Fig. 2. Developmental changes in chimpanzee pelvic morphology from perinatal stage to adulthood. (A, B) Bivariate plots of shape variation along PC1 (39.7% of total sample variance), PC2 (26.6%) and PC3 (6.6%); red symbols: females; blue symbols: males (labels A-D denote four ontogenetic stages: A: perinatal; B: eruption of deciduous dentition; C: eruption of M1/M2, and D: M3 fully erupted). (C) Visualization of sex-specific and stage-specific pelvic mean shapes (anterior and superior views). To facilitate visual comparisons all shapes are represented at the same size (centroid size=1); see supplementary Figure S1 for visualizations of pelvic form (size and shape).

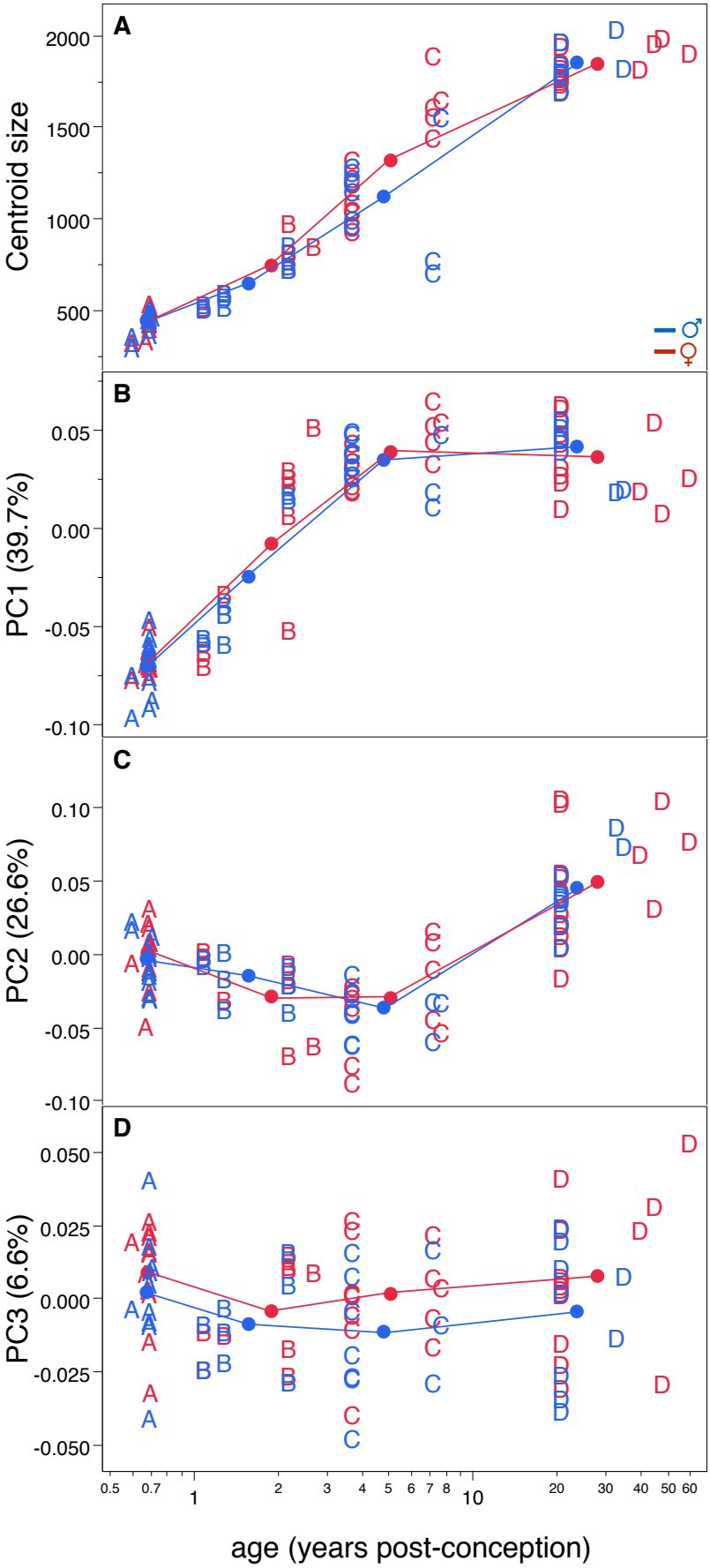

Fig. 3. Age-related change in chimpanzee pelvic size and shape. Colors and symbols as in Fig. 2; the age axis is scaled logarithmically in post-conception years (specimens with unknown age at death are assigned to stage-specific mean ages).

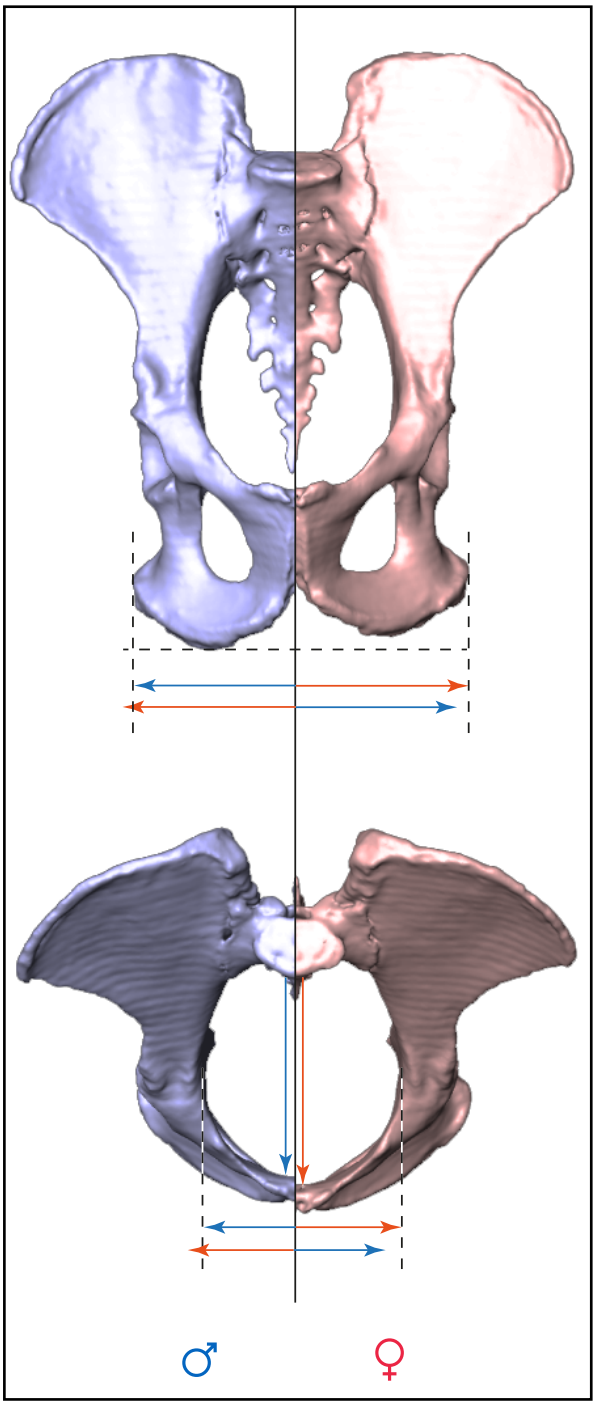

Fig. 4. Sexual dimorphism in the adult chimpanzee pelvis. Note more capacious inlet and outlet regions in females (red) compared to males (blue). The visualizations were generated by morphing the pelvic surface of one actual specimen into female and male mean shapes, respectively, using the landmarks defined in Tables S1 and S2 as nodes of a thin-plate spline interpolation function.

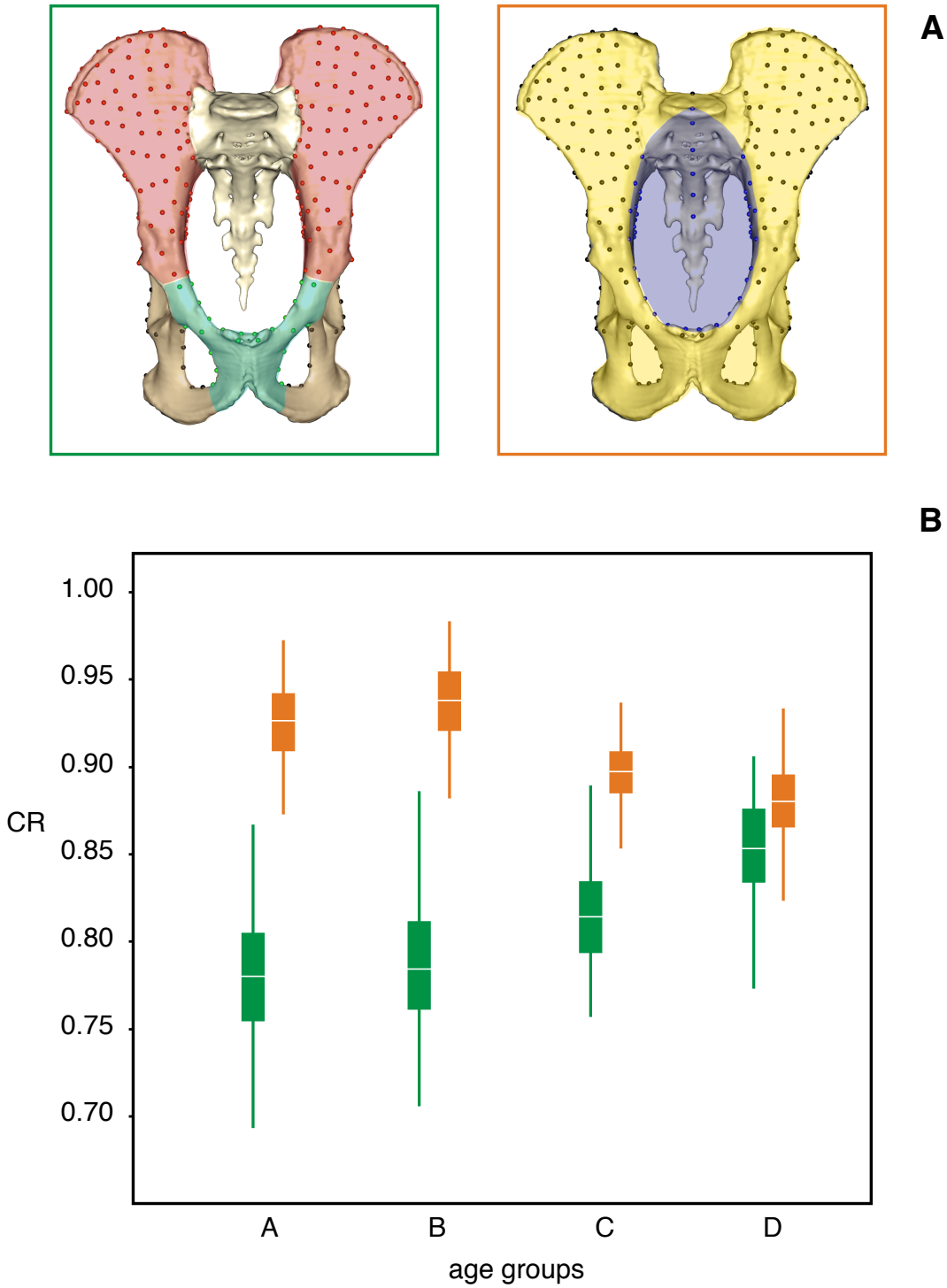

Fig. 5. Ontogenetic changes in covariation between pelvic units. (A) Visualization of developmental units (ilium: red, ischium: brown, pubis: light green) and functional units (obstetric/abdominal: blue, locomotor: yellow). (B) Ontogenetic changes in covariance ratio CR for developmental units (dark green symbols) and functional units (orange symbols); box-and-whisker symbols represent 25th, 50th, 75th percentiles, and range of CR distributions evaluated from 100 bootstrap samples. Note increase in CR from stages B to D for developmental units, and decrease for functional units.

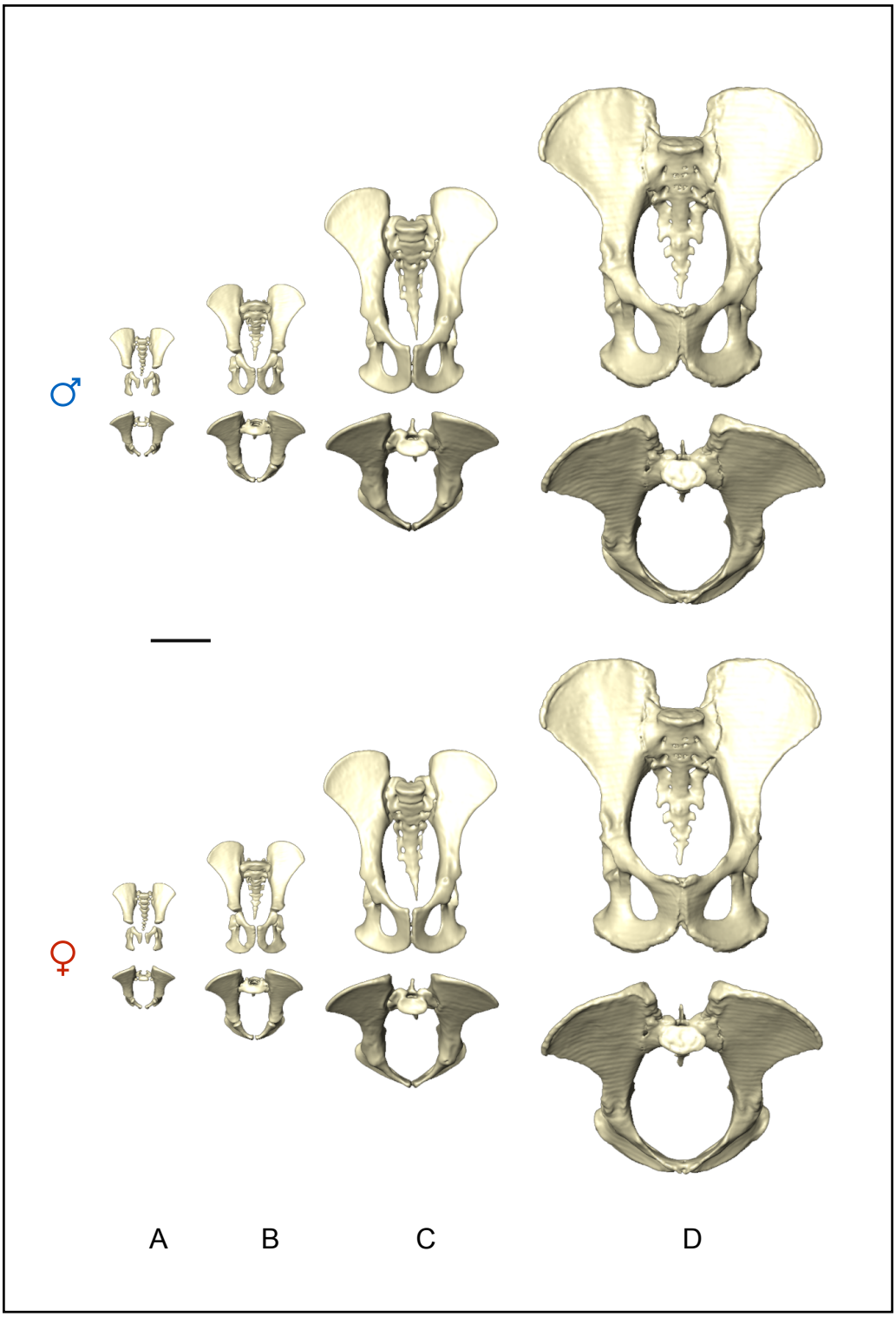

Fig. S1. Visualization of sex-specific and stage-specific pelvic mean forms (size and shape) at ontogenetic stages A to D (anterior and superior views; scale bar is 5cm).

Table 1. Sample structure.

Developmental stage	group label	age range, y	males	females	wet	dry	total
perinatal	A	-0.08 to 0.01	11	11	22	0	22
infants*	B	0.4 to 2	8	8+1	11	6	17
juveniles*	C	3 to 7	10	13	5	18	23
young adults	D	~20 to ~30	5+2	11	4	14	18
old adults	D	~30+	2	4	6	0	6

*infants include one, and juveniles include two bonobo specimens

Table 2. Comparison of female and male pelvic shapes at different developmental stages (results of Procrustes ANOVA).

Age range	df	SS	MS	Rsq	F	*P*
perinatal to infants	1	0.0034	0.0034	0.0262	0.9952	0.4006
Residuals	37	0.1272	0.0034			
Total	38	0.1306				
juvenile to adults	1	0.0061	0.0061	0.0269	1.2418	0.2577
Residuals	45	0.2196	0.0049			
Total	46	0.2256				
perinatal to adults	1	0.0054	0.0054	0.0147	1.2531	0.2248
Residuals	84	0.3608	0.0043			
Total	85	0.3661				

df, degrees of freedom; F, F-value; MS, mean square; *P* = P value; Rsq, R^2; SS, sum of squares.

Table 3. Ontogenetic changes in CR values.

	developmental units			functional units		
difference between stages[1]	mean	std error	*P*	mean	std error	*P*
A-B	0.0101	0.0048	0.1499	0.0111	0.0031	0.0021
B-C	0.0246	0.0048	<0.0001	0.0389	0.0031	<0.0001
C-D	0.0380	0.0048	<0.0001	0.0185	0.0031	<0.0001
regression slope[2]	0.0243	0.0015	<0.0001	-0.0178	0.0011	<0.0001

1 results of Tukey HSD test; 2 results of linear regression of CR on stages A-D; std error, standard error; *P* = P value.

Table S1. Definition of fixed landmarks.

LM number	Description
1-2	Pubic symphysis: superiormost anterior point
3-4	Pubic symphysis: superiormost posterior point
5-6	Ischiopubic juncture: pubis - posterior fusion point
7-8	Ischiopubic juncture: ischium - posterior fusion point
9-10	Ischiopubic juncture: pubis - obturator foramen inferior fusion point
11-12	Ischiopubic juncture: ischium - obturator foramen inferior fusion point
13-14	Ischiopubic juncture: pubis - obturator foramen superior fusion point
15-16	Ischiopubic juncture: ischium - obturator foramen superior fusion point
17-18	Ischium: posteriormost point (superior from ischial tuberosity)
19-20	Ischium: inferiormost midpoint
21-22	Ilioischial juncture: ischium - fusion point
23-24	Ilioischial juncture: ilium - fusion point
25-26	Ilioischial juncture: ischium - acetabulum lateral fusion point
27-28	Ilioischial juncture: ilium - acetabulum lateral fusion point
29-30	Acetabulum: superiormost lateral point
31-32	Acetabulum: point on pubic part of lunate surface
33-34	Iliopubic juncture: pubis - superior fusion point
35-36	Iliopubic juncture: ilium - superior fusion point
37-38	Iliopubic juncture: pubis - fusion point on pelvic brim
39-40	Iliopubic juncture: ilium - fusion point on pelvic brim
41-42	Pubis: anterior midpoint
43-44	Acetabulum: inferiormost lateral point on lunate surface
45-46	Acetabulum: deepest point on acetabular center (acetabular fossa)
47-48	Pelvic brim and sacroiliac joint: intersection point
49-50	Sacroiliac joint: superiormost point
51	S1: superiormost anterior point
52	S1: superiormost posterior point
53	S1: anterior midpoint
54	S2: anterior midpoint
55	S3: anterior midpoint
56	S4: anterior midpoint
57-58	Anterior supuperior iliac spine
59-60	Iliac crest: posteriormost point (end point)
61-62	Posterior inferior iliac spine
63	S5: anterior midpoint

Table S2. Definition of semilandmarks.

LM number	Description
Iliac crest	Right: start LM 57, end LM 59; Left: start LM 58, end LM 60 with eight subdivisions
Posterior iliac spines	Right: start LM 59, end LM 61; Left: start LM 60, end LM 62 with four subdivisions
Greater sciatic notch	Right: start LM 61, end LM 23; Left: start LM 62, end LM 24 with four subdivisions
Acetabulum: on ilium	Right: start LM 27, end LM 29; Left: start LM 28, end LM 30 with four subdivisions
Anterior iliac spines	Right: start LM 57, end LM 29; Left: start LM 58, end LM 30 with four subdivisions
Acetabulum: on ischium	Right: start LM 25, end LM 43; Left: start LM 26, end LM 44 with four subdivisions
Obturator foramen posterior	Right: start LM 15, end LM 11; Left: start LM 16, end LM 12 with four subdivisions
Obturator foramen anterior	Right: start LM 13, end LM 9; Left: start LM 14, end LM 10 with four subdivisions
Sacroiliac joint	Right: start LM 49, end LM 47; Left: start LM 50, end LM 48 with four subdivisions
Pelvic brim1	Right: start LM 47, end LM 39; Left: start LM 48, end LM 40 with four subdivisions
Pelvic brim2	Right: start LM 37, end LM 3; Left: start LM 38, end LM 4 with four subdivisions
Pubis posterior	Right: start LM 3, end LM 5; Left: startLeft: start LM 4, end LM 6 with two subdivisions
Ischium posterior	Right: start LM 7, end LM 21; Left: start LM 8, end LM 22 with eight subdivisions

References:

Abzhanov A, Kuo WP, Hartmann C, Grant BR, Grant PR, Tabin CJ. 2006. The calmodulin pathway and evolution of elongated beak morphology in Darwin's finches. Nature 442:563–567.

Abzhanov A, Protas M, Grant BR, Grant PR, Tabin CJ. 2004. Bmp4 and morphological variation of beaks in Darwin's finches. Science 305:1462–1465.

Adams DC, Collyer ML, Sherratt E. 2015. *geomorph*: Software for geometric morphometric analyses. R package version 2.1.7. http://cran.r-project.org/web/ packages/geomorph/ index.html. Available from: http://cran.r-project.org/web/ packages/geomorph/index.html

Adams DC, Otárola Castillo E. 2013. *geomorph*: an R package for the collection and analysis of geometric morphometric shape data. Methods Ecol Evol 4:393–399.

Adams DC. 2016. Evaluating modularity in morphometric data: challenges with the RV coefficient and a new test measure. Methods Ecol Evol 7:565–572.

Armbruster WS, Pélabon C, Bolstad GH, Hansen TF. 2014. Integrated phenotypes: understanding trait covariation in plants and animals. Philos Trans R Soc B 369:20130245–20130245.

Berge C. 1998. Heterochronic processes in human evolution: An ontogenetic analysis of the hominid pelvis. Am J Phys Anthropol 105:441–459.

Bernstein P, Crelin ES. 1967. Bony pelvic sexual dimorphism in the rat. Anat Rec 157:517–525.

Bookstein FL. 1997. Morphometric tools for landmark data: geometry and biology. Cambridge University Press.

Bookstein FL. 2016. The inappropriate symmetries of multivariate statistical analysis in geometric morphometrics. Evol Biol 43:277–313.

Callebaut W, Rasskin-Gutman D. 2005. Modularity. MIT Press.

Capellini TD, Handschuh K, Quintana L, Ferretti E, Di Giacomo G, Fantini S, Vaccari G, Clarke SL, Wenger AM, Bejerano G, Sharpe J, Zappavigna V, Selleri L. 2011. Control of pelvic girdle development by genes of the Pbx family and Emx2. Developmental Dynamics 240:1173–1189.

Clune J, Mouret J-B, Lipson H. 2013. The evolutionary origins of modularity. Proc R Soc B 280:20122863–20122863.

Delezene LK. 2015. Modularity of the anthropoid dentition: Implications for the evolution of the hominin canine honing complex. J Hum Evol 86:1–12.

Esteve-Altava B, Marugán Lobón J, Botella H, Bastir M, Rasskin-Gutman D. 2013. Grist for Riedl's mill: a network model perspective on the integration and modularity of the human skull. J Exp Zool B Mol Dev Evol 320:489–500.

Esteve-Altava B. 2015. Systematic review of the research on morphological modularity. bioRxiv:027144.

Gonzalez PN, Oyhenart EE, Hallgrimsson B. 2011. Effects of environmental perturbations during postnatal development on the phenotypic integration of the skull. J Exp Zool B Mol Dev Evol 316B:547–561.

González PN, Hallgrimsson B, Oyhenart EE. 2011. Developmental plasticity in covariance structure of the skull: effects of prenatal stress. J Anat 218:243–257.

Goswami A, Binder WJ, Meachen J, O'Keefe FR. 2015. The fossil record of phenotypic integration and modularity: A deep-time perspective on developmental and evolutionary dynamics. Proc Natl Acad Sci USA 112:4891–4896.

Goswami A, Polly PD. 2010. The influence of modularity on cranial morphological disparity in carnivora and primates (Mammalia). PLoS ONE 5:e9517.

Goswami A, Smaers JB, Soligo C, Polly PD. 2014. The macroevolutionary consequences of phenotypic integration: from development to deep time. Philos Trans R Soc B 369:20130254–20130254.

Grabowski MW, Polk JD, Roseman CC. 2011. Divergent patterns of integration and reduced constraint in the human hip and the origins of bipedalism. Evolution 65:1336–1356.

Grabowski MW. 2012. Hominin obstetrics and the evolution of constraints. Evol Biol 40:57–75.

Gruss LT, Schmitt D. 2015. The evolution of the human pelvis: changing adaptations to bipedalism, obstetrics and thermoregulation. Philos Trans R Soc Lond, B, Biol Sci 370:20140063–20140063.

Gunz P, Mitteroecker P, Bookstein FL. 2005. Semilandmarks in three dimensions. In: Slice DE, editor. Modern morphometrics in physical anthropology. Developments in Primatology: Progress and Prospects. New York: Kluwer Academic Publishers-Plenum Publishers. p 73–98.

Hallgrimsson B, Jamniczky H, Young NM, Rolian C, Parsons TE, Boughner JC, Marcucio RS. 2009. Deciphering the palimpsest: studying the relationship between morphological integration and phenotypic covariation. Evol Biol 36:355–376.

Hansen TF, Houle D. 2008. Measuring and comparing evolvability and constraint in multivariate characters. Journal of Evolutionary Biology 21:1201–1219.

Hansen TF. 2003. Is modularity necessary for evolvability? Remarks on the relationship between pleiotropy and evolvability. Biosystems 69:83–94.

Hendrikse JL, Parsons TE, Hallgrimsson B. 2007. Evolvability as the proper focus of evolutionary developmental biology. Evol Dev 9:393–401.

Hirata S, Fuwa K, Sugama K, Kusunoki K, Takeshita H. 2011. Mechanism of birth in chimpanzees: humans are not unique among primates. Biology Letters 7:686–688.

Huseynov A, Zollikofer CPE, Coudyzer W, Gascho D, Kellenberger C, Hinzpeter R, Ponce de León MS. 2016. Developmental evidence for obstetric adaptation of the human female pelvis. Proc Natl Acad Sci USA 113:5227–5232.

Iguchi T, Irisawa S, Fukazawa Y, Uesugi Y, Takasugi N. 1989. Morphometric analysis of the development of sexual dimorphism of the mouse pelvis. Anat Rec 224:490–494.

Kitano H. 2004. Biological robustness. Nat Rev Genet 5:826–837.

Klingenberg CP, Duttke S, Whelan S, KIM M. 2012. Developmental plasticity, morphological variation and evolvability: a multilevel analysis of morphometric integration in the shape of compound leaves. Journal of Evolutionary Biology 25:115–129.

Klingenberg CP, Marugán Lobón J. 2013. Evolutionary covariation in geometric morphometric data: analyzing integration, modularity, and allometry in a phylogenetic context. Syst Biol 62:591–610.

Klingenberg CP, Mebus K, Auffray JC. 2003. Developmental integration in a complex morphological structure: how distinct are the modules in the mouse mandible? Evol Dev 5:522–531.

Klingenberg CP, Zaklan SD. 2000. Morphological integration between development compartments in the Drosophila wing. Evolution 54:1273.

Klingenberg CP. 2004. Integration and modularity of quantitative trait locus effects on geometric shape in the mouse mandible. Genetics 166:1909–1921.

Klingenberg CP. 2005. Developmental constraints, modules, and evolvability. In: Hallgrimsson B, Hall BK, editors. Themes on Variation. San Diego: Academic Press. p 219–247.

Klingenberg CP. 2008. Morphological integration and developmental modularity. Annu Rev Ecol Evol Syst 39:115–132.

Klingenberg CP. 2009. Morphometric integration and modularity in configurations of landmarks: tools for evaluating a priori hypotheses. Evol Dev 11:405–421.

Klingenberg CP. 2010. Evolution and development of shape: integrating quantitative approaches. Nat Rev Genet 11:623–635.

Klingenberg CP. 2014. Studying morphological integration and modularity at multiple levels: concepts and analysis. Philos Trans R Soc Lond, B, Biol Sci 369:20130249.

Kuratani S. 2009. Modularity, comparative embryology and evo-devo: Developmental dissection of evolving body plans. Developmental Biology 332:61–69.

LaVelle M. 1995. Natural selection and developmental sexual variation in the human pelvis. Am J Phys Anthropol 98:59–72.

Lewton KL. 2012. Evolvability of the primate pelvic girdle. Evol Biol 39:126–139.

Lovejoy CO. 2005. The natural history of human gait and posture. Gait & Posture 21:95–112.

Matsuzawa T. 2006. Sociocognitive Development in Chimpanzees: A Synthesis of Laboratory Work and Fieldwork. In: Matsuzawa T, Tomonaga M, Tanaka M, editors. Cognitive Development in Chimpanzees. Cognitive Development in Chimpanzees. Tokyo: Springer-Verlag. p 3–33.

McGuigang K. 2006. Studying phenotypic evolution using multivariate quantitative genetics. Mol Ecol 15:883–896.

Melo D, Marroig G. 2015. Directional selection can drive the evolution of modularity in complex traits. Proc Natl Acad Sci USA 112:470–475.

Milella M, Zollikofer CPE, Ponce de León MS. 2015. Virtual reconstruction and geometric morphometrics as tools for paleopathology: a new approach to study rare developmental disorders of the skeleton. Anat Rec 298:335–345.

Mitteroecker P, Bookstein F. 2008. The evolutionary role of modularity and integration in the hominoid cranium. Evolution 62:943–958.

Pomikal C, Streicher J. 2010. 4D−analysis of early pelvic girdle development in the mouse (Mus musculus). J Morphol 271:116–126.

Ponce de León MS, Golovanova L, Doronichev V, Romanova G, Akazawa T, Kondo O, Ishida H, Zollikofer CPE. 2008. Neanderthal brain size at birth provides insights into the evolution of human life history. Proc Natl Acad Sci USA 105:13764–13768.

Rolian C. 2014. Genes, development, and evolvability in primate evolution. Evol Anthropol 23:93–104.

Ruff C, Holt B, Trinkaus E. 2006. Who's afraid of the big bad Wolff?: 'Wolff's law' and bone functional adaptation. Am J Phys Anthropol 129:484–498.

Scheuer L, Black S, Cunningham C. 2000. Developmental juvenile osteology. London: Academic Press.

Schlager S. 2013. Soft-tissue reconstruction of the human nose: population differences and sexual dimorphism. PhD thesis. Universität Freiburg. Available from: http://www.freidok.uni-freiburg.de/volltexte/9181/

Schlager S. 2016. Morpho: Calculations and visualisations related to geometric morphometrics. R package version 2.3.1.1. Available from: http://sourceforge.net/projects/morpho-rpackage/ https://github.com/zarquon42b/Morpho

Schultz AH. 1949. Sex differences in the pelves of primates. Am J Phys Anthropol 7:401–423.

Smilde AK, Kiers HAL, Bijlsma S, Rubingh CM, van Erk MJ. 2009. Matrix correlations for high-dimensional data: the modified RV-coefficient. Bioinformatics 25:401–405.

Striedter GF. 2005. Principles of brain evolution (Sinauer, Sunderland, MA).

Tague RG. 2003. Pelvic sexual dimorphism in a metatherian, Didelphis Virginiana: implications for eutherians. Journal of Mammalogy 84:1464–1473.

Tague RG. 2005. Big-bodied males help us recognize that females have big pelves. Am J Phys Anthropol 127:392–405.

Uesugi Y, Taguchi O, Noumura T, Iguchi T. 1992. Effects of sex steroids on the development of sexual dimorphism in mouse innominate bone. Anat Rec 234:541–548.

Wagner GP, Pavlicev M, Cheverud JM. 2007. The road to modularity. Nat Rev Genet 8:921–931.

Wagner GP, Zhang J. 2011. The pleiotropic structure of the genotype–phenotype map: the evolvability of complex organisms. Nat Rev Genet 12:204–213.

Wagner GP. 1990. A comparative study of morphological integration in Apis mellifera (Insecta, Hymenoptera). Journal of Zoological Systematics and Evolutionary Research 28:48–61.

Wells JCK, DeSilva JM, Stock JT. 2012. The obstetric dilemma: an ancient game of Russian roulette, or a variable dilemma sensitive to ecology? Am J Phys Anthropol 149:40–71.

Wells JCK. 2015. Between Scylla and Charybdis: renegotiating resolution of the "obstetric dilemma" in response to ecological change. Philos Trans R Soc Lond, B, Biol Sci 370:20140067–20140067.

Williams FL, Orban R. 2007. Ontogeny and phylogeny of the pelvis in Gorilla, Pongo, Pan, Australopithecus and Homo. Folia Primatol 78:99–117.

Willmore KE, Leamy L, Hallgrimsson B. 2006. Effects of developmental and functional interactions on mouse cranial variability through late ontogeny. Evol Dev 8:550–567.

Young NM, Wagner GP, Hallgrimsson B. 2010. Development and the evolvability of human limbs. Proc Natl Acad Sci USA 107:3400–3405.

Zelditch ML, Mezey J, Sheets HD, Lundrigan BL, Garland T. 2006. Developmental regulation of skull morphology II: ontogenetic dynamics of covariance. Evol Dev 8:46–60.

Zelditch ML, Wood AR, Bonett RM, Swiderski DL. 2008. Modularity of the rodent mandible: Integrating bones, muscles, and teeth. Evol Dev 10:756–768.

Zollikofer CPE, Ponce de León MS. 2005. Virtual reconstruction: a primer in computer-assisted paleontology and biomedicine. Hoboken, N. J.: Wiley-Liss.

Zollikofer CPE, Scherrer M, Ponce de León MS. (*accepted*). Development of pelvic sexual dimorphism in hylobatids: testing the obstetric constraints hypothesis. Anat Rec.

Chapter 3

Shared patterns of adult pelvic sexual dimorphism in great apes and humans

Reference: *ready to submit to Scientific Reports*

Abstract

Adult modern humans exhibit a strong sexual dimorphism in the pelvis, which is typically interpreted as an obstetric adaptation to give birth to large-brained, large-bodied babies. In contrast, the great apes are obstetrically unconstrained and exhibit only little adult pelvic sexual dimorphism. Here we investigate commonalities and differences between great ape and human patterns of dimorphism with methods of biomedical imaging and geometric morphometrics. The results show that the basic patterns of pelvic sexual dimorphism in adult chimpanzees, gorillas and orangutans are similar to the human pattern, although less expressed in birth canal dimensions such as inlet and outlet pelvic regions, as well as inter-spinal and inter-ischial dimensions. These findings indicate a shared ancestral pattern of pelvic sexual dimorphism in great apes and humans, which likely evolved before the evolution of obstetric constraints and bipedal locomotion in the human lineage.

Key words: pelvis, adult, sexual dimorphism, great apes, humans

INTRODUCTION

Differences between males and females in various body parts or body dimensions are known as somatic sexual dimorphism (Badyaev, 2002; McPherson and Chenoweth, 2012), and are typically the result of hormonally regulated sex-biased autosomal gene expression (Williams and Carroll, 2009; Callewaert et al., 2010; Parsch and Ellegren, 2013). Such sex-specific differences are especially marked in the human pelvis, but also present in non-human primates (Schultz, 1949; Leutenegger, 1970; Gingerich, 1972; Leutenegger, 1974; Rosenberg, 1992; LaVelle, 1995; Tague, 1995; Lovejoy, 2005; Wittman and Wall, 2007; Weiner et al., 2008; Gruss and Schmitt, 2015; Wells, 2015; Huseynov et al., 2016; Ponce de León et al., 2016), in rodents (Bernstein and Crelin, 1967; Iguchi et al., 1989; Uesugi et al., 1992; Berdnikovs et al., 2006) and other vertebrates (Chapman et al., 1994; Tague, 2003).

It is generally agreed that the human female pelvis is adapted to obstetric constraints. Accordingly, pelvic sexual dimorphism (PSD) has traditionally been explained by the obstetrical dilemma (OD) hypothesis (Washburn, 1960) where antagonistic selective regimes constitute the "dilemma": selection for biomechanical efficiency (narrow pelves) versus selection for large-brained/large-bodied neonates requiring obstetrical efficiency (wide female pelves) (Rosenberg, 1992; LaVelle, 1995). The OD hypothesis, however, has recently been questioned along several lines of evidence. Direct experimental measurements indicate that there is no correlation between pelvic width and locomotor efficiency (Dunsworth et al., 2012; Warrener et al., 2014), and it appears that human birth is constrained by metabolic limitations of the mother rather than the tight fit between the female pelvis and the neonate head (Dunsworth et al., 2012). On the other hand, a recent study showed that human PSD largely results from changes in female (rather than male) pelvic morphology, which are correlated with changes in estradiol levels during puberty, and again during postmenopausal live (Huseynov et al., 2016; Ponce de León et al., 2016). Human pelvic morphology thus exhibits a certain level of developmental plasticity (Wilson, 1894) in response to changing physiological and environmental factors (Wells et al., 2012; Wells, 2015).

PSD in apes has been shown to be minimal compared to that observed in humans (Schultz, 1949; Tague, 2005). The relationship between PSD and body size [femoral size] dimorphism has only weak correlation, and body mass dimorphism is not associated with PSD in primates including humans (Schultz, 1949; Tague, 2005). Intriguingly, however, there is evidence that PSD in the obstetrically unconstrained great apes (Schultz, 1949; Tague, 2003; Huseynov et al., accepted) exhibits similar patterns as in obstetrically constrained

species such as humans and gibbons (*Hylobates lar*) (Huseynov et al., 2016; Zollikofer et al., accepted). This suggests that the evolution of PSD in apes predates the evolution of obstetric constraints. Based on these observations, we analyze patterns of PSD in chimpanzees, gorillas and orangutans, compare them with PSD in humans, and test the hypothesis of PSD pattern similarity among these species. Support for this hypothesis would indicate a shared ancestral pattern of PSD, whose evolutionary origins are unrelated to obstetric constraints. According to this hypothesis, the PSD of modern humans does not represent evolutionary novelty, but reflects a basal great-ape pattern that had increased in magnitude because of obstetric selection.

RESULTS

Three-dimensional (3D) pelvic shape was quantified in a sample of adult humans and great apes (humans: *n*=174; chimpanzees: *n*=24; gorillas: *n*=19; and orangutans: *n*=14; see also Table 1), using methods of Computed Tomography (CT) and geometric morphometrics (see Materials and Methods). Figure 1.A graphs pelvic shape variation in great apes and humans along the first three principal components (PCs) of shape space. PC1, which accounts for 84 % of the total sample variance, captures major differences between human and great ape pelvic morphologies, PC2 (5%) mostly captures species-specific differences, and PC3 (3%) reflects the sex-specific differences within species. Figure 1.B visualizes species-specific pelvic mean shapes, as well as pelvic sexual dimorphism within each species. The figure reproduces the well-known differences between human and great ape pelvic morphologies, such as a more anteroposterior orientation of the iliac blades, and supero-inferiorly reduced versus anteroposterior increased overall dimensions of the human pelvis. In all species, however, the female compared to the male pelvis exhibits relatively wider inlet and outlet regions, and larger inter-spinal and inter-ischial dimensions.

Figure 2 represents a heat map and dendrograms of the phenetic distances between taxon-specific pelvic mean shapes in morphospace. These distance values are color-coded from lower (towards dark red) to larger (towards light yellow) distances. Here the relatively small average distance is observed between *Homo* and *Gorilla* (0.284, p=0.001) as opposed to *Homo* and *Pan* (0.364, p=0.001) distance, while *Homo* and *Pongo* distances take an intermediate position (0.312, p=0.001).

Given the general similarity of PSD patterns among species (Fig. 1A) we analyze shared patterns of PSD in greater detail . Figure 3.A graphs pelvic shape variation in the

pooled great ape and human sample adjusted for species-mean differences (see Materials and Methods). PC1 (22% of total sample variation) accounts for variation among sexes, while PC2 (19%) captures a shared human-great ape pattern of between-sex variation. Figure 4 graphs (in the same manner as Fig. 2) the heat map and phenetic dendrograms of distances between male and female group means of taxon-adjusted great ape and human data. This basically shows that – after adjustment for species-mean differences – the major shape differences are between sexes, not between taxa. Here the significant differences are observed between average great ape male and female groups (0.026, p=0.007) as well as human male and female average distance values (0.050, p=0.001) as expected. Additionally perform Procrustes ANOVA that show similar results (as in Fig. 4) for significant great ape and human PSD (see Table 2). The sexual size dimorphism as indicated by mean centroid size per sex and per taxon looks generally similar for *Homo* and *Pan*, little more different in *Pongo*, and even more different *Gorilla*, such differences are correlated with average body weight (in general: r^2=0.84; for males: r^2=0.95; for females: r^2=0.76) where males typically weigh more than females (see Fig. 5, body weight data taken from National Primate Research Center http://pin.primate.wisc.edu, and National Center for Health Statistics http://www.cdc.gov/nchs/). Size related shape variation was evaluated via regression of all PCs on centroid size for taxon-adjusted and non-adjusted data: only PC2 (5%) of non-adjusted data yielded significant correlation with centroid size (males: r^2=0.53; females: r^2=0.31), and on taxon-adjusted data only PC1 (22%) correlates weakly with taxon-adjusted centroid size (males: r=0.31, r^2=0.10; females: r=0.32, r^2=0.11).

DISCUSSION

Our findings show that great apes and humans share largely similar patterns of sexual dimorphism in pelvic shape (Fig. 1, 3-4). Taxon-specific sex-neutral and the actual taxon-specific male-female pelvic morphologies differ fundamentally *between* species, however *within* species the pattern of PSD is largely similar. However, the magnitude of sexual dimorphism (measured as the shape distance between female and male mean shapes) is clearly large in humans than in great apes. Overall, these data provide support for the hypothesis of shared processes of sex-specific development in humans and great apes that predate the evolution of obstetric constraints in hominins. This is consistent with previous hypothesis that human PSD have evolved via disruptive selection (LaVelle, 1995), so that

males and female have different adaptive (fitness) peaks most probably due to different reproductive strategies and relative investment in offspring raising, sometimes called the Bateman's principle (Bateman, 1948).

The question is why did PSD evolve? Schultz (1949) suggested that PSD is due to a "...very marked trend for divergent development of the two sexes" (Schultz, 1949, p 419), and/or global somatic sex-specific differences are partly reflected in pelvis. However, the primary sexual differences in reproductive organs might be linked to sex-specific internal/ abdominal organ configuration and partially reflect great ape PSD. On the other hand, correlation between average pelvic centroid size and average body mass in great ape and humans might indicate that the size of the pelvis is a good estimator of body size or weight in general. Gorillas and orangutans show greater sex-specific differences in body size (in both centroid size and in body mass) whereas humans and chimpanzees exhibit only moderate pattern (Fig. 5).

Despite close phylogenetic distance between humans and chimpanzees (Perelman et al., 2012) pelvis shape data shows that humans are more closer to gorillas than to chimpanzees (Fig. 1B-C, Fig. 2). This suggests that shared phylogenetic similarities do not always mean shared phenotypic/morphological similarities of closely related species. Greater similarity of human pelvic shape with gorillas than chimpanzees or orangutans (Fig. 1-2) was previously observed (Marchal, 2000; Lycett and Cramon-Taubadel, 2013) and interpreted as: "...possibility for this convergence in pelvic shape … due to loading factors (i.e., upper body mass in the case of *Gorilla* and bipedal locomotion in the case of *Homo*)" (Lycett and Cramon-Taubadel, 2013), or alternatively, because humans and gorillas are morphologically closer to the ancestral/basal state of pelvic shape than chimpanzees (Almécija et al., 2013). However this could also be due to species-specific molecular/developmental programs that probably lead to phenotypic convergence (Rosenblum et al., 2014). Also, the lack of a phylogenetic signal indicates that pelvic morphology does not follow a pattern of "neutral evolution" but rather represents taxon-specific adaptations. Moreover, pelvis may also possess relatively high degree of phenotypic plasticity in general, so that in order to "see the phylogeny in pelvis" or any other possible structure one would need to look at mid-embryonic development of great apes and humans (i.e pharyngula/phylotypic stage) where the embryos look most alike (Gilbert, 2013). Such evidence, also called the developmental hourglass model, already exist for most vertebrates (Domazet-Lošo and Tautz, 2010; Kalinka et al., 2010; Irie and Kuratani, 2011; Gilbert, 2013; Piasecka et al., 2013; Wang et al., 2013).

These results are puzzling and interesting at the same time, here we may conclude that sex-related differences in great ape and human pelvic morphology is likely due to shared processes of sex-specific development. Finally, we assume that modular developmental programs (Klingenberg, 2014; Huseynov et al., accepted) are crucial for facilitating evolution and development of PSD in primates, pointing to a shared pattern of modular organization of the pelvis. Relative independence of both developmental (ilium, ischium and pubis) and functional (obstetric versus other functions) pelvic modules at different ontogenetic stages would let natural selection to act differently on each module resulting in less integration and high evolvability of primate pelvis in general (Grabowski et al., 2011; Grabowski, 2012; Lewton, 2012; Rolian, 2014; Huseynov et al., accepted).

MATERIALS AND METHODS

Our sample size consists of *n*=174 *Homo sapiens*, *n*=24 *Pan troglodytes spp.*, *n*=19 *Gorilla gorilla spp.*, and *n*=14 *Pongo spp.* adult specimens, total great ape sample makes up *n*=57 specimens (see Table 1 for details). Because the adult sample size per great ape taxon is relatively small (see again Table 1) we performed mean-centering procedures (using multiple regressions) removing the taxon-specific differences between great apes and humans which resulted in a pooled dataset and relatively larger sample sizes for great ape males *n*=30 and females *n*=27 (see Table 1). Great ape data sources are the Collections of the Anthropological Institute (University of Zurich), and the Digital Morphology Museum of the Primate Research Institute (Kyoto University), human data consist of mixed forensic cases from the Virtopsy® data base of the Institute of Forensic Medicine of the University of Zurich and the digital autopsy data base of the Catholic University of Leuven, Belgium (KU Leuven), and clinical data sets from the Institute of Diagnostic and Interventional Radiology of the University of Zurich as well as clinical data sets freely available from the OsiriX web-page (http://www.osirix-viewer.com). During data preselection, cases showing congenital or acquired pathologies of the pelvic girdle were excluded from the sample.

Volumetric data of all specimens were acquired with medical computed tomography (CT), using the following acquisition and image reconstruction parameters: beam collimation 1mm; in-plane pixel size between 0.2x0.2 and 0.7x0.7 mm^2, slice increment between 0.2 and 1.0 mm. 3D surface models of the bony pelvis were generated with Avizo 6.3.1 (FEI Visualization Sciences Group), and subsequent mesh cleaning was performed with Geomagic XOS (3D Systems). Only well-preserved pelves were utilized. Some specimens (humans: *n*=14 with

ages between 50 and 80 years; chimpanzees: n=8; gorilla: n=12; orangutans: n=6) required virtual reconstruction (completion of missing parts on one side with mirror-imaged counterparts, and of virtual alignment of coxal bones with sacrum) following previously published protocols (Zollikofer and Ponce de León, 2005; Ponce de León et al., 2008; Milella et al., 2015).

The shape of the pelvis was quantified with K=377 3D anatomical landmarks, which denote locations of biological and/or geometric homology among specimens of the sample. These consist of fixed landmarks (K_f=63), curve semilandmarks (K_c=90), and surface (K_s=224) (see Tables S1-S2, and Fig. S1). The fixed landmarks set comprises 14 landmark pairs, which eventually fuse during pelvic development. For geometric morphometric analyses, the mean position was calculated for each pair, resulting in K_f=49 fixed landmarks, and a total of K=363 landmarks. Surface semilandmarks were generated from an arbitrary specimen's point cloud, following the procedures described in ref. (Gunz et al., 2005), although alternative methods can be used (Schlager and Goepper, 2016; Rüdell and Schlager). In order to minimize among-specimen differences in user-defined semilandmarks positions, iterative semilandmark sliding procedures as described in ref. (Gunz et al., 2005) were applied. Semilandmark sliding was performed relative to the symmetrized mean configuration, using the minimum bending energy criterion. All procedures were performed with the R package Morpho, version 2.3.1.1. (Schlager, 2016). We performed principal components analysis (PCA) to reduce the dimensionality of the procrustes data, and to explore major patterns of shape variation in the sample. Graphs of the data scatter in the low-dimensional shape space represented by the first few principal components (PCs) were produced with software JMP, version 12.1. It should be noted that PCs represent statistical rather than biological entities, which facilitate the visualization of patterns of variation in multivariate data sets. In this study, the actual morphological patterns of pelvic shape change were visualized with stage-specific mean shapes. Similarly, patterns of pelvic sexual dimorphism were visualized by comparing mean adult female and male pelvic shapes. To test for differences between male and female pelvic shapes (Table S2), Procrustes ANOVA was performed using the R package geomorph, version 3.0.2 (Adams and Otárola Castillo, 2013; Adams et al., 2015), and distance matrices of between male and female group means were computed using R package Morpho, version 2.3.1.1. (Schlager, 2016).

ACKNOWLEDGEMENTS

We would like to thank Naoki Morimoto (Kyoto University), Marco Milella (University of Zurich) Patrick Kircher (VetSuisse Faculty, University of Zurich) for acquiring/providing great ape CT data, and Michael Thali, Dominic Gascho, Lars Ebert, Steffen Ross (Institute of Forensic Medicine, University of Zurich) and Wim Develter (Katholieke University Leuven) for preparing the anonymized forensic data, and Ricarda Hinzpeter (University Hospital of Zurich) for preparing anonymized clinical data. This study was supported by Swiss NSF grant #31003A_135470/1 to C. P. E. Z., and the A. H. Schultz Foundation.

Figures and Tables

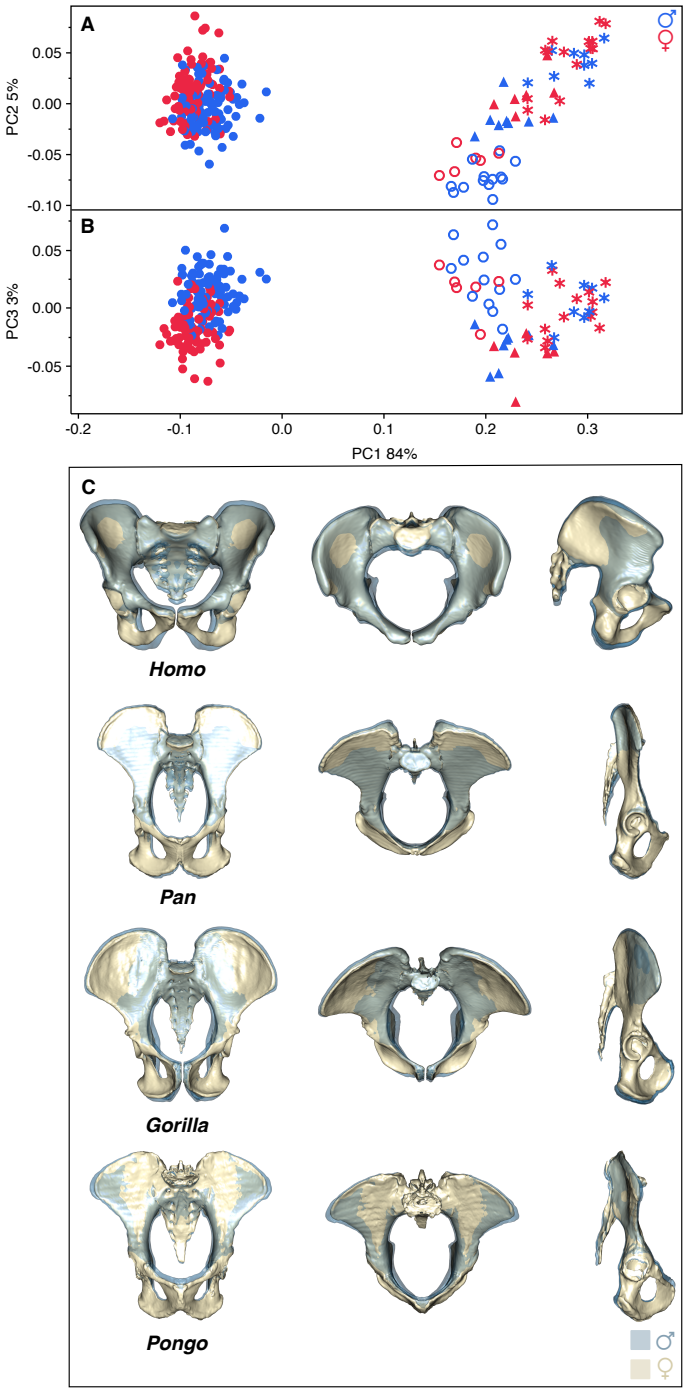

Fig. 1. Pelvic shape variation in adult great apes and humans. (A and B) Bivariate plots of shape variation along PC1 (84% of total sample variance) and PC2 (5%) (B), and along PC1 and PC3 (3%) (B). Red symbols are females and blue are males; filled circles indicate humans, stars indicate chimpanzees, open circles indicate gorilla, and filled triangles indicate orangutans. (C) Anterior, superior and lateral views showing female (solid) and male (transparent) pelvic mean shapes of humans and great ape species; note shared/similar male-female differences between humans and great apes.

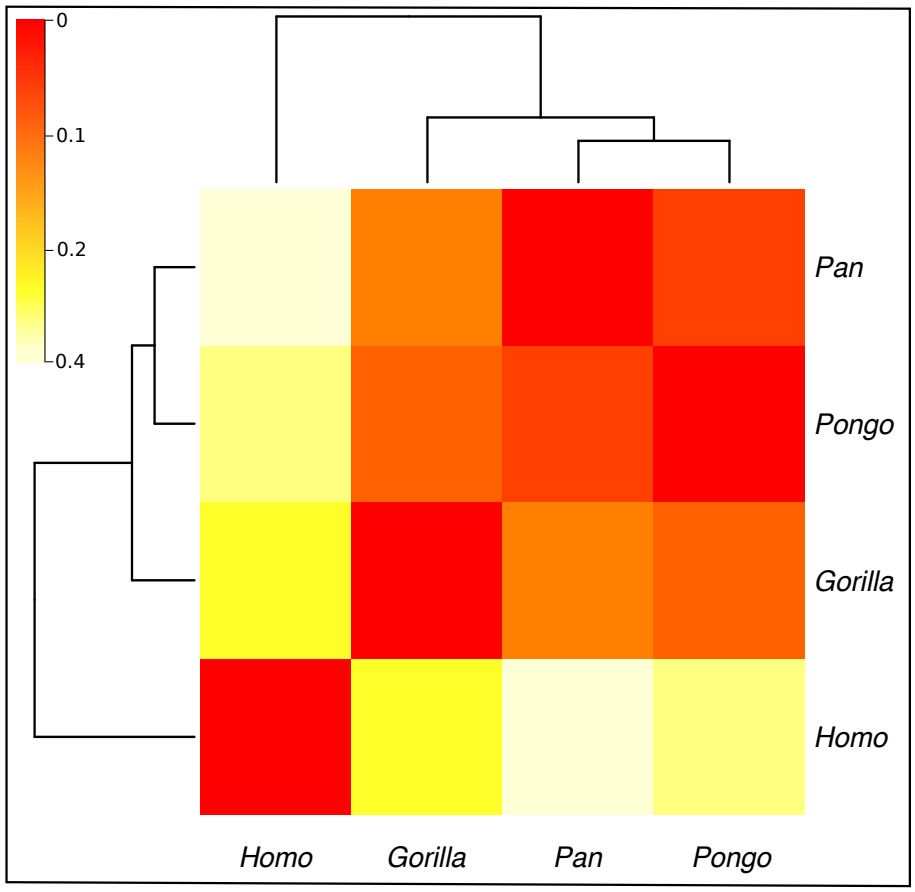

Fig. 2. Heat map and phenetic dendrograms of distance matrix (color coded) between taxon-specific group means of great apes and humans. Note relatively small average distance between *Homo* and *Gorilla* versus larger *Homo* and *Pan* distance. The relative distance values are color-coded from lower (towards dark red) to larger (towards light yellow) distances.

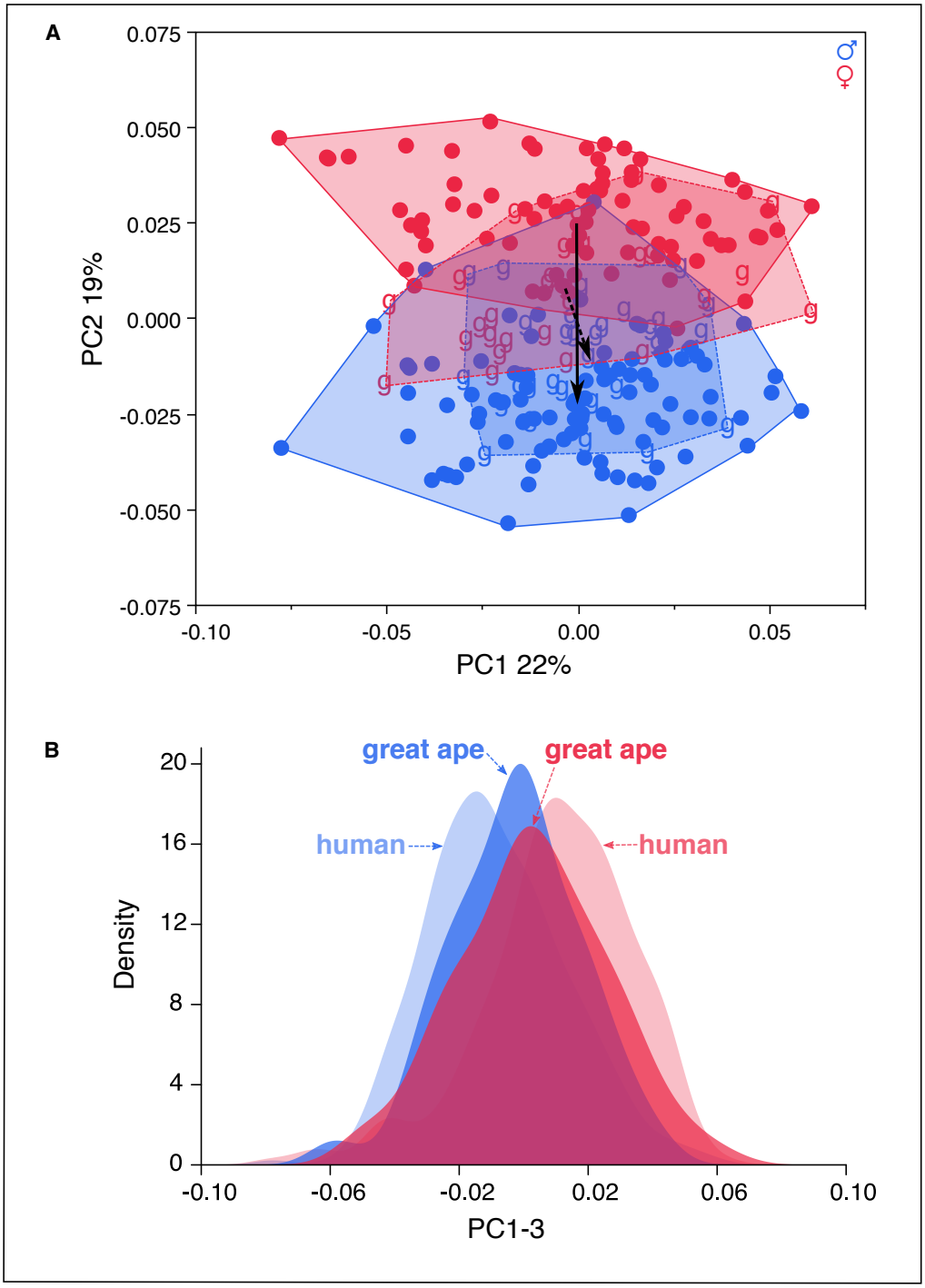

Fig. 3. Patterns of pelvic shape variation in the pooled great ape and human sample adjusted for species-mean differences. (A) Bivariate plots of variation along PC1 (22 % of total sample variance) and PC2 (19%); red/blue: females/males; filled circles: humans, letter g: great apes; dashed contours indicate convex hulls around female/male great apes; solid contours are for humans; arrows connect female and male average values indicating similarity of great ape and human patterns. (B) Density plot of histogram for the first three PCs (51% of total sample variance); note the intermediate position of great ape males and females to relative to those of humans.

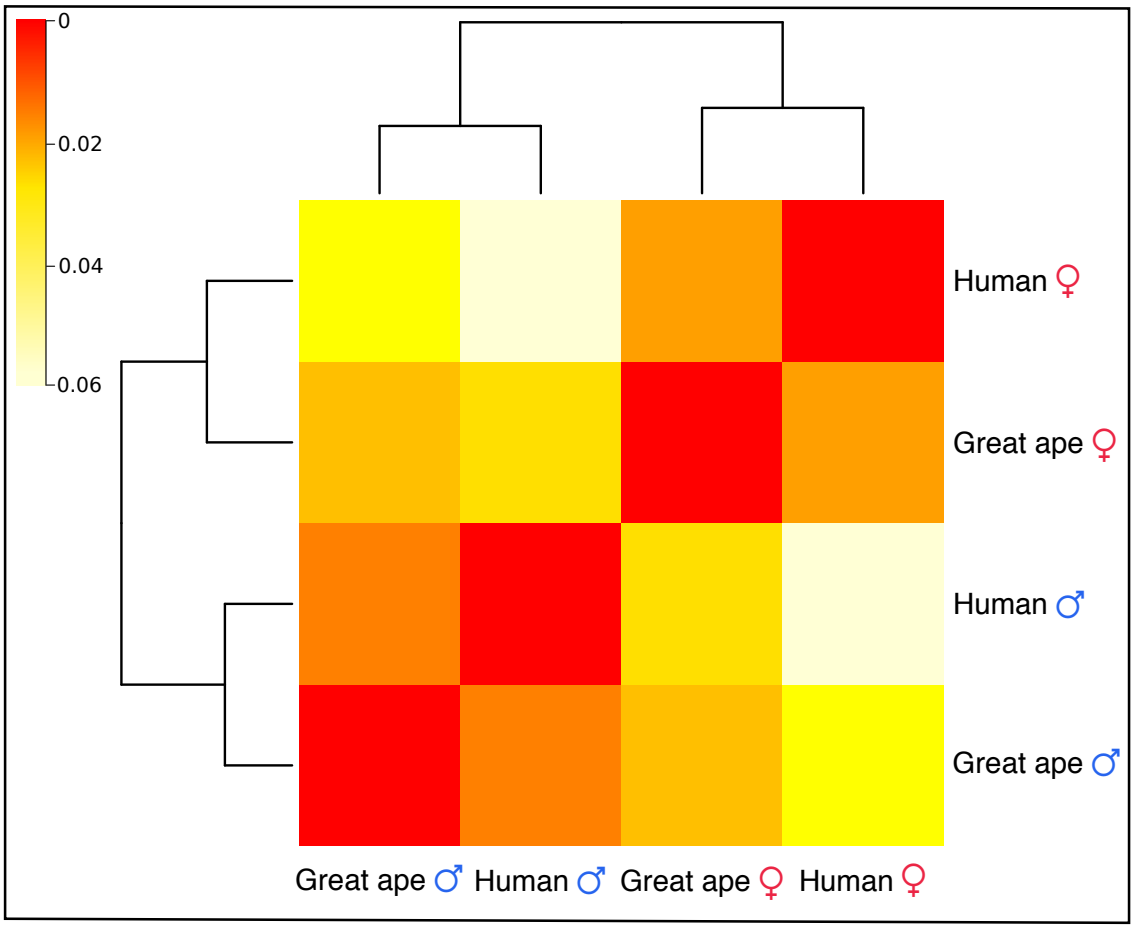

Fig. 4. Heat map and phenetic dendrograms of distance matrix (color coded) between male and female group means of taxon-adjusted great ape and human data. Note the significant difference between great ape male and female group means. The relative distance values are color-coded from lower (towards dark red) to larger (towards light yellow) distances.

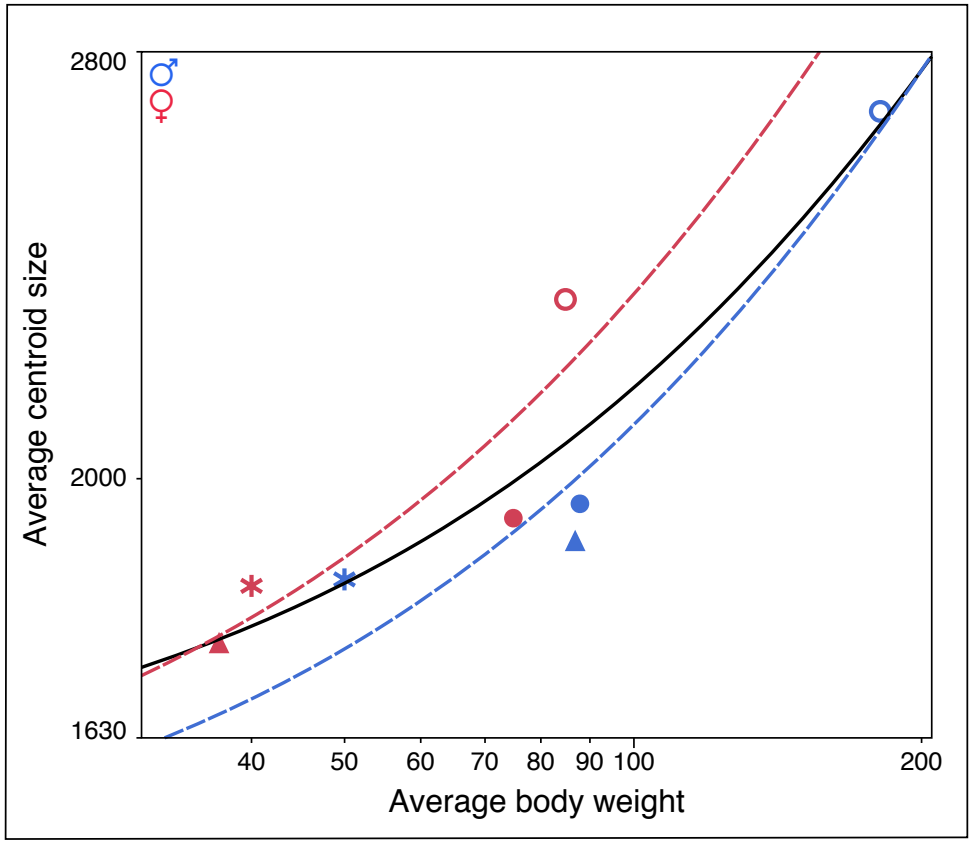

Fig. 5. Correlation plot of sex-specific differences in average adult pelvic size (centroid size) and average body weight for great apes and humans. Regressions sex-specific (dashed line, colors and symbols as in Fig.1) and sex-neutral (solid line, black color); the axes are scaled logarithmically.

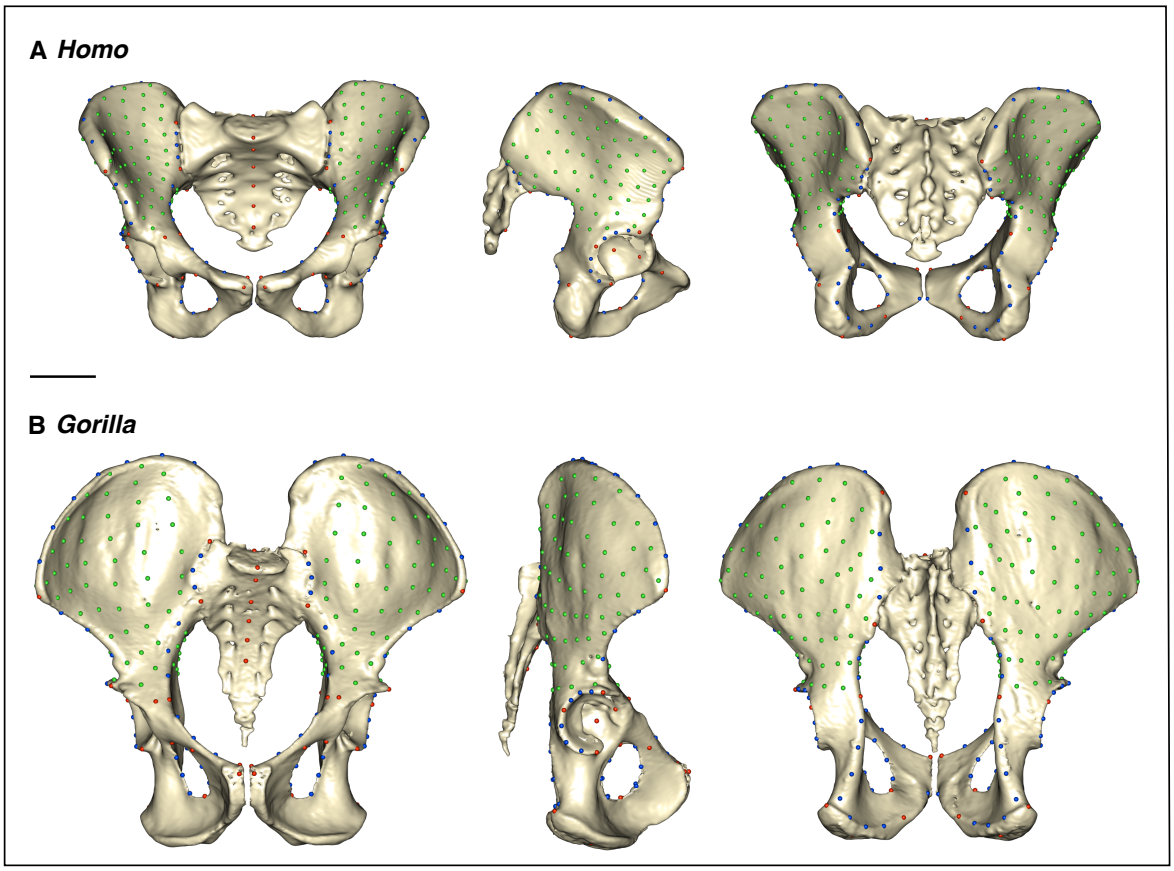

Fig. S1. Anterior, lateral , and posterior views of an adult human (A) and adult gorilla (B) pelves showing pelvic landmarks and semilandmarks. Fixed landmarks are shown in red, curve semilandmarks in blue, and surface semilandmarks in green. (Scale bar, 5 cm).

Table 1. Sample structure of adult specimens.

Taxon	*group symbols*	*males*	*females*	*wet*	*dry*	*total*
Homo sapiens	filled circles	96	78	174	0	174
Pan troglodytes spp.	stars	9	15	10	14	24
Gorilla gorilla spp.	open circles	13	6	4	15	19
*Pongo spp.**	filled triangles	8	6	3	11	14
Great apes**	g	30	27	17	40	57

*includes three *Pongo abelii* and eleven *Pongo pygmaeus* specimens
**includes all the specimens of chimpanzees, gorillas and orangutans together/pooled

Table 2. Sexual dimorphism within great apes and humans (results of Procrustes ANOVA on taxon-adjusted data).

Taxon	df	SS	MS	Rsq	F	*P*
Great ape	1	0.0098	0.0098	0.0493	2.8572	0.0069
Residuals	55	0.1888	0.0034			
Total	56	0.1986				
Human	1	0.1065	0.1065	0.1821	38.314	0.0009
Residuals	172	0.4781	0.0027			
Total	172	0.5846				

df, degrees of freedom; F, F-value; MS, mean square; *P* = P value; Rsq, R^2; SS, sum of squares.

Table S1. Definition of fixed landmarks.

LM number	Description
1-2	Pubic symphysis: superiormost anterior point
3-4	Pubic symphysis: superiormost posterior point
5-6	Ischiopubic juncture: pubis - posterior fusion point
7-8	Ischiopubic juncture: ischium - posterior fusion point
9-10	Ischiopubic juncture: pubis - obturator foramen inferior fusion point
11-12	Ischiopubic juncture: ischium - obturator foramen inferior fusion point
13-14	Ischiopubic juncture: pubis - obturator foramen superior fusion point
15-16	Ischiopubic juncture: ischium - obturator foramen superior fusion point
17-18	Ischium: posteriormost point (superior from ischial tuberosity)
19-20	Ischium: inferiormost midpoint
21-22	Ilioischial juncture: ischium - fusion point
23-24	Ilioischial juncture: ilium - fusion point
25-26	Ilioischial juncture: ischium - acetabulum lateral fusion point
27-28	Ilioischial juncture: ilium - acetabulum lateral fusion point
29-30	Acetabulum: superiormost lateral point
31-32	Acetabulum: point on pubic part of lunate surface
33-34	Iliopubic juncture: pubis - superior fusion point
35-36	Iliopubic juncture: ilium - superior fusion point
37-38	Iliopubic juncture: pubis - fusion point on pelvic brim
39-40	Iliopubic juncture: ilium - fusion point on pelvic brim
41-42	Pubis: anterior midpoint
43-44	Acetabulum: inferiormost lateral point on lunate surface
45-46	Acetabulum: deepest point on acetabular center (acetabular fossa)
47-48	Pelvic brim and sacroiliac joint: intersection point
49-50	Sacroiliac joint: superiormost point
51	S1: superiormost anterior point
52	S1: superiormost posterior point
53	S1: anterior midpoint
54	S2: anterior midpoint
55	S3: anterior midpoint
56	S4: anterior midpoint
57-58	Anterior supuperior iliac spine
59-60	Iliac crest: posteriormost point (end point)
61-62	Posterior inferior iliac spine
63	S5: anterior midpoint

Table S2. Definition of semilandmarks.

LM number	Description
Iliac crest	Right: start LM 57, end LM 59; Left: start LM 58, end LM 60 with eight subdivisions
Posterior iliac spines	Right: start LM 59, end LM 61; Left: start LM 60, end LM 62 with four subdivisions
Greater sciatic notch	Right: start LM 61, end LM 23; Left: start LM 62, end LM 24 with four subdivisions
Acetabulum: on ilium	Right: start LM 27, end LM 29; Left: start LM 28, end LM 30 with four subdivisions
Anterior iliac spines	Right: start LM 57, end LM 29; Left: start LM 58, end LM 30 with four subdivisions
Acetabulum: on ischium	Right: start LM 25, end LM 43; Left: start LM 26, end LM 44 with four subdivisions
Obturator foramen posterior	Right: start LM 15, end LM 11; Left: start LM 16, end LM 12 with four subdivisions
Obturator foramen anterior	Right: start LM 13, end LM 9; Left: start LM 14, end LM 10 with four subdivisions
Sacroiliac joint	Right: start LM 49, end LM 47; Left: start LM 50, end LM 48 with four subdivisions
Pelvic brim1	Right: start LM 47, end LM 39; Left: start LM 48, end LM 40 with four subdivisions
Pelvic brim2	Right: start LM 37, end LM 3; Left: start LM 38, end LM 4 with four subdivisions
Pubis posterior	Right: start LM 3, end LM 5; Left: startLeft: start LM 4, end LM 6 with two subdivisions
Ischium posterior	Right: start LM 7, end LM 21; Left: start LM 8, end LM 22 with eight subdivisions

References:

Adams DC, Collyer ML, Sherratt E. 2015. *geomorph*: Software for geometric morphometric analyses. R package version 2.1.7. http://cran.r-project.org/web/ packages/geomorph/ index.html. Available from: http://cran.r-project.org/web/ packages/geomorph/index.html

Adams DC, Otárola Castillo E. 2013. *geomorph*: an R package for the collection and analysis of geometric morphometric shape data. Methods Ecol Evol 4:393–399.

Almécija S, Tallman M, Alba DM, Pina M, Moyà-Solà S, Jungers WL. 2013. The femur of Orrorin tugenensis exhibits morphometric affinities with both Miocene apes and later hominins. Nat Commun 4:2888.

Badyaev AV. 2002. Growing apart: an ontogenetic perspective on the evolution of sexual size dimorphism. Trends Ecol Evol 17:369–378.

Bateman AJ. 1948. lntra-sexual selection in Drosophila. Heredity.

Berdnikovs S, Bernstein M, Metzler A, German RZ. 2006. Pelvic growth: ontogeny of size and shape sexual dimorphism in rat pelves. J Morphol 268:12–22.

Bernstein P, Crelin ES. 1967. Bony pelvic sexual dimorphism in the rat. Anat Rec 157:517–525.

Callewaert F, Sinnesael M, Gielen E, Boonen S, Vanderschueren D. 2010. Skeletal sexual dimorphism: relative contribution of sex steroids, GH-IGF1, and mechanical loading. J Endocrinol 207:127–134.

Chapman A, Hall LS, Bennett MB. 1994. Sexual Dimorphism in the Pelvic Girdle of Australian Flying Foxes. Aust J Zool 42:261–265.

Domazet-Lošo T, Tautz D. 2010. A phylogenetically based transcriptome age index mirrors ontogenetic divergence patterns. Nature 468:815–818.

Dunsworth HM, Warrener AG, Deacon T, Ellison PT, Pontzer H. 2012. Metabolic hypothesis for human altriciality. Proc Natl Acad Sci USA 109:15212–15216.

Gilbert SF. 2013. Developmental Biology. 10 ed. Sinauer Associates.

Gingerich PD. 1972. The development of sexual dimorphism in the bony pelvis of the squirrel monkey. Anat Rec 172:589–595.

Grabowski MW, Polk JD, Roseman CC. 2011. Divergent patterns of integration and reduced constraint in the human hip and the origins of bipedalism. Evolution 65:1336–1356.

Grabowski MW. 2012. Hominin obstetrics and the evolution of constraints. Evol Biol 40:57–75.

Gruss LT, Schmitt D. 2015. The evolution of the human pelvis: changing adaptations to bipedalism, obstetrics and thermoregulation. Philos Trans R Soc Lond, B, Biol Sci 370:20140063–20140063.

Gunz P, Mitteroecker P, Bookstein FL. 2005. Semilandmarks in three dimensions. In: Slice DE, editor. Modern morphometrics in physical anthropology. Developments in Primatology: Progress and Prospects. New York: Kluwer Academic Publishers-Plenum Publishers. p 73–98.

Huseynov A, Ponce de León MS, Zollikofer CPE. (*accepted*). Development of modular organization in the chimpanzee pelvis. Anat Rec.

Huseynov A, Zollikofer CPE, Coudyzer W, Gascho D, Kellenberger C, Hinzpeter R, Ponce de León MS. 2016. Developmental evidence for obstetric adaptation of the human female pelvis. Proc Natl Acad Sci USA 113:5227–5232.

Iguchi T, Irisawa S, Fukazawa Y, Uesugi Y, Takasugi N. 1989. Morphometric analysis of the development of sexual dimorphism of the mouse pelvis. Anat Rec 224:490–494.

Irie N, Kuratani S. 2011. Comparative transcriptome analysis reveals vertebrate phylotypic period during organogenesis. Nat Commun 2:248.

Kalinka AT, Varga KM, Gerrard DT, Preibisch S, Corcoran DL, Jarrells J, Ohler U, Bergman CM, Tomancak P. 2010. Gene expression divergence recapitulates the developmental hourglass model. Nature 468:811–814.

Klingenberg CP. 2014. Studying morphological integration and modularity at multiple levels: concepts and analysis. Philos Trans R Soc Lond, B, Biol Sci 369:20130249.

LaVelle M. 1995. Natural selection and developmental sexual variation in the human pelvis. Am J Phys Anthropol 98:59–72.

Leutenegger W. 1970. Relation between newborn size and sex dimorphism of pelvis in simian primates. Folia Primatol 12:224–235.

Leutenegger W. 1974. Functional aspects of pelvic morphology in simian primates. J Hum Evol 3:207–222.

Lewton KL. 2012. Evolvability of the primate pelvic girdle. Evol Biol 39:126–139.

Lovejoy CO. 2005. The natural history of human gait and posture. Gait & Posture 21:95–112.

Lycett SJ, Cramon-Taubadel von N. 2013. Understanding the comparative catarrhine context of human pelvic form: a 3D geometric morphometric analysis. J Hum Evol 64:300–310.

Marchal F. 2000. A new morphometric analysis of the hominid pelvic bone. J Hum Evol 38:347–365.

McPherson FJ, Chenoweth PJ. 2012. Mammalian sexual dimorphism. Animal Repr Sci 131:109–122.

Milella M, Zollikofer CPE, Ponce de León MS. 2015. Virtual reconstruction and geometric morphometrics as tools for paleopathology: a new approach to study rare developmental disorders of the skeleton. Anat Rec 298:335–345.

Parsch J, Ellegren H. 2013. The evolutionary causes and consequences of sex-biased gene expression. Nat Rev Genet 14:83–87.

Perelman P, Johnson WE, Roos C, Seuánez HN, Horvath JE, Moreira MAM, Kessing B, Pontius J, Roelke M, Rumpler Y, Schneider MPC, Silva A, O'Brien SJ, Pecon-Slattery J. 2012. A Molecular Phylogeny of Living Primates. PLOS Genet 7:e1001342.

Piasecka B, Lichocki P, Moretti S, Bergmann S, Robinson-Rechavi M. 2013. The Hourglass and the Early Conservation Models—Co-Existing Patterns of Developmental Constraints in Vertebrates. PLOS Genet 9:e1003476.

Ponce de León MS, Golovanova L, Doronichev V, Romanova G, Akazawa T, Kondo O, Ishida H, Zollikofer CPE. 2008. Neanderthal brain size at birth provides insights into the evolution of human life history. Proc Natl Acad Sci USA 105:13764–13768.

Ponce de León MS, Huseynov A, Zollikofer CPE. 2016. Reply to Mitteroecker and Fischer: Developmental solutions to the obstetrical dilemma are not Gouldian spandrels. Proc Natl Acad Sci USA 113:E3597–8.

Rolian C. 2014. Genes, development, and evolvability in primate evolution. Evol Anthropol 23:93–104.

Rosenberg KR. 1992. The evolution of modern human childbirth. Am J Phys Anthropol 35:89–124.

Rosenblum EB, Parent CE, Brandt EE. 2014. The Molecular Basis of Phenotypic Convergence. Annu Rev Ecol Evol Syst 45:203–226.

Rüdell A, Schlager S. (*in press*) Sexual dimorphism and population affinity in the human zygomatic structure - comparing surface to outline data. Anat Rec.

Schlager S, Goepper M. 2016. Model based facial soft-tissue estimation from dry skull. Am J Phys Anthropol.

Schlager S. 2016. Morpho: Calculations and visualisations related to geometric morphometrics. R package version 2.3.1.1. Available from: http://sourceforge.net/projects/morpho-rpackage/ https://github.com/zarquon42b/Morpho

Schultz AH. 1949. Sex differences in the pelves of primates. Am J Phys Anthropol 7:401–423.

Tague RG. 1995. Variation in pelvic size between males and females in nonhuman anthropoids. Am J Phys Anthropol 97:213–233.

Tague RG. 2003. Pelvic sexual dimorphism in a metatherian, Didelphis Virginiana: implications for eutherians. Journal of Mammalogy 84:1464–1473.

Tague RG. 2005. Big-bodied males help us recognize that females have big pelves. Am J Phys Anthropol 127:392–405.

Uesugi Y, Taguchi O, Noumura T, Iguchi T. 1992. Effects of sex steroids on the development of sexual dimorphism in mouse innominate bone. Anat Rec 234:541–548.

Wang Z, Pascual-Anaya J, Zadissa A, Li W, Niimura Y, Huang Z, Li C, White S, Xiong Z, Fang D, Wang B, Ming Y, Chen Y, Zheng Y, Kuraku S, Pignatelli M, Herrero J, Beal K, Nozawa M, Li Q, Wang J, Zhang H, Yu L, Shigenobu S, Wang J, Liu J, Flicek P, Searle S, Wang J, Kuratani S, Yin Y, Aken B, Zhang G, Irie N. 2013. The draft genomes of soft-shell turtle and green sea turtle yield insights into the development and evolution of the turtle-specific body plan. Nature Genetics 45:701–706.

Warrener AG, Lewton KL, Pontzer H, Lieberman DE. 2014. A wider pelvis does not increase locomotor cost in humans, with implications for the evolution of childbirth. PLoS ONE 10:e0118903–e0118903.

Washburn SL. 1960. Tools and Human Evolution. Sci Am 203:62–75.

Weiner S, Monge J, Mann A. 2008. Bipedalism and parturition: an evolutionary imperative for Cesarean delivery? Clinics Perinatol 35:469–478.

Wells JCK, DeSilva JM, Stock JT. 2012. The obstetric dilemma: an ancient game of Russian roulette, or a variable dilemma sensitive to ecology? Am J Phys Anthropol 149:40–71.

Wells JCK. 2015. Between Scylla and Charybdis: renegotiating resolution of the “obstetric dilemma” in response to ecological change. Philos Trans R Soc Lond, B, Biol Sci 370:20140067–20140067.

Williams TM, Carroll SB. 2009. Genetic and molecular insights into the development and evolution of sexual dimorphism. Nat Rev Genet 10:797–804.

Wilson EB. 1894. The embryological criterion of homology. Biol Lect MBL, Woods Hole: 101–124.

Wittman AB, Wall LL. 2007. The evolutionary origins of obstructed labor: bipedalism, encephalization, and the human obstetric dilemma. Obstetr Gynecol Survey 62:739–748.

Zollikofer CPE, Ponce de León MS. 2005. Virtual reconstruction: a primer in computer-assisted paleontology and biomedicine. Hoboken, N. J.: Wiley-Liss.

Zollikofer CPE, Scherrer M, Ponce de León MS. (*accepted*). Development of pelvic sexual dimorphism in hylobatids: testing the obstetric constraints hypothesis. Anat Rec.

Appendix: Materials and Methods

The total sample consist of ontogenetic series (from late fetal stages to late adulthood) of humans (*n*=275) and chimpanzees (*n*=86), then the adult gorillas (*n*=19) and adults orangutans (*n*=14) (see Table 1). The great ape data sources are the Collections of the Anthropological Institute (University of Zurich), and the Digital Morphology Museum of the Primate Research Institute (Kyoto University). Human data consist of mixed forensic sources from the Virtopsy® data base of the Institute of Forensic Medicine of the University of Zurich and the digital autopsy data base of the Catholic University of Leuven, Belgium (KU Leuven), and clinical data sets from the Institute of Diagnostic and Interventional Radiology of the University of Zurich together with freely available data sets from the OsiriX web-page (http://www.osirix-viewer.com). During data preselection, cases showing congenital or acquired pathologies of the pelvic girdle were excluded from the sample.

Volumetric data of all specimens were acquired with medical computed tomography (CT) using the following acquisition and image reconstruction parameters: beam collimation 1mm; in-plane pixel size between 0.2x0.2 and 0.7x0.7 mm^2, slice increment between 0.2 and 1.0 mm. Virtual surface models of the pelvis were generated with Avizo 6.3.1 (FEI Visualization Sciences Group), and subsequent mesh cleaning was performed with Geomagic XOS (3D Systems). Only well-preserved pelves were utilized. A number of specimens (humans: n = 9 with ages <8 y, n = 5 with ages 12-15 y, and n = 14 with ages 50-80 y; chimpanzees: n = 8 with ages <2 years, and n = 16 with ages >8 years) required virtual reconstruction (completion of missing parts on one side with mirror-imaged counterparts) following previously published protocols (Zollikofer and Ponce de León, 2005; Ponce de León et al., 2008; Milella et al., 2015).

Nowadays multimodal CT, image processing/analysis tools and geometric morphometrics (GM) (Bookstein, 1997; Gunz et al., 2005; Zollikofer and Ponce de León, 2005) permit a more detailed look at skeletal changes in basically any morphological structure including the bony pelvis, during development, for example quantify and analyze modularity/ integration patterns in ontogenetic datasets. As compared to other methods of classical/ traditional multivariate morphometric analysis utilizing linear and/or angular measurements GM is advantageous in several aspects. First, GM quantifies morphology/form by the a set of 3D anatomical landmarks that are assumed to represent points of biological and/or geometric homology between the specimens of the sample. Second, GM can mathematically/statistically

separate the two main components of morphology, namely size (extent) and shape (geometry) hat are preserved in each specimen's landmark configuration. And finally, GM permits simultaneous representation of patterns of shape variation in high-dimensional multivariate spaces and in 3-dimensional physical space, thus maintaining the links between statistical and real-space representation of the results.

The shape of the pelvis was quantified with K=377 3D anatomical landmarks, which denote (as previously mentioned) locations of biological and/or geometric homology among specimens of the sample. These consist of fixed landmarks (K_f=63), curve semilandmarks (K_c=90), and surface (K_s=224) (see Tables 2-3). The fixed and curve semilandmarks were quantified manually on each pelvis using using in-house software FoRM-IT (Fossil Reconstruction and Morphometry Interactive Toolkit) (Zollikofer and Ponce de León, 1995). The fixed landmarks set comprises 14 landmark pairs, which eventually fuse during pelvic development. For geometric morphometric analyses, the mean position was calculated for each pair, resulting in K_f=49 fixed landmarks, and a total of K=363 landmarks. Surface semilandmarks were generated from an arbitrary specimen's point cloud, following largely the procedures described in ref. (Gunz et al., 2005), although alternative methods were proposed and utilized by refs. (Schlager and Goepper, 2016; Rüdell and Schlager). Alternatively, one can use arbitrary specimen, decimate point could (shape) of this specimen and manually adjust the surface landmarks, then export point cloud as ascii file for FoRM-IT or Geomagic XOS or R. There are also ways to digitize surface semilandmarks using software: Landmark Editor (http://www.idav.ucdavis.edu/research/EvoMorph) or Stratovan (https://www.stratovan.com/blog/landmark-editor).

In order to digitize surface semilandmarks on all pelvises I created an shape atlas which represents a full (K=377) landmark configuration of a random specimen. From this atlas surface semilandmarks were warped to all specimens using Thin-plate spline (TPS) interpolation function ensuring that all surface semilandmarks are then projected on to corresponding surfaces - i.e along surface normals. Then, in order to minimize among-specimen differences in user-defined semilandmarks positions, iterative semilandmark sliding procedures as described in ref. (Gunz et al., 2005) were applied. Semilandmark sliding was performed relative to the symmetrized mean configuration, using the minimum bending energy criterion. All procedures were performed with the R (R Core Team, 2016) package Morpho (Schlager, 2016) version 2.3.1.1. I utilized principal components analysis (PCA) to reduce the dimensionality of the procrustes data, and to explore major patterns of shape

variation in the sample. Graphs of the data scatter in the low-dimensional shape space represented by the first few principal components (PCs) were produced with software JMP, version 12.1. Directions of developmental trajectories through shape space were compared using the methods proposed in ref. (Collyer et al., 2015). Procrustes ANOVA was performed to test for sex-specific or any differences in pelvic shape using R package geomorph, version 3.0.2 (Adams and Otárola Castillo, 2013; Adams et al., 2015). To explore patterns of morphological change along developmental trajectories (mostly for visual proposes) I calculated sex-specific moving averages of PC scores, centroid size, and angular and linear pelvic dimensions. Distance matrices of between taxon-specific and male-female group means were computed using R package Morpho, version 2.3.1.1. (Schlager, 2016). In this thesis, the actual morphological patterns of pelvic shape change were visualized with stage-specific mean shapes, similarly, the patterns of pelvic sexual dimorphism were visualized by comparing mean adult female and male pelvic shapes.

Modularity and integration was quantified and analyzed according to the methods proposed by Adams (2016). The ratio of covariance between versus within modules was typically measured by the so-called RV coefficient (Klingenberg, 2009); however, it has been shown that RV tend to depend on the dimensionality of the multivariate data, and on sample size (Smilde et al., 2009; Adams, 2016). Thus, in this thesis I use the covariance ratio (CR), which is insensitive to dimensionality and sample size (Adams, 2016). Here I tested developmental modularity: landmarks were attributed to three subsets, corresponding to ilium, ischium and pubis); and functional modularity: landmarks were attributed to two subsets, corresponding to hypothetical structures that are mainly involved in “obstetric” or “abdominal” functions (the pelvic inlet region, and/or true pelvis (McKinley and O'loughlin, 2006)), and structures hypothesized to be mainly involved in “non-obstetric” functions (mostly locomotor: muscle attachment regions, and/or false pelvis (McKinley and O'loughlin, 2006)). The developmental units of the pelvis are pretty straightforward and mostly correspond to true developmental/embryonic regions. Whereas the functional units are mostly based on previous observations and hypotheses (Lovejoy, 2005; Hirata et al., 2011; Grabowski, 2012; Gruss and Schmitt, 2015). Modularity/integration was also analyzed in left versus right coxal bones, as well as in “random modules” consisting of user-defined bilaterally symmetrical landmark patches.

Following are the examples of **R scripts for GM analyses**. Other detailed examples of GM-related functions can be found in R packages *Morpho* (https://cran.r-project.org/web/packages/Morpho/index.html) and *geomorph* (https://cran.r-project.org/web/packages/geomorph/index.html) user manuals.

Short script to read landmark data:

```
# install all the libraries below
# e.g. install.packages("Morpho")

# load the libraries
library(rgl)
library(Rvcg)
library(shapes)
library(aqfig)
library(mgcv)
library(MASS)
library(pls)
library(abind)
library(Morpho)
library(geomorph)
library(parallel)
library(plyr)

# load the data. in my case they are in .NTS format. If they are in .VER the you need to use only first 3 columns.

setwd("~/Desktop/R/pelvis_analysis/") # e.g. to set the current working directory
getwd() # tells u in which directory you are. like pwd in Linux

# make an atlas to get the surface semilandmarks
patch_homo<-read.table(file="fullbody3_patch_hs.NTS",header=F,skip=3) # load .nts file of surface semilandmarks
patch_homo<-as.matrix(patch_homo)
landmarks_homo<-read.table(file="fullbody03_pelvis_final.NTS",header=F,skip=3) # load .nts file of fixed + curve semilandmarks
landmarks_homo<-as.matrix(landmarks_homo)
mesh_homo<-file2mesh("~/Desktop/R/pelvis_analysis/surfaces_stl/fullbody03_pelvis_final.stl") # load the corresponding mesh file
atlas_homo<-createAtlas(mesh_homo,landmarks_homo,patch_homo) # create atlas
plotAtlas(atlas_homo,pt.size=1.5,add=F,render="s",point="s",meshcol=bone3,bg3d("black")) # plot atlas to check

lm_list<-list.files() # list files in the current directory
lm_all<-ldply(lm_list,read.table,skip=3) # reads the data as data.frame and skips first 3 rows. if you have it in .VER the do not use skip.
```

```
lm_all_r<-arrayspecs(lm_all,63,3) # makes the array in case of .NTS. 63 means total number of lms and 3 means the dimensions => 3d
lm_all_r<-arrayspecs(lm_all[,1:3],63,3) # makes the array in case of .VER

# define some arguments for sliding process
sur<-("~/Desktop/R/pelvis_analysis/surfaces_stl/") # path to surfaces
left<-c(2,4,6,..) # all left lms
right<-c(1,3,5,7,..) # all right lms
pairedLM<-cbind(left,right) # matrix of paired lms

SMvector=c(1:63) # a vector with fixed lmd
outlines=list(c(57,125:131,59),c(58,135:141,60),....) # list of curve-lms. e.g. lm 57 is staring fixed point and 59 end fixed point and 125 to 131 are the curve-lms
surp=c(154:377) # vector of surface semi-lms.

# sliding process
slid_spec<-
slider3d(lm_all_r,SMvector=SMvector,outlines=outlines,surp=surp,sur.path=sur,deselect=T,pairedLM=pairedLM,iterations=0,sur.type="stl",fixRepro=F)
# check how the lms look like after sliding

checkLM(slid_spec
$dataslide,path=path,begin=1,alpha=1,col=bone3,render="s",point="s",pt.size=0.5,atlas=NULL,text.lm=T,suffix=".stl")

# GPA or GLS
proc_data<-procSym(slid_spec$dataslide,pairedLM=pairedLM) # does procrustes analysis
# write a .csv file of centroid size and first 6 PCscores
write.csv(abind(proc_data$size,proc_data$PCscore_sym[,1:6]),"give_file_name.csv")
```

Example of Procrustes (multivariate) anova:

```
library(geomorph)
devo_fet_inf_age_mf<-(c(rep("females",length(1:20)),rep("males",length(49:67)))) # define your dummy variable with two levels
devo_fet_inf_age_mf<-as.factor(devo_fet_inf_age_mf) # make it as factor with two levels
stats_fet_inf_age_mf<-
procD.lm(proc_pan_lm363$PCscore_sym[c(1:20,49:67),]~devo_fet_inf_age_mf,iter=1000,RRPP = F) # first is your array of shape dat, then dummy variable.
summary(stats_fet_inf_age_mf) # summarized results into anova table.
```

Example of visualization of transformed shapes:

```
# visualize female to male
# human
# get the landmarks from shape data
hX.adl_f<-arrMean3(proc_hs_adl_lm363$Sym[,,c(1:78)]) # calculate mean shape
hX.adl_m<-arrMean3(proc_hs_adl_lm363$Sym[,,c(79:174)]) # calculate mean shape
# load corresponding .stl
adult4_fullbody09<-vcgSmooth(file2mesh("~/Desktop/R/pelvis_analysis/pelvisDevo_movie/
fullbody09_pelvis_final.stl"))
# warp the loaded .stl(s) in to corresponding mean shapes config.
hX.adl_f_stl<-tps3d(adult4_fullbody09,slid_homo_cadv_lm363[,,48],hX.adl_f)
hX.adl_m_stl<-tps3d(adult4_fullbody09,slid_homo_cadv_lm363[,,48],hX.adl_m)
#check the warped meshes
shade3d(hX.adl_f_stl, col="lemonchiffon1",alpha=1) # loads the mesh
shade3d(hX.adl_m_stl,col="steelblue", alpha=0.35)
```

Example how to calculate mean between 2 landmarks

```
slid_adl_pan_lm363<-slid_adl_pan$dataslide # assign a new name to array
# for loop computes the mean values between landmarks 5 and 7
for(i in 1:24){
 if(!exists("lm5_7_slid_adl_pan_lm363"))
 {
  lm5_7_slid_adl_pan_lm363<-apply(slid_adl_pan_lm363[c(5,7),,i],2,mean)
 }
 else{temp_lm5_7_slid_adl_pan_lm363<-apply(slid_adl_pan_lm363[c(5,7),,i],2,mean)
     lm5_7_slid_adl_pan_lm363<-
abind(lm5_7_slid_adl_pan_lm363,temp_lm5_7_slid_adl_pan_lm363,along = 2)
     rm(temp_lm5_7_slid_adl_pan_lm363)}
}
lm5_7_slid_adl_pan_lm363<-t(lm5_7_slid_adl_pan_lm363) # assign to a new matrix

# for loop computes the mean values between landmarks 5 and 7
for(i in 1:24){
 if(!exists("lm6_8_slid_adl_pan_lm363"))
 {
  lm6_8_slid_adl_pan_lm363<-apply(slid_adl_pan_lm363[c(6,8),,i],2,mean)
 }
 else{temp_lm6_8_slid_adl_pan_lm363<-apply(slid_adl_pan_lm363[c(6,8),,i],2,mean)
     lm6_8_slid_adl_pan_lm363<-
abind(lm6_8_slid_adl_pan_lm363,temp_lm6_8_slid_adl_pan_lm363,along = 2)
     rm(temp_lm6_8_slid_adl_pan_lm363)}
}
lm6_8_slid_adl_pan_lm363<-t(lm6_8_slid_adl_pan_lm363) # assign to a new matrix
```

... Continue for all the specimens (here there are 24 specimens) depending for how many landmarks you do it.

Example to calculate angles and interlandmark distances.

```
allLms_hs<-proc_homo_cadv_lm363$Sym # your array of shape data
# write a fuction/loop for angle calculation in radians#
angle<-function(Vr,Vl){
  dot.prod<-Vr%*%Vl
  norm.Vr<-norm(Vr,type="2")
  norm.Vl<-norm(Vl,type="2")
  theta<-acos(dot.prod / (norm.Vr * norm.Vl))
  as.numeric(theta)
  degrees<-(180*theta/pi)
}

# calculate verctors between landmarks 5,50; 6,51
Vr<-allLms_hs[5,,]-allLms_hs[50,,]
Vl<-allLms_hs[6,,]-allLms_hs[51,,]

# calculate subpubic angle in all specimens in degrees
for(i in 1:276){
  if(!exists("subPub_angle"))
  {
    subPub_angle<-angle(t(Vr[,i]),Vl[,i])
  }
  else{temp_subPub_angle<-angle(t(Vr[,i]),Vl[,i])
       subPub_angle<-abind(subPub_angle,temp_subPub_angle)
       rm(temp_subPub_angle)}
}
subPub_angle<-t(subPub_angle)
dimnames(subPub_angle)[[1]]<-dimnames(proc_homo_cadv_lm363$Sym)[[3]] # make some
names
dimnames(subPub_angle)[[2]]<-c("Subpubic_angle(deg)")
```

```
# Calculate procrustes distance:

# one way
sin(riemdist(shape1, shape2)) # according to R package shapes

# second way to is using permutation test from Morpho pacakge
# make some groupings
groups_g_apes_taxon4<-
(c(rep("homo",length(c(48:125,181:276))),rep("pan",dim(placed_pan[,,c(34:48,78:86)])
[3]),rep("gorilla",dim(placed_gorilla[,,c(18:23,36:48)])[3]),
                    rep("pongo",dim(placed_pongo[,,c(12:17,32:39)])[3])))
# run the permunation test
dist.m_hs_gApes_taxon<-
permudist_modified(proc_g_apes_ald_lm363$PCscore_sym,as.factor(groups_g_apes_taxon4
),rounds = 1000) # first is your shape data, or PC scores, then groups.

# Example to calculate moving averages for user-defined parameters

# matlab script example by CPE Zollikofer

function [Xdiscrete, Ysmooth]=mvg_avg1(X,Y,nbins,navg)
%   [Xdiscrete, Ysmooth]=mvg_avg1(X,Y,nbins,navg):
%   creates bins of Y along X
%       nbins is scalar: number of bins along X
%       nbins is array: edges of bins along X
%   then computes moving average with navg-neighborhood
[N,edges,bin] = histcounts(X,nbins); % bin contains the bin indices of each element of X

%% calculate Ymeans for each X bin
Ymean=NaN(1,length(N)); % preallocate array for Ymean
for i=1:length(N)
idx= bin==i; % find row indices of all specimens fitting into bin i
Ymean(i)=mean(Y(idx)); % calculate mean value per bin
end

% calculate moving average along bins
mov_avg_width=navg; % convolution kernel width for moving average
kernel = ones(1, mov_avg_width) / mov_avg_width;
Ymean_pad=padarray(Ymean,[0, mov_avg_width],'rep'); % add replicated elements at the
array boundaries to equalize the effects of convolution
Ysmooth = conv(Ymean_pad, kernel, 'valid');
if mod(navg,2)>0 % odd number of bins
pad_diff=(length(Ysmooth)-length(Ymean))/2;
Ysmooth=Ysmooth(pad_diff+1:end-pad_diff); % cut off the replicated elements
else % even number of bins
pad_diff=round((length(Ysmooth)-length(Ymean))/2);
Ysmooth=Ysmooth(pad_diff+1:end-pad_diff+1); % cut off the replicated elements
end
```

```
Xdiscrete=(edges(1:end-1)+edges(2:end))./2; % shift to midpoints


# translated to R, the order is the same as in matlab example

m.a.<-function(x,y,nbins,navg){
  bin<-histc(x,nbins)
  bin_counts<-hist(x,nbins,plot = F)
  Ymean<-rep(NaN, length(bin_counts$counts))
  for(i in 1:length(bin_counts$counts)){
    idx= bin$bin==i
    Ymean[i]<-mean(y[idx])
  }
  mov_avg_width<-navg
  kernel<-matrix(1, mov_avg_width)/mov_avg_width
  Ymean_pad=padarray(Ymean,c(0, mov_avg_width),"replicate")
  Ysmooth = convolve(Ymean_pad, rev(kernel),type = "open")
  Xdiscrete<-bin_counts$mids
  out<-cbind(Xdiscrete,Ysmooth[6:24]) # remove first 6 and the last values
  return(out)
}
```

Table 1. List of specimens

Id	Taxon	Sex	Age1	Age (years)	Age2	Dental Eruption	Status
AM195	*Homo sapiens*	m	infant	0.2?	1	i1&i2 started to erupt	cadaver
AM6162-1	*Homo sapiens*	m	fetus	>6 months	-1	none erupted	cadaver
AM6162-2	*Homo sapiens*	m	fetus	>6 months	-1	none erupted	cadaver
AM6163-1	*Homo sapiens*	m	fetus	>6 months	-1	none erupted	cadaver
AM6163-2	*Homo sapiens*	m	fetus	>6 months	-1	none erupted	cadaver
AM6414	*Homo sapiens*	f	fetus	>6 months	-1	none erupted	cadaver
AM6637	*Homo sapiens*	f	fetus	>6 months	-1	none erupted	cadaver
AM6637-2nd	*Homo sapiens*	f	fetus	>6 months	-1	none erupted	cadaver
amnesix	*Homo sapiens*	m	adult	68	5	M3?	cadaver
an10000	*Homo sapiens*	f	neonate	1 day/14 days?	0	none erupted	cadaver
AN5124	*Homo sapiens*	f	neonate	1 day/14 days?	0	none erupted	cadaver
AN537	*Homo sapiens*	f	neonate	1 day/14 days?	0	none erupted	cadaver
AN697	*Homo sapiens*	m	infant	0.2	1	no skull	cadaver
aneurix	*Homo sapiens*	m	adult	68	5	M3?	cadaver
assurancetourix	*Homo sapiens*	m	adult		5		cadaver
brebix	*Homo sapiens*	f	adult		5		cadaver
colonix	*Homo sapiens*	m	adult		5		cadaver
enterix	*Homo sapiens*	f	adult		5	M3?	cadaver
fullbody01	*Homo sapiens*	m	infant	6	2	dm2	cadaver
fullbody02	*Homo sapiens*	m	infant	5	2	dm2	cadaver
fullbody03	*Homo sapiens*	f	infant	2	2	dm2	cadaver
fullbody04	*Homo sapiens*	f	infant	3	1	dm1, dm^2 erupted,dm_2 started to erupted	cadaver
fullbody05	*Homo sapiens*	f	infant	0.5	1	i1&i2 started to erupt	cadaver
fullbody06	*Homo sapiens*	f	infant	3	2	dm2	cadaver
fullbody07	*Homo sapiens*	m	infant	max 1.5	1	dm1 almost erupted	cadaver
fullbody09	*Homo sapiens*	f	adult	20	5	M2	cadaver
fullbody10	*Homo sapiens*	m	infant	11 months	1	i_1 erupted i^2 started to erupt	cadaver
fullbody11	*Homo sapiens*	f	adult	39	5	M3	cadaver
fullbody12	*Homo sapiens*	f	adult	45	5	M3	cadaver
fullbody13	*Homo sapiens*	f	adult	30	5	M3	cadaver
fullbody14	*Homo sapiens*	f	infant	4	2	dm2 erupted	cadaver
fullbody16	*Homo sapiens*	f	fetus	>6 months	-1	none erupted	cadaver

fullbody17	*Homo sapiens*	m	infant	10 months	1	i_1 erupted i_2 started to erupt	cadaver
fullbody18	*Homo sapiens*	m	infant	0.6	1	i1&i2 started to erupt	cadaver
fullbody19	*Homo sapiens*	m	juvenile	9	3	M1	cadaver
fullbody20	*Homo sapiens*	m	juvenile	13	4	M2	cadaver
fullbody21	*Homo sapiens*	f	juvenile	11	4	M1	cadaver
fullbody22	*Homo sapiens*	f	juvenile	7	4	M1	cadaver
fullbody23	*Homo sapiens*	f	juvenile	7	4	M1	cadaver
fullbody24	*Homo sapiens*	f	adult	80	5	M3	cadaver
irm02	*Homo sapiens*	m	infant	0.2	1	i1 started to erupt	cadaver
irm03	*Homo sapiens*	m	juvenile	8.5	3	M1	cadaver
irm04	*Homo sapiens*	f	infant	1.3	1	dm1	cadaver
irm05	*Homo sapiens*	m	neonate	2 days	0	none erupted	cadaver
irm06	*Homo sapiens*	m	juvenile	16	4	M2	cadaver
irm07	*Homo sapiens*	f	infant	3.9	2	dm2	cadaver
irm08	*Homo sapiens*	f	juvenile	7.5	3	M1 erupted, M2 started to erupt	cadaver
irm09	*Homo sapiens*	f	infant	0.2	1	i1 started to erupt	cadaver
irm10	*Homo sapiens*	m	infant	0.2	1	i1 started to erupt	cadaver
irm11	*Homo sapiens*	f	juvenile	16.9	4	M2	cadaver
irm12	*Homo sapiens*	m	adult	18	4	M2	cadaver
irm13	*Homo sapiens*	f	infant	3.5	2	dm2	cadaver
irm14	*Homo sapiens*	m	adult	18.3	4	M2	cadaver
irm15	*Homo sapiens*	f	juvenile	8.4	3	M1 erupted, M2 started to erupt	cadaver
irm16	*Homo sapiens*	m	infant	3	2	dm2	cadaver
irm18	*Homo sapiens*	f	neonate	2 days	0	none erupted	cadaver
irm19	*Homo sapiens*	m	neonate	4 days	0	none erupted	cadaver
irm21	*Homo sapiens*	m	infant	3.7	2	dm2	cadaver
irm22	*Homo sapiens*	f	infant	4.1	2	dm2?	cadaver
irm23	*Homo sapiens*	m	infant	ca 2	1	dm1 erupted, dm2 started to erupt	cadaver
irm24	*Homo sapiens*	m	infant	6.3	2	dm2 erupted, M1 started to erupt	cadaver
irm25	*Homo sapiens*	m	infant	4.3	2	dm2	cadaver
irm26	*Homo sapiens*	m	neonate	0	0	none erupted	cadaver
irm27	*Homo sapiens*	m	neonate	1 week	0	none erupted	cadaver
irm28	*Homo sapiens*	m	infant	0.9	1	i1 started to erupt	cadaver
irm29	*Homo sapiens*	f	neonate	2 days	0	none erupted	cadaver
irm30	*Homo sapiens*	f	neonate	2 days	0	none erupted	cadaver
irm33	*Homo sapiens*	f	neonate	3 days	0	none erupted	cadaver
irm34	*Homo sapiens*	f	neonate	2 days	0	none erupted	cadaver

irm35	*Homo sapiens*	f	neonate	2 days	0	none erupted	cadaver
irm36	*Homo sapiens*	f	neonate	1 week	0	none erupted	cadaver
irm37	*Homo sapiens*	f	neonate	3 days	0	none erupted	cadaver
irm42	*Homo sapiens*	f	infant	1.9	1	dm1	cadaver
irm43	*Homo sapiens*	m	infant	11 months	1	i1&i2 erupted	cadaver
irm44	*Homo sapiens*	m	infant	3 months	1	i1&i2 started to erupt	cadaver
irm45	*Homo sapiens*	m	infant	2 months	1	i1&i2 started to erupt	cadaver
irm46	*Homo sapiens*	m	infant	1 months	1	i1&i2 started to erupt	cadaver
irm47	*Homo sapiens*	f	infant	1 months	1	i1&i2 started to erupt	cadaver
irm48	*Homo sapiens*	m	juvenile	6	3	M1 erupting	cadaver
irm49	*Homo sapiens*	m	infant	3	2	dm2	cadaver
keskonrix	*Homo sapiens*	f	adult	84	5	M3?	cadaver
macoessix	*Homo sapiens*	m	adult		5	M3?	cadaver
mecanix	*Homo sapiens*	m	adult		5	M3?	cadaver
melanix	*Homo sapiens*	f	adult	42	5	M2, M3 not erupted	cadaver
obelix	*Homo sapiens*	m	adult	43	5	M3?	cadaver
osirix	*Homo sapiens*	m	adult		5	M3?	cadaver
panoramix	*Homo sapiens*	m	adult		5	M3?	cadaver
pelvix	*Homo sapiens*	f	adult	46	5	M3?	cadaver
petcetix	*Homo sapiens*	f	adult	81	5	M3?	cadaver
prostatix	*Homo sapiens*	m	adult	72	5	M3?	cadaver
vis_hum_fem	*Homo sapiens*	f	adult		5	M3	cadaver
VSD01	*Homo sapiens*	m	adult	89	5	M3	cadaver
VSD02	*Homo sapiens*	f	adult	78	5	M3	cadaver
VSD03	*Homo sapiens*	f	adult	90	5	M3	cadaver
VSD04	*Homo sapiens*	m	adult	89	5	M3	cadaver
VSD05	*Homo sapiens*	m	adult	22	5	M3 erupted	cadaver
VSD06	*Homo sapiens*	f	adult	51	5	M3	cadaver
VSD07	*Homo sapiens*	m	adult	56	5	M3	cadaver
VSD08	*Homo sapiens*	f	adult	60	5	M3	cadaver
VSD09	*Homo sapiens*	m	adult	60	5	M3	cadaver
VSD10	*Homo sapiens*	f	adult	45	5	M3	cadaver
VSD12	*Homo sapiens*	m	adult	81	5	M3	cadaver
VSD13	*Homo sapiens*	m	adult	77	5	M3	cadaver
VSD14	*Homo sapiens*	f	adult	30	5	M3	cadaver
VSD15	*Homo sapiens*	m	adult	81	5	M3	cadaver
VSD16	*Homo sapiens*	f	adult	95	5	M3	cadaver
VSD17	*Homo sapiens*	f	adult	19	5	M3 erupted	cadaver

VSD18	*Homo sapiens*	m	adult	32	5	M3	cadaver
VSD19	*Homo sapiens*	m	adult	56	5	M3	cadaver
VSD20	*Homo sapiens*	f	adult	83	5	M3	cadaver
VSD22	*Homo sapiens*	f	adult	43	5	M3	cadaver
VSD23	*Homo sapiens*	m	adult	74	5	M3	cadaver
VSD25	*Homo sapiens*	f	adult	64	5	M3	cadaver
VSD26	*Homo sapiens*	f	adult	53	5	M3	cadaver
VSD27	*Homo sapiens*	m	adult	23	5	M2	cadaver
VSD28	*Homo sapiens*	m	adult	28	5	M3	cadaver
VSD29	*Homo sapiens*	f	adult	44	5	M3	cadaver
VSD30	*Homo sapiens*	m	adult	20	5	M2, M3 started to erupt	cadaver
VSD31	*Homo sapiens*	m	adult	39	5	M3	cadaver
VSD33	*Homo sapiens*	m	adult	42	5	M3	cadaver
VSD34	*Homo sapiens*	f	adult	46	5	M3	cadaver
VSD35	*Homo sapiens*	f	adult	78	5	M3	cadaver
VSD36	*Homo sapiens*	m	juvenile	17	4	M2, M3 started to erupt	cadaver
VSD37	*Homo sapiens*	f	adult	62	5	M3	cadaver
VSD38	*Homo sapiens*	f	adult	57	5	M3	cadaver
VSD39	*Homo sapiens*	m	adult	53	5	M3	cadaver
VSD40	*Homo sapiens*	m	adult	46	5	M3	cadaver
VSD41	*Homo sapiens*	m	adult	33	5	M3	cadaver
VSD42	*Homo sapiens*	m	adult	78	5	M3	cadaver
z01	*Homo sapiens*	m	adult	77	5	M3	cadaver
z02	*Homo sapiens*	m	adult	58	5	M3	cadaver
z03	*Homo sapiens*	m	adult	65	5	M3	cadaver
z04	*Homo sapiens*	m	adult	65	5	M3	cadaver
z05	*Homo sapiens*	m	adult	66	5	M3	cadaver
z06	*Homo sapiens*	m	adult	38	5	M3	cadaver
z07	*Homo sapiens*	m	adult	60	5	M3	cadaver
z08	*Homo sapiens*	m	adult	76	5	M3	cadaver
z09	*Homo sapiens*	m	adult	27	5		cadaver
z10	*Homo sapiens*	f	adult	70	5	M3	cadaver
z11	*Homo sapiens*	m	adult	85	5	M3	cadaver
z12	*Homo sapiens*	m	adult	32	5	M3	cadaver
z13	*Homo sapiens*	f	adult	42	5	M3	cadaver
z14	*Homo sapiens*	m	adult	58	5	M3	cadaver
z15	*Homo sapiens*	m	adult	22	5		cadaver
z16	*Homo sapiens*	m	adult	34	5	M3	cadaver
z17	*Homo sapiens*	m	adult	53	5	M3	cadaver
z19	*Homo sapiens*	m	adult	59	5	M3	cadaver

z20	*Homo sapiens*	m	adult	41	5	M3	cadaver
z21	*Homo sapiens*	m	adult	50	5	M3	cadaver
z22	*Homo sapiens*	m	adult	54	5	M3	cadaver
z23	*Homo sapiens*	f	adult	48	5	M3	cadaver
z24	*Homo sapiens*	f	adult	58	5	M3	cadaver
z25	*Homo sapiens*	m	adult	96	5	M3	cadaver
z26	*Homo sapiens*	m	adult	74	5	M3	cadaver
z27	*Homo sapiens*	f	adult	38	5	M3	cadaver
z28	*Homo sapiens*	m	adult	62	5	M3	cadaver
z29	*Homo sapiens*	m	adult	63	5	M3	cadaver
z30	*Homo sapiens*	f	adult	31	5	M3	cadaver
z31	*Homo sapiens*	m	adult	66	5	M3	cadaver
z32	*Homo sapiens*	m	adult	59	5	M3	cadaver
z33	*Homo sapiens*	m	adult	88	5	M3	cadaver
z34	*Homo sapiens*	m	adult	38	5	M3	cadaver
z35	*Homo sapiens*	f	adult	57	5	M3	cadaver
z36	*Homo sapiens*	m	adult	53	5	M3	cadaver
z37	*Homo sapiens*	m	adult	46	5	M3	cadaver
z38	*Homo sapiens*	m	adult	26	5	M3	cadaver
z39	*Homo sapiens*	f	adult	62	5	M3	cadaver
z40	*Homo sapiens*	f	adult	76	5	M3	cadaver
z41	*Homo sapiens*	m	adult	71	5	M3	cadaver
z42	*Homo sapiens*	m	adult	46	5	M3	cadaver
z43	*Homo sapiens*	m	adult	39	5	M3	cadaver
z44	*Homo sapiens*	m	adult	35	5	M3	cadaver
z45	*Homo sapiens*	m	adult	27	5	M3	cadaver
z46	*Homo sapiens*	m	adult	77	5	M3	cadaver
z47	*Homo sapiens*	f	adult	37	5	M3	cadaver
z48	*Homo sapiens*	m	adult	86	5	M3	cadaver
z49	*Homo sapiens*	m	adult	67	5	M3	cadaver
z50	*Homo sapiens*	f	adult	40	5	M3	cadaver
z51	*Homo sapiens*	m	adult	44	5	M3	cadaver
z52	*Homo sapiens*	f	adult	74	5	M3	cadaver
z53	*Homo sapiens*	m	adult	70	5	M3	cadaver
z54	*Homo sapiens*	m	adult	86	5	M3	cadaver
z55	*Homo sapiens*	m	adult	89	5	M3	cadaver
z56	*Homo sapiens*	m	adult	79	5	M3	cadaver
z57	*Homo sapiens*	f	adult	66	5	M3	cadaver
z58	*Homo sapiens*	f	adult	54	5	M3	cadaver
z59	*Homo sapiens*	f	adult	47	5	M3	cadaver
z60	*Homo sapiens*	f	adult	44	5	M3	cadaver
z61	*Homo sapiens*	f	adult	39	5	M3	cadaver

z63	*Homo sapiens*	m	adult	89	5	M3	cadaver
z64	*Homo sapiens*	f	adult	83	5	M3	cadaver
z65	*Homo sapiens*	m	adult	77	5	M3	cadaver
z66	*Homo sapiens*	m	adult	69	5	M3	cadaver
z67	*Homo sapiens*	f	adult	62	5	M3	cadaver
z68	*Homo sapiens*	f	adult	58	5	M3	cadaver
z69	*Homo sapiens*	m	adult	55	5	M3	cadaver
z70	*Homo sapiens*	m	adult	55	5	M3	cadaver
z71	*Homo sapiens*	f	adult	52	5	M3	cadaver
z72	*Homo sapiens*	f	adult	49	5	M3	cadaver
z73	*Homo sapiens*	f	adult	48	5	M3	cadaver
z74	*Homo sapiens*	m	adult	41	5	M3	cadaver
z75	*Homo sapiens*	m	adult	41	5	M3	cadaver
z76	*Homo sapiens*	m	adult	39	5	M3	cadaver
z77	*Homo sapiens*	f	adult	26	5	M3	cadaver
z78	*Homo sapiens*	f	adult	20	5	M3	cadaver
f1	*Homo sapiens*	f	infant	13.83	3		cadaver
f2	*Homo sapiens*	f	juvenile	16.08	4		cadaver
f3	*Homo sapiens*	f	infant	12.21	3		cadaver
f4	*Homo sapiens*	f	juvenile	16.30	4		cadaver
f5	*Homo sapiens*	f	juvenile	16.16	4		cadaver
f6	*Homo sapiens*	f	infant	13.46	3		cadaver
f7	*Homo sapiens*	f	juvenile	17.42	4		cadaver
f8	*Homo sapiens*	f	infant	10.98	3		cadaver
f9	*Homo sapiens*	f	juvenile	14.83	4		cadaver
f10	*Homo sapiens*	f	juvenile	14.02	4		cadaver
f11	*Homo sapiens*	f	juvenile	14.49	4		cadaver
m1	*Homo sapiens*	m	juvenile	14.12	4		cadaver
m2	*Homo sapiens*	m	juvenile	15.79	4		cadaver
m3	*Homo sapiens*	m	infant	12.65	3		cadaver
m4	*Homo sapiens*	m	juvenile	15.20	4		cadaver
m5	*Homo sapiens*	m	juvenile	17.44	4		cadaver
m6	*Homo sapiens*	m	juvenile	15.23	4		cadaver
m7	*Homo sapiens*	m	juvenile	15.15	4		cadaver
m8	*Homo sapiens*	m	juvenile	15.42	4		cadaver
m9	*Homo sapiens*	m	infant	9.80	3		cadaver
m10	*Homo sapiens*	m	infant	12.20	3		cadaver
m11	*Homo sapiens*	m	juvenile	15.76	4		cadaver
irm50	*Homo sapiens*	m	juvenile	16	4	M2	cadaver
irm51	*Homo sapiens*	m	juvenile	16	4	M2	cadaver
irm52	*Homo sapiens*	m	juvenile	16	4	M2	cadaver

irm53	*Homo sapiens*	f	infant	11	3	M1, M2 started to erupt	cadaver
irm54	*Homo sapiens*	m	infant	10	3	M1, M2 started to erupt	cadaver
irm55	*Homo sapiens*	m	juvenile	16	4	M2	cadaver
irm56	*Homo sapiens*	m	infant	12	3	M1, M2 started to erupt	cadaver
irm57	*Homo sapiens*	f	infant	13	3	M2	cadaver
z79	*Homo sapiens*	m	adult	21	5	M3	cadaver
z80	*Homo sapiens*	m	adult	18	5	M3	cadaver
z81	*Homo sapiens*	m	adult	21	5	M3	cadaver
z82	*Homo sapiens*	f	adult	19	5	M3	cadaver
z83	*Homo sapiens*	m	adult	24	5	M3	cadaver
z84	*Homo sapiens*	m	adult	24	5	M3	cadaver
z85	*Homo sapiens*	m	adult	22	5	M3	cadaver
z86	*Homo sapiens*	m	adult	24	5	M3	cadaver
z87	*Homo sapiens*	m	adult	21	5	M3	cadaver
z88	*Homo sapiens*	m	adult	18	5	M3	cadaver
z89	*Homo sapiens*	m	adult	19	5	M3	cadaver
z90	*Homo sapiens*	m	adult	23	5	M3	cadaver
z91	*Homo sapiens*	f	adult	24	5	M3	cadaver
z92	*Homo sapiens*	m	juvenile	17	4	M2	cadaver
z93	*Homo sapiens*	m	adult	24	5	M3	cadaver
z94	*Homo sapiens*	m	adult	23	5	M3	cadaver
z95	*Homo sapiens*	m	juvenile	17	4	M2	cadaver
fullbody25_adult	*Homo sapiens*	f	adult	30	5	M3	cadaver
fullbody25_fetus	*Homo sapiens*	m	fetus	7th months	-1	none	cadaver
usz1	*Homo sapiens*	f	adult	31.6	5		cadaver
usz2	*Homo sapiens*	f	adult	32.6	5		cadaver
usz3	*Homo sapiens*	f	adult	34.2	5		cadaver
usz4	*Homo sapiens*	f	adult	39	5		cadaver
usz5	*Homo sapiens*	f	adult	29.11	5		cadaver
usz6	*Homo sapiens*	f	adult	32.2	5		cadaver
usz7	*Homo sapiens*	f	adult	37.11	5		cadaver
usz8	*Homo sapiens*	f	adult	34	5		cadaver
usz9	*Homo sapiens*	f	adult	36.10	5		cadaver
usz10	*Homo sapiens*	f	adult	31.9	5		cadaver
usz11	*Homo sapiens*	f	adult	24.10	5		cadaver
usz12	*Homo sapiens*	f	adult	24.7	5		cadaver
usz13	*Homo sapiens*	f	adult	32.1	5		cadaver
usz14	*Homo sapiens*	f	adult	37.7	5		cadaver

usz15	*Homo sapiens*	f	adult	37.4	5		cadaver
usz16	*Homo sapiens*	f	adult	35.8	5		cadaver
usz17	*Homo sapiens*	f	adult	33	5		cadaver
usz18	*Homo sapiens*	f	adult	29.6	5		cadaver
usz19	*Homo sapiens*	f	adult	36.6	5		cadaver
usz20	*Homo sapiens*	f	adult	36.3	5		cadaver
usz21	*Homo sapiens*	f	adult	24.11	5		cadaver
AM10342	*Pan troglodytes*	m	infant		1	dm1 almost erupted	cadaver
AM10532	*Pan troglodytes*	f	neonate		0	none erupted	cadaver
AM11451	*Pan troglodytes*	f	infant		1	dm1 started to erupt	cadaver
AM11454	*Pan troglodytes*	m	neonate		0	none erupted	cadaver
AM13302	*Pan troglodytes*	f	neonate	1 day	0	none erupted	cadaver
AM13305	*Pan troglodytes*	m	neonate		0	none erupted	cadaver
AM13306	*Pan troglodytes*	f	neonate		0	none erupted	cadaver
AM13307	*Pan troglodytes*	m	neonate	1 day	0	none erupted	cadaver
AM13308	*Pan troglodytes*	m	neonate		0	none erupted	cadaver
AM13311	*Pan troglodytes*	m	neonate		0	none erupted	cadaver
AM5559	*Pan troglodytes*	f	neonate	6 days	0	none erupted	cadaver
AM6807	*Pan troglodytes*	m	fetus		-1	none erupted	cadaver
AM6830	*Pan troglodytes*	f	fetus		-1	none erupted	cadaver
AM7283	*Pan troglodytes*	m	juvenile		4	M2	cadaver
AM7529	*Pan troglodytes*	m	neonate		0	none erupted	cadaver
AM7653	*Pan troglodytes*	f	neonate		0	none erupted	cadaver
AM8346	*Pan troglodytes*	m	neonate		0	none erupted	cadaver
AM9361	*Pan troglodytes*	f	neonate		0	none erupted	cadaver
AM9404	*Pan troglodytes*	f	neonate		0	none erupted	cadaver
as443	*Pan troglodytes*	f	neonate		0	none erupted	cadaver
AS445	*Pan troglodytes*	m	fetus		-1	none erupted	cadaver
blacky	*Pan troglodytes*	f	adult	59	5	M3	cadaver
chimp1	*Pan troglodytes*	f	juvenile		4	M2	cadaver
chimp2	*Pan troglodytes*	f	adult		5	M_3	cadaver
chimp3	*Pan troglodytes*	m	adult		5	M_3	cadaver
chimp4	*Pan troglodytes*	f	adult		5	M3	cadaver
prict34	*Pan troglodytes verus*	f	adult	20	5	M3	cadaver
prict452	*Pan troglodytes verus*	m	adult	32	5	M3	cadaver
prict496	*Pan troglodytes verus*	f	adult	39	5	M3	cadaver
prict611	*Pan troglodytes*	f	adult	44	5	M3	cadaver
prict650	*Pan troglodytes*	f	juvenile		3	M1	cadaver

prict660	*Pan troglodytes verus*	m	adult	34	5	M3	cadaver
Sch-302	*Pan troglodytes*	f	fetus		-1	none erupted	cadaver
10533	*Pan troglodytes*	m	adult		5	M3? No skull	dry
10768	*Pan troglodytes*	f	infant		2	dm2	dry
5920	*Pan troglodytes*	m	adult		5		dry
6670	*Pan troglodytes*	m	infant		2	dm2	dry
6695	*Pan troglodytes*	m	juvenile		3	M1	dry
6876	*Pan troglodytes*	m	adult		5	M3?	dry
6892	*Pan troglodytes*	f	infant		2	dm2	dry
6972	*Pan troglodytes*	m	juvenile		3	M1	dry
7127	*Pan troglodytes*	f	adult		5	M3	dry
8606	*Pan troglodytes*	m	infant		2	dm2	dry
8620	*Pan troglodytes schweinfurthii*	m	adult		5	M3	dry
AS1586	*Pan troglodytes*	f	adult		5	M3	dry
AS1745	*Pan troglodytes*	f	adult		5	M3	dry
AS1760	*Pan troglodytes*	m	infant		2	dm2	dry
AS1763	*Pan troglodytes*	f	adult		5	M3	dry
AS1784	*Pan troglodytes*	f	adult		5	M3	dry
as1789	*Pan troglodytes*	f	juvenile		4	M2	dry
AS1810	*Pan troglodytes*	m	adult		5	M3	dry
AS1814	*Pan troglodytes*	f	juvenile		3	M1	dry
PAL4	*Pan troglodytes*	f	infant		2	dm2	dry
PAL130	*Pan troglodytes*	f	juvenile		4	M2	dry
PAL154	*Pan troglodytes*	f	juvenile		3	M1	dry
PAL156	*Pan troglodytes*	f	juvenile		3	M1?	dry
PAL163	*Pan troglodytes*	m	juvenle		3	M1	dry
PAL192	*Pan troglodytes*	m	juvenle		3	M1	dry
PAL194	*Pan troglodytes*	m	juvenile		3	M1?	dry
PAL195	*Pan troglodytes*	m	juvenile		3	M1?	dry
PAL197	*Pan troglodytes*	f	juvenile		3	M1	dry
PAL198	*Pan troglodytes*	f	juvenile		3	M1	dry
PAL215	*Pan troglodytes*	f	adult		5	M3	dry
PAL217	*Pan troglodytes*	f	adult		5	M3	dry
PAL219	*Pan troglodytes*	f	adult		5	M3	dry
PAL220	*Pan troglodytes*	m	adult		5	M3	dry
PAL221	*Pan troglodytes*	m	juvenile		3	M1	dry
PAL222	*Pan troglodytes*	f	juvenile		3	M1	dry
PAL223	*Pan troglodytes*	f	juvenile		4	M2	dry
PAL226	*Pan troglodytes*	f	juvenile		4	M2	dry
PAL53	*Pan troglodytes*	f	juvenle		3	M1	dry

prict975	*Pan troglodytes verus*	m	neonate	5 days	0	none erupted	frech cadaver
prict845	*Pan troglodytes verus*	f	adult	47?	5	M3?	fresh cadaver
8500	*Pan paniscus*	m	juvenile		4	M2	frozen
AM11450	*Pan troglodytes*	m	infant		1	dm1 started to erupt	frozen
AM11452	*Pan troglodytes*	f	infant		2	dm2	frozen
AM11453	*Pan troglodytes*	f	infant		1	dm1 almost erupted	frozen
AM13301	*Pan troglodytes*	m	infant		1	dm1	frozen
AM13303	*Pan troglodytes*	f	neonate		0	none erupted	frozen
AM13304	*Pan troglodytes*	f	infant		1	dm1 started to erupt	frozen
AM13309	*Pan troglodytes*	m	infant		1	dm1 started to erupt	frozen
AM13310	*Pan troglodytes*	m	infant		1	dm1 almost erupted	frozen
AM8501	*Pan paniscus*	f	infant	2-3	2	dm2?	frozen
AM8503	*Pan paniscus*	m	juvenile	7	4	M2?	frozen
am8504	*Pan troglodytes*	f	infant		2	dm2	frozen
AM6686	*Pan troglodytes*	m	neonate		0	none erupted	wet
prict1350	*Gorilla gorilla*	m	adult	38	5		cadaver
prict293	*Gorilla gorilla gorilla*	f	adult	54	5	M3	cadaver
prict308	*Gorilla gorilla gorilla*	m	adult	46	5	M3	cadaver
13488	*Gorilla gorilla*	f	adult		5	M3	dry
6680	*Gorilla gorilla*	m	adult		5	M3	dry
6878	*Gorilla gorilla*	m	adult		5	M3	dry
7148	*Gorilla gorilla*	m	adult		5		dry
7487	*Gorilla gorilla*	m	adult		5	M3	dry
9787	*Gorilla gorilla*	f	adult		5		dry
as1690	*Gorilla gorilla*	m	adult		5	M3	dry
pal1	*Gorilla gorilla*	m	adult		5	M3	dry
pal2	*Gorilla gorilla*	f	adult		5	M3	dry
pal8	*Gorilla gorilla*	m	adult		5	M3	dry
PAL11	*Gorilla gorilla gorilla*	m	adult		5	M3	dry
PAL12	*Gorilla gorilla*	m	adult		5	M3	dry
PAL13	*Gorilla gorilla*	m	adult		5	M3	dry
PAL14	*Gorilla gorilla*	f	adult		5	M3	dry
PAL241	*Gorilla gorilla*	m	adult		5	M3	dry
nache	*Gorilla gorilla gorilla*	f	adult	32	5	M2	frozen
AM103141	*Pongo pygmaeus*	m	adult		5	M3, old individual	cadaver
prict1342	*Pongo abelii*	f	adult	49	5		cadaver

prict738	*Pongo pygmaeus*	f	adult	42	5	M3	cadaver
8609	*Pongo pygmaeus*	m	adult		5	M3	dry
11444	*Pongo abelii*	f	adult	ca 20 years	5	M3?	dry
AM9149	*Pongo pygmaeus*	m	adult		5	no skull	dry
AS1077	*Pongo abelii*	m	adult		5	M3	dry
as1528	*Pongo pygmaeus*	f	adult		5	M3?	dry
as1529	*Pongo pygmaeus*	m	adult		5	M3	dry
AS1554	*Pongo pygmaeus*	f	adult		5	M3	dry
as1561	*Pongo pygmaeus*	m	adult		5	M3	dry
PAL101	*Pongo pygmaeus*	m	adult		5	M3	dry
AS1531	*Pongo pygmaeus*	m	adult?		5	no skull	dry
AS1677	*Pongo pygmaeus*	f	adult?	12	5	no skull	dry

Table 2. Definition of fixed landmarks.

LM number	Description
1-2	Pubic symphysis: superiormost anterior point
3-4	Pubic symphysis: superiormost posterior point
5-6	Ischiopubic juncture: pubis - posterior fusion point
7-8	Ischiopubic juncture: ischium - posterior fusion point
9-10	Ischiopubic juncture: pubis - obturator foramen inferior fusion point
11-12	Ischiopubic juncture: ischium - obturator foramen inferior fusion point
13-14	Ischiopubic juncture: pubis - obturator foramen superior fusion point
15-16	Ischiopubic juncture: ischium - obturator foramen superior fusion point
17-18	Ischium: posteriormost point (superior from ischial tuberosity)
19-20	Ischium: inferiormost midpoint
21-22	Ilioischial juncture: ischium - fusion point
23-24	Ilioischial juncture: ilium - fusion point
25-26	Ilioischial juncture: ischium - acetabulum lateral fusion point
27-28	Ilioischial juncture: ilium - acetabulum lateral fusion point
29-30	Acetabulum: superiormost lateral point
31-32	Acetabulum: point on pubic part of lunate surface
33-34	Iliopubic juncture: pubis - superior fusion point
35-36	Iliopubic juncture: ilium - superior fusion point
37-38	Iliopubic juncture: pubis - fusion point on pelvic brim
39-40	Iliopubic juncture: ilium - fusion point on pelvic brim
41-42	Pubis: anterior midpoint
43-44	Acetabulum: inferiormost lateral point on lunate surface
45-46	Acetabulum: deepest point on acetabular center (acetabular fossa)
47-48	Pelvic brim and sacroiliac joint: intersection point
49-50	Sacroiliac joint: superiormost point
51	S1: superiormost anterior point
52	S1: superiormost posterior point
53	S1: anterior midpoint
54	S2: anterior midpoint
55	S3: anterior midpoint
56	S4: anterior midpoint
57-58	Anterior supuperior iliac spine
59-60	Iliac crest: posteriormost point (end point)
61-62	Posterior inferior iliac spine
63	S5: anterior midpoint

Table S3. Definition of semilandmarks.

LM number	Description
Iliac crest	Right: start LM 57, end LM 59; Left: start LM 58, end LM 60 with eight subdivisions
Posterior iliac spines	Right: start LM 59, end LM 61; Left: start LM 60, end LM 62 with four subdivisions
Greater sciatic notch	Right: start LM 61, end LM 23; Left: start LM 62, end LM 24 with four subdivisions
Acetabulum: on ilium	Right: start LM 27, end LM 29; Left: start LM 28, end LM 30 with four subdivisions
Anterior iliac spines	Right: start LM 57, end LM 29; Left: start LM 58, end LM 30 with four subdivisions
Acetabulum: on ischium	Right: start LM 25, end LM 43; Left: start LM 26, end LM 44 with four subdivisions
Obturator foramen posterior	Right: start LM 15, end LM 11; Left: start LM 16, end LM 12 with four subdivisions
Obturator foramen anterior	Right: start LM 13, end LM 9; Left: start LM 14, end LM 10 with four subdivisions
Sacroiliac joint	Right: start LM 49, end LM 47; Left: start LM 50, end LM 48 with four subdivisions
Pelvic brim1	Right: start LM 47, end LM 39; Left: start LM 48, end LM 40 with four subdivisions
Pelvic brim2	Right: start LM 37, end LM 3; Left: start LM 38, end LM 4 with four subdivisions
Pubis posterior	Right: start LM 3, end LM 5; Left: startLeft: start LM 4, end LM 6 with two subdivisions
Ischium posterior	Right: start LM 7, end LM 21; Left: start LM 8, end LM 22 with eight subdivisions

References:

Adams DC, Collyer ML, Sherratt E. 2015. *geomorph*: Software for geometric morphometric analyses. R package version 2.1.7. http://cran.r-project.org/web/ packages/geomorph/ index.html. Available from: http://cran.r-project.org/web/ packages/geomorph/index.html

Adams DC, Otárola Castillo E. 2013. *geomorph*: an R package for the collection and analysis of geometric morphometric shape data. Methods Ecol Evol 4:393–399.

Adams DC. 2016. Evaluating modularity in morphometric data: challenges with the RV coefficient and a new test measure. Methods Ecol Evol 7:565–572.

Bookstein FL. 1997. Morphometric tools for landmark data: geometry and biology. Cambridge University Press.

Collyer ML, Sekora DJ, Adams DC. 2015. A method for analysis of phenotypic change for phenotypes described by high-dimensional data. Heredity 115:357–365.

Grabowski MW. 2012. Hominin obstetrics and the evolution of constraints. Evol Biol 40:57–75.

Gruss LT, Schmitt D. 2015. The evolution of the human pelvis: changing adaptations to bipedalism, obstetrics and thermoregulation. Philos Trans R Soc Lond, B, Biol Sci 370:20140063–20140063.

Gunz P, Mitteroecker P, Bookstein FL. 2005. Semilandmarks in three dimensions. In: Slice DE, editor. Modern morphometrics in physical anthropology. Developments in Primatology: Progress and Prospects. New York: Kluwer Academic Publishers-Plenum Publishers. p 73–98.

Hirata S, Fuwa K, Sugama K, Kusunoki K, Takeshita H. 2011. Mechanism of birth in chimpanzees: humans are not unique among primates. Biology Letters 7:686–688.

Klingenberg CP. 2009. Morphometric integration and modularity in configurations of landmarks: tools for evaluating a priori hypotheses. Evol Dev 11:405–421.

Lovejoy CO. 2005. The natural history of human gait and posture. Gait & Posture 21:95–112.

McKinley MP, O'loughlin VD. 2006. Human anatomy. McGraw-Hill Higher Education.

Milella M, Zollikofer CPE, Ponce de León MS. 2015. Virtual reconstruction and geometric morphometrics as tools for paleopathology: a new approach to study rare developmental disorders of the skeleton. Anat Rec 298:335–345.

Ponce de León MS, Golovanova L, Doronichev V, Romanova G, Akazawa T, Kondo O, Ishida H, Zollikofer CPE. 2008. Neanderthal brain size at birth provides insights into the evolution of human life history. Proc Natl Acad Sci USA 105:13764–13768.

R Core Team. 2016. R: A language and environment for statistical computing. R Foundation for Statistical Computing, Vienna, Austria. Available from: https://www.R-project.org/

Rüdell A, Schlager S. Sexual dimorphism and population affinity in the human zygomatic structure - comparing surface to outline data. Anat Rec.

Schlager S, Goepper M. 2016. Model based facial soft-tissue estimation from dry skull. Am J Phys Anthropol.

Schlager S. 2016. Morpho: Calculations and visualisations related to geometric morphometrics. R package version 2.3.1.1. Available from: http://sourceforge.net/projects/morpho-rpackage/ https://github.com/zarquon42b/Morpho

Smilde AK, Kiers HAL, Bijlsma S, Rubingh CM, van Erk MJ. 2009. Matrix correlations for high-dimensional data: the modified RV-coefficient. Bioinformatics 25:401–405.

Zollikofer CPE, Ponce de León MS. 1995. Tools for rapid prototyping in the biosciences. IEEE Comput Grap Appl 15:48–55.

Zollikofer CPE, Ponce de León MS. 2005. Virtual reconstruction: a primer in computer-assisted paleontology and biomedicine. Hoboken, N. J.: Wiley-Liss.

Acknowledgements

Making this PhD thesis is not an individual experience, but rather it takes place in complex social environment and includes a number of people, whom I would like to thank sincerely!

First of all, I wish to express my enormous gratitude to my joint PhD supervisors, Dr. Marcia S. Ponce de León and Prof. Dr. Christoph P.E. Zollikofer, for their huge support at different levels during all these years in Zurich.

Besides my advisors, I would like to thank the rest of my thesis committee: Prof. Dr. Marcelo Sánchez, Prof. Dr. Carel van Schaik and Prof. Dr. Robert Tague, for their insightful comments and encouragement.

I would like to thank all my colleagues and friends from Anthropological Institute, Institute of Forensic Medicine at Zurich, University Hospital of Zurich and Dept. of Radiology at Katholieke University Leuven for their support and collaboration at all levels.

My big thanks goes to my wife, Natalia, for her love, her patience with me and with my career aspirations, to my family in Azerbaijan and relatives in Germany for their constant encouragement.

This PhD work was supported by the A.H. Schultz Foundation and Swiss National Science Foundation Grant 31003A_135470/1 (to Prof. Dr. Christoph P.E. Zollikofer).

SURNAME

HUSEYNOV

Name

Alik

Date of birth

24.04.1985

Nationality

German

Education

2002 N23 Public Secondary School, Sumqayit, Azerbaijan

2002-2006 BA History/Political Science, Baku State University, Azerbaijan

2007-2008 Guest student in Bio/Earth Sciences, Goethe-University Frankfurt am Main, Germany

2008-2010 Msc in Quaternary Science and Prehistory, Natural Museum of Natural History Museum at Paris, France

Title: *Patterns of dental sexual dimorphism in early hominins: a comparative account.*

09/2011-now PhD candidate in Life Science/Evolutionary Biology, University of Zurich, Switzerland

Publications

Huseynov, A. Ponce de León, M.S. & Zollikofer, C.P.E. (*accepted*) Development of modular organization in the chimpanzee pelvis, Anat Rec.

Ponce de León, M.S., **Huseynov, A.** & Zollikofer, C.P.E. (2016) Reply to Mitteroecker and Fischer: Developmental solutions to the obstetrical dilemma are not Gouldian spandrels. Proc. Natl. Acad. Sci. USA.: 201607209.

Huseynov, A., Zollikofer, C.P.E., Coudyzer, W., Gascho, D., Kellenberger, C., Hinzpeter, R. & Ponce de León, M.S. (2016) Developmental evidence for obstetric adaptation of the human female pelvis. Proc. Natl. Acad. Sci. USA. 113(19): 5227-5232.

Workshop/Summer school participation

Zurich Center for Experimental and Clinical Imaging Technologies (EXCITE) - Summer School on Biomedical Engineering, basics of multiscale Biomedical Imaging (including

lectures, practical day, and hands-ons), blitz poster/one slide PhD work presentation, (ETH, Zurich, Switzerland 09/2014).

Teaching

05/2013 Practicum assistant, Biomedical Imaging and Scientific Visualization (BIO219), University of Zurich,

2011-2016 Teaching assistant, Anthropology practicum (BIO133), University of Zurich,

2011-2016 Teaching assistant, Morphometric Analysis (BIO208), University of Zurich,

2011-2016 Teaching assistant, Evolutionary and functional morphology of primates (BIO202) University of Zurich, University of Zurich,

2011-2016 Teaching assistant, Evolutionary and functional morphology of primates (BIO202) University of Zurich, University of Zurich.

Fellowships/Grants/Employment

06/2012-12/2016 Employed as PhD student, University of Zurich

09/2011-05/2012 A.H. Schultz Foundation grant for PhD start-up, University of Zurich